DESIGN AND ANALYSIS OF MICROSTRIP PATCH ANTENNA FOR WHITE SPACE TV BAND

A thesis submitted to
Delhi Technological University
for the Award of Degree of
Doctor of Philosophy
In

Electronics and Communication Engineering
by
RICHA

(Enrollment No.: 2K18/PHDEC/508)

Under the Supervision of
Dr. ASOK DE

&

Dr. N. S. RAGHAVA

Professor

Department of Electronics and Communication Engineering

Delhi Technological University (Formerly DCE)

Bawana Road, Delhi - 110042, India.

January, 2023.

DECLARATION

I declare that the research work reported in this thesis entitled "**Design and Analysis of Microstrip Patch Antenna for White Space TV Band**" for the award of the degree of *Doctor of Philosophy in Electronics and Communication Engineering* has been carried out by me under the supervision of Prof. Asok De and Prof. N.S. Raghava, Department of Electronics and Communication Engineering, Delhi Technological University, Delhi, India.

The research work embodied in this thesis, except where otherwise indicated, is my original research. This thesis has not been submitted by me earlier in part or full to any other University or Institute for the award of any degree or diploma. This thesis does not contain other person's data, graphs or other information, unless specifically acknowledged.

Date: (Richa)

Enrollment no.: 2K18/PHDEC/508

Department of ECE

Delhi Technological University,

Delhi-110042, India

CERTIFICATE

This is to certify that the research work embodied in the thesis entitled **"Design and Analysis of Microstrip Patch Antenna for White Space TV Band"** submitted by **Ms. Richa** with enrollment number **(2K18/PHDEC/508)** is the result of her original research carried out in the Department of Electronics and Communication Engineering, Delhi Technological University, Delhi, for the award of **Doctor of Philosophy** under the supervision of **Prof. Asok De** and **Prof. N.S. Raghava.**

It is further certified that this work is original and has not been submitted in part or fully to any other University or Institute for the award of any degree or diploma.

This is to certify that the above statement made by the candidate is correct to the best of our knowledge.

(Prof. Asok De)   **(Prof. N.S.Raghava)**
Supervisor   Co-Supervisor
Professor   Professor
Department of ECE   Department of ECE
Delhi Technological University   Delhi Technological University
Delhi-110042   Delhi-110042

ACKNOWLEDGEMENT

Above all, I would like to express my heartiest thanks to all my family members whose blessings and affection have been remained constant source of inspiration. I have no words to express my gratitude to my father Mr. Ravi Bhushan, my mother Ms. Veena, my father-in-law Mr. Sukhpal Sharma, my mother-in-law Ms. Kanta Sharma and my brother Mr. Piyush Sharma.

Words cannot express my deep sense of gratitude to my life partner Mr. Avdhesh Kumar Sharma for his unwavering support and encouragement throughout my PhD journey. His love and understanding have been a constant source of strength and motivation for me. His willingness to listen and offer guidance has been invaluable in helping me navigate the challenges. He is always there cheering me up and stood by me through the good and bad times equally.

I would like to extend my deepest gratitude to my children Himadri Bhardwaj and Parth Bhardwaj, for their unwavering love and support throughout my PhD journey. Their understanding and patience during my time spent on research and writing has been truly invaluable. Their presence in my life has been a constant source of inspiration and motivation, and I am deeply grateful to have them by my side. I could not have completed this thesis without their love and support. Thank you from the bottom of my heart.

Last, but not least, I would like to dedicate my thesis to my beloved husband and loving parents for their endless love, patience and understanding.

Date :   **(Richa)**

Place : Delhi, India

DEDICATED TO MY LOVING PARENTS

Mr. Ravi Bhushan & Ms. Veena

&

MY BELOVED HUSBAND

Mr. Avdhesh Kumar Sharma

CONTENTS

Abstract

Federal Communications Commission regulates the radio spectrum with designation of three bands (54 -88 MHz, 174-216MHz and 470-806MHz) for broadcasting terrestrial television. Television stations are often operated in geographically separate areas to avoid interference. Furthermore, all television stations are not used in some parts of the nation due to population density. The frequency designated to these unused television stations and the spectrum between TV stations are called white spaces. Many researchers have been investigated and demonstrated that this untapped spectrum may be utilize to deliver broadband Internet access while getting along with nearby TV channels. White space is an important possibility in the context of our evolving wireless mobile environment. This portion of the spectrum is primed for experimentation and innovation. Due to introduction of 4G, 5G and IoT services the frequency spectrum above the 806 MHz becomes very crowded. White space TV band frequencies fascinate researcher because of large available spectrum, good propagation characteristics, excellent penetration, and of course no cost. As the frequency of TV band is small as compared to the most of the available wireless devices, the biggest challenge at this frequency is the largest physical size of the antenna. Planar antenna is the one of the solutions to reduce size of TV band antenna. There is some disadvantage of planar antenna like low gain, narrow bandwidth etc. Various bandwidth and gain enhancement techniques are available in literature to overcome the disadvantages of planar antennas.

In this thesis, microstrip patch antennas are designed to operate in white space TV band. The gain and bandwidth enhancement techniques are used to achieve ultra-wide band and high gain antennas. Fractal geometry is used to further reduce the size of the antenna with multiband characteristics. The different applications of these antennas are RFID, IEEE 802.11, 'Super Wi-Fi' and for long distance communication in the presence of obstacles such as wall, hill, mountains etc. The thesis is organized into six chapters as described below.

In the first chapter, a brief introduction of white space TV band and its spectrum is explained with the availability of TV band for different applications. Antennas were designed for high gain and bandwidth. This introduction lays the foundation that is needed to appreciate the work performed in this thesis.

In the second chapter, circular patch antenna is designed for RFID application. In India, the frequency band used for RFID applications is 865–867 MHz with 2MHz bandwidth. In

comparison to the currently existing RFID antenna, the proposed antenna is compact in dimensions. Four concentric rings are sliced from a circular microstrip patch, and a shorting pin is used to connect the patch to the ground. The design was done on FR4, which is a fairly common and durable substrate. The antenna design's gain and directivity are 7.6dBi and 9.9 dB, respectively. The antenna may operate on two bands in the intended frequency spectrum, namely 479- 492 MHz and 643 -653MHz. The bandwidth obtained in these bands are 13 MHz and 10 MHz, individually, that is higher than commercially available UHF RFID antenna. The bands have a return loss of -29dB and -14dB, respectively. Parameters of design antenna have been compared with the commercially available RFID antenna. The proposed antenna is having the lowest VSWR of 1.07 as compared to 1.4 for all compared antennas. Bandwidth is also increased from 3MHz to 13MHz. It was observed that the proposed design has a compact size with a good agreement of gain, bandwidth, VSWR, and front-to-back ratio and limited ground size

Extending the work performed in second chapter, again circular microstrip patch antenna with three circular rings is designed. In 1st design we are able to achieve desirable gain and multiband, but the bandwidth is small. After changing the position of rings and size of ground plane proposed antenna can be used in complete TV band with a compromise in gain. In the presented paper a novel application of microstrip circular patch antenna with three rings on patch is proposed. The bandwidth and efficiency of the proposed antenna can be compared with the work already published in the white space TV band. It was observed that the proposed antenna is having good bandwidth and efficiency with considerable gain.

In the fourth chapter, inverted stacked parasitic patch antenna with two layers is explored. In this design, two layers are stacked on each other with coaxial feed at the lower circular patch. The two top circular patches are placed in an inverted position and electromagnetically coupled with a lower patch. The substrate used is FR4. The proposed antenna can operate between 499-650MHz frequency band with 5.6dBi gain. The proposed antenna is having an efficiency of 98%. A parametric analysis is done to cater to the requirements of the antenna size, gain, and radiation pattern. The parametric study found that when both top patches are elliptical, the lowest size with the largest gain is achieved. After variation of the eccentricity of top two patches, it was concluded that for compactness of antenna top patch eccentricity should be 0.5 with increased gain of 5.6dBi. Depending upon the requirement, the proposed antenna can be

used for base station and as user terminal. These low frequencies allow signals to penetrate things like walls, trees, etc., better than higher frequencies, and they can be used for various purposes, such as IEEE 802.11, in the 470–806 MHz band between TV channels.

In the fifth chapter, fractal patch antenna is designed. The effect of fractal slots on patch and cross slots in ground are investigated. In the proposed design 4 iteration Koch snowflakes patch is used to get dual band. 4th iteration Koch snowflake patch is placed 18mm above the air. FR4 is placed 65mm above the ground plane as superstrate. As no of iteration increased size of antenna is going to reduce. Further 4th iteration Koch snowflakes slots have been created in patch to get three bands. Last two bands have been combined to get higher bandwidth by creating 4th iteration cross slots in the ground plane. The antenna is working in multi-polarization in the received bands. The physical size of antenna is reduced by 38 mm with a gain of 4.5dBi

In the end, the sixth chapter consists of the overall conclusion and future scope of the thesis. In this thesis, we designed circular microstrip patch antenna with circular rings, inverted stacked parasitic circular patch antenna and Koch fractal patch antenna to achieve high gain and considerable bandwidth in white space TV band with reduced size. These antennas can be used as RFID application, IEEE 802.11, super wide band and any application which requires TV band frequency.

In this way, this thesis will discuss size reduction, bandwidth and gain enhancement techniques by using slots, stacking and fractal shapes.

List of Figures

List of Tables

List of Acronyms

ADS	Advanced Design System
C&S TV	Cable & Satellite television
CAD	Computer-Aided Design
CLS	Capacitive Loaded Strips
CMSA	Circular Microstrip Patch Antenna
CP	Circular Polarization
CRLH	Composite Right- or Left-Handed
CRP	Closed Ring Pair
CSSMA	Compact Stacked Square Microstrip Antenna
DECT	Digital Enhanced Cordless Telecommunication
DGS	Defected Ground Structure
EBG	Electromagnetic Band Gap
FBR	Front-to-Back Ratio
FCC	Federal Communications Commission
FDTD	Finite-Difference Time-Domain
GSM	Global System for Mobile Communication
HFSS	High Frequency Simulation Software
HPBW	Half Power Beam Width
IDMA	Interleave Division Multiple Access
IFDGS	Inclined Fractal Defected Ground Structure
IFS	Iterated Function System
INSAT	Indian National Satellite
MTM	Metamaterials
NLOS	Non-Line-of-Sight

NRW	Nicolson Ross Weir
OTM	Over-The-Mesh
PBG	Photonic Band Gap
PCB	Printed Circuit Board
PCS	Personal Communications Service
RFID	Radio Frequency Identification
SITE	Satellite Instructional Television Experiment
SRR	Split Ring Resonator
TL	Transmission Line
TV	Television
TVWS	Television White Space
UHF	Ultra-High Frequency
UMTS	Universal Mobile Telecommunications System
VHF	Very High Frequency
VNA	Vector Network Analyzer
VSWR	Voltage Standing Wave Ratio
Wi-Fi	Wireless Fidelity
WiMAX	Worldwide Interoperability for Microwave Access
WLAN	Wireless Local Area Networks
WPT	Wireless Power Transfer

CHAPTER 1

Introduction

1.1 Introduction to TVWS band

In 1959, television was introduced to India, and in 1975, Satellite Television Experiment introduced satellite television. The launch of the Indian National Satellite (INSAT) in 1982 led to a fast increase in color television users and a spike in the use of private television sets. Early in the 1990s, Cable & Satellite television (C&S TV), a new satellite television format, and foreign material were introduced to Indian households. C&S TV is now available in one-third of Indian television households. The first technological social experiment in human history, called SITE (Satellite Instructional Television Experiment), was used to launch satellite television in India. That was followed by several other experiments, including School Television, Jhabua Development Communication Project, SITE Continuity, Country Wide Class Room, and Gyan Darshan for educational and social development. Technologies by themselves offer the potential for democratization, but they also raise problems about access and control for those who do not own them. It also notes that although satellite television has advanced much in India since the SITE days in 1975, it has consistently been used by those who 'had' and 'had' other technology. In Figure 1.1, the radio spectrum for the TV band is depicted. For broadcasting terrestrial television, three bands were designated. Since these bands were licensed, nobody was allowed to utilize them for personal use. This band was utilized by 69 channels in total for TV broadcasts. Radio astronomy was only permitted on channels 1 through 37 [107].
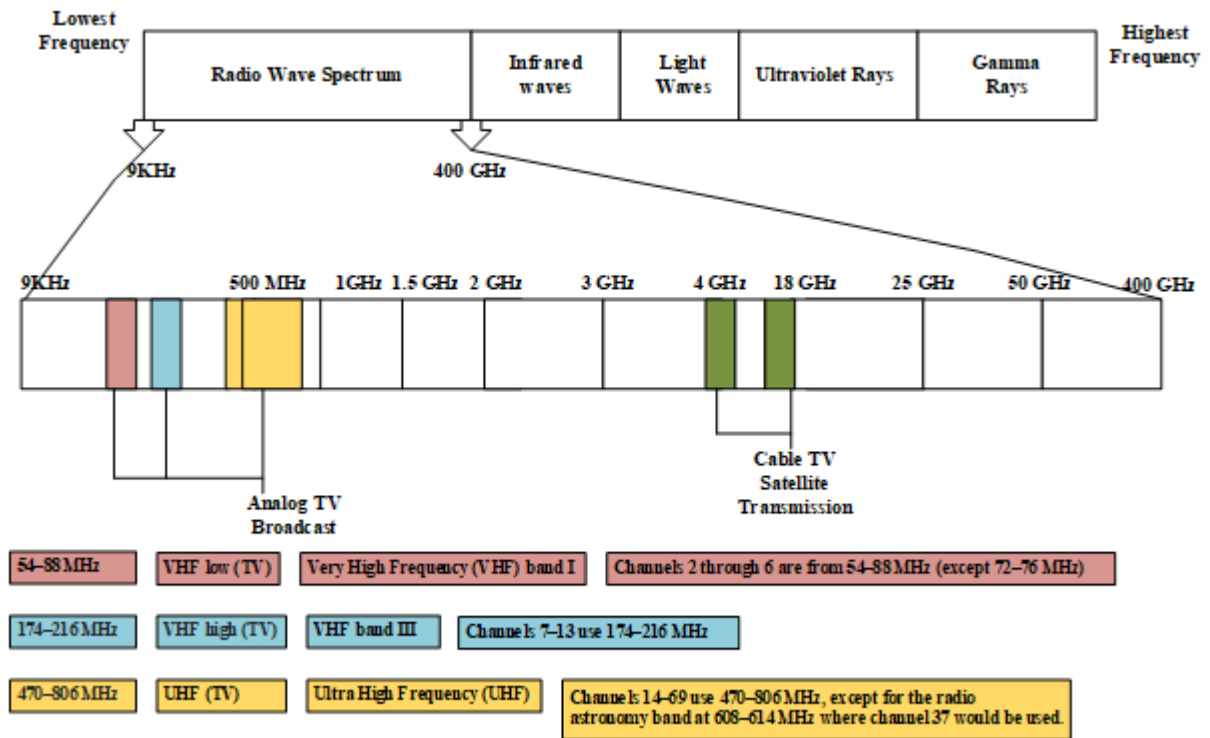
Fig. 1.1 Radio Spectrum for TV Transmission

Channels 2 to 6 are used in the VHF low band between 54 and 88 MHz, with a 6 MHz band for each channel. The frequency band between 88-173 MHz is reserved for FM Broadcasting, Aircraft, Ham radio, and Mobile or marine (150 and 173 MHz) use. Channels 7 to 13 of TV broadcasting used a frequency spectrum of 174–216 MHz. Channels 14 to 69 utilized the UHF TV band for broadcasting signals. To avoid interference between adjacent channels, guard bands are provided between channels and are also operated in geographically separate regions. Additionally, not all channels are utilized due to geographical conditions. These unutilized frequencies between TV stations are called white spaces [140]. In India, Door Darshan is the only television service provider and as a result, roughly 12 (80%) of the 15 channels in the "TV-UHF band-IV" are available as TVWS, according to a study done by the IIT-Bombay.

This unused and underutilized frequency spectrum gives a new opportunity to researchers to work in the TVWS band. This band is yet to be explored for new applications.

1.2 Definition of TV White Space (TVWS)

The term "white space" refers to a portion of the spectrum that is available for a particular time at a particular location for a radio communication application without interfering with other services. In simple terms, the space between licensed and unlicensed frequency bands is known as white space as shown in Figure 1.2. In almost every part of the world, many TV broadcast channels are unused. These unused channels are blocks of the spectrum which we call 'TV white space'
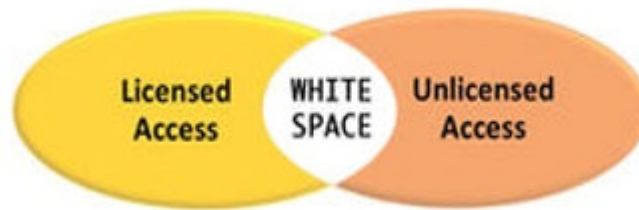
Fig. 1.2 White Space

Geographical characteristics might have a major impact on the quantity of TVWS spectrum that is accessible in a certain area [174,175]. The availability of TVWS can be mainly categorized as.

i   **Frequency:** In some geographical areas for avoiding interference, guard bands are employed between active channels.

ii   **Height:** The availability of TVWS in a particular region is defined by the height of the TVWS antenna about the reception of nearby broadcast television coverage.

iii   **Space:** The concept of utilizing geographic areas that are outside of traditional television coverage to expand broadcasting capabilities is a unique approach. These areas, often referred to as "dead zones," lack a current signal and are prime for development. Additionally, it is also possible to use these geographic locations as separation zones between locations that use the same television channels, allowing for more efficient use of broadcasting resources.

iv   **Time domain**: TVWS can be available on a time-sharing basis. A licensed channel is not receiving the assigned frequency during a particular time. At this time licensed channel can be used as TVWS.

1.3 Need for TVWS Technology

The following are some key points that need to be explored for better utilization of the TVWS spectrum [186]:

- There is a huge increase in the adaptation of data-intensive applications and rapid growth among mobile users. Spectrum is currently overburdened, and regulatory bodies demand maximum efficiency in its utilization. This can be accomplished by implementing spectrum sharing by licensed but underutilized or unutilized spectrum for various spectrum demands [113]

- Due to difficult geographical conditions, connecting in rural and remote areas becomes difficult. Connecting these areas with fixed-line services is very difficult and expensive. A wireless connectivity solution is a more feasible solution to connect these areas with the modern era. In this place, TVWS technology comes into play, as this technology

can communicate over a larger distance with high penetration and does not require extra infrastructure [75].

1.4 Motivation and Objective of The Thesis

There is an endless demand for wireless spectrum but a limited supply of it, which leads to a spectrum crunch. Ironically, out of the 100% spectrum allocated, the actual utilization is only 5 to 15%. The main reason for such a low utilization rate is that spectrum today is allocated in a fixed manner. If we could use the underutilized spectrum dynamically without interfering with the incumbents, this would open up huge opportunities to serve user needs. One alternative method of spectrum utilization is the efficient use of TVWS technology. TVWS is the first wireless technology to employ dynamic spectrum utilization. This band of frequencies is ready for experiments and innovation aimed at expanding the spectrum's capacity for users. The Federal Communications Commission (FCC) is actively working to make use of white spaces, or unused spectrum, to benefit the users and service providers. FCC published a report that allows for unlicensed frequency users to operate in TVWS frequency, effectively freeing up the white space spectrum for new and innovative technologies such as Wi-Fi. The commission's ongoing efforts aim to maximize the potential of white spaces and create new opportunities for growth and innovation in the industry. White space TV band frequencies have qualities like a large available spectrum, good propagation characteristics, excellent penetration, and of course no cost, which is the main motivation to work in this band. This band offers numerous opportunities to work [205, 188, 207] with existing bandwidth and gain enhancement techniques.

The objective of this work is to design an antenna for white space TV band communication. This band has not been explored yet. It has a very good chance of working. This technology has larger coverage with high penetration. To use the above-mentioned TVWS quality in antenna design, we will need a high-gain, wideband antenna. The objective of the thesis is to design a wideband, high-gain & compact-sized TVWS antenna.

The main objectives of the work are listed below:

- ❖ To design wideband & multiband antenna which can work in TV Band.
- ❖ To design a stacked parasitic patch antenna which can work in the TVWS band.
- ❖ To investigate Fractal Antenna, compact in size for TV range and can work in multiband.
- ❖ To investigate whether it can be used for multi-polarization.
- ❖ To investigate the antenna with the defective ground plane.

1.5 TVWS Technology

TVWS is the television white space band between the used frequencies of the UHF TV band. There are many technologies available for communication but TVWS is better as shown in Figure 1.3.
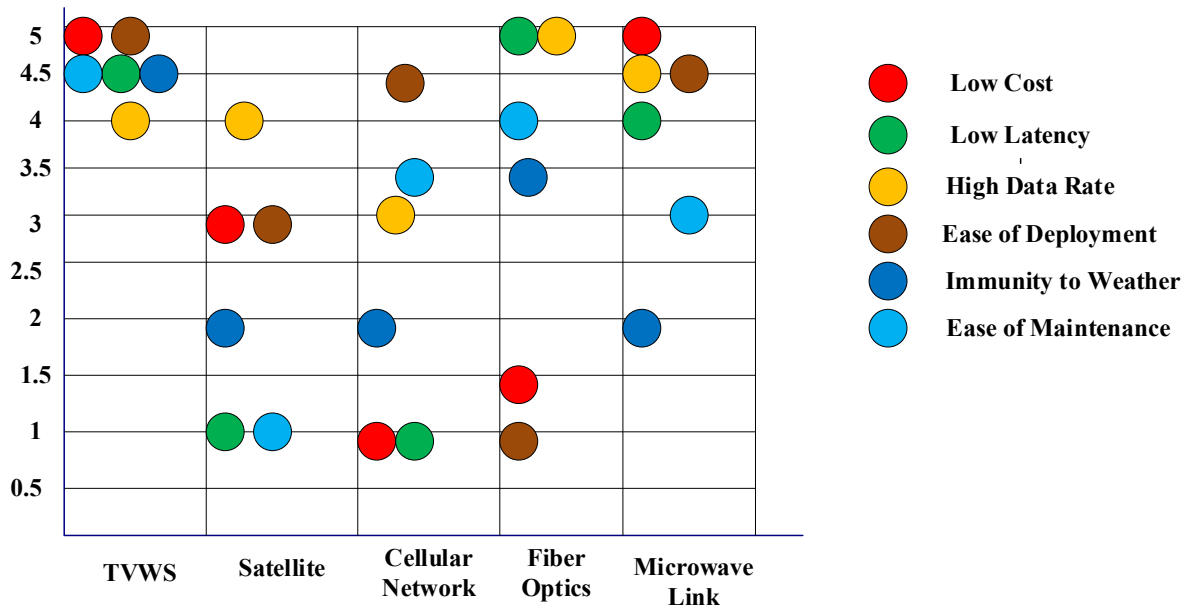
Fig. 1.3 Comparison between different communication techniques

TVWS technology is compared with satellite, cellular network, fiber optics, and microwave links and it was found that TVWS technology has low cost, low latency, high data rate, easy to deploy, immunity to weather, and easy maintenance.

1.5.1 Advantages of TVWS Technology

There are a number of advantages of TVWS technology as given below:

- Better coverage
- Non-Line-of-Sight (NLOS) Performance
- A New Broadband Possibility – Connecting More People
- Beyond Broadband – Connecting More Things
- Interference-Free Operations

Better Coverage: TV White Space technology has a superior range compared to traditional Wi-Fi, and it can cover vast areas of up to 10 kilometers in diameter [80]. This feature makes it a game-changing technology and it is dubbed as "Super Wi-Fi" due to its superior range and

7

penetration capabilities [181]. TVWS is more reliable than Wi-Fi, as a conventional Wi-Fi router covers a shorter range approximately less than 100 meters.

Non-Line-of-Sight (NLOS) Performance: In wireless communication, the microwave link requires line-of-sight communication. This line-of-sight communication, however, is not possible in rural, remote, rugged, or forested terrain. In big towers, line-of-sight communication becomes costly and unfeasible. TVWS technology is a viable alternative to microwaves because it uses low frequency, which can penetrate objects and cover a larger area without any additional infrastructure.

A New Broadband Possibility – Connecting More People: nowadays, people are more dependent on technology for various services on the internet, like data transfer, banking, education, business work, etc. We can now say that connectivity has become a human right. Unfortunately, this human right cannot be provided to people living in rural and remote areas due to environmental barriers, low population density, and distance from major ISPs. Rural communities often face significant challenges when it comes to connectivity, such as expensive and complex networks, and a lack of options. However, Carlson Wireless' Rural Connect radio aims to address these issues. The technology is well-suited for developing regions as it can act as a backhaul to nearby networks, utilize more open channels, be deployed quickly even in difficult terrain, and require less equipment and infrastructure to provide coverage over longer distances, thereby saving customers money. Additionally, Rural Connect is not limited to rural areas alone. As it can be used in urban areas as well. This is due to the "Super Wi-Fi" [83] effect which allows more people to be connected in more places than ever before.

Beyond Broadband – Connecting More Things: In addition to connecting people, TV White Space can connect things. TV White Space technology offers a unique opportunity to provide

a wideband signal that can handle the high volume of data being transmitted by multiple devices over long distances. This innovative technology has the potential to enable the development of smart cities, with a wide range of connected devices, from sports stadiums and shopping malls to municipal areas and more. It will be an enabler for many new applications and services that are yet to be imagined.

Interference-Free Operations: The people living in rural areas connect with the spectrum using TVWS, which can penetrate objects. The spectrum can be utilized without any interference.

If these underutilized bands are used effectively, they will become a key to rural connectivity, which is one of the goals of 'Digital India'. TVWS can be used to connect all Wi-Fi networks, and the fiber network used for the interconnection of urban or village gram panchayats can be replaced. Further, this technology can be used to connect rural and remote locations where the deployment of fiber is not possible. The following rules can be made to efficient use of the white space band:

- The database of free TV channels has to be created and maintained by the companies authorized by the commission. The interference of TVWS devices can be prevented by sharing geolocation capabilities with the available TV channels.
- A database of licensed wireless users and authorized unlicensed users should be maintained and protected. Furthermore, two channels should be kept clean and free from unregistered devices for a specific location to allow wireless devices to operate without a license.

- Furthermore, rules should be made for the registration of multiple TV stations, as well as for temporary broadcast fixed links. After making clear rules, there will be no interference from TV white space devices.

1.6 Requirements of Antenna for TVWS

TVWS communication technology demands transmitting and receiving signals from a longer distance. In the new coming era, this technology is suggested to work in rural, remote, rugged, and forested terrain areas. The importance of antennas in communication technology cannot be overstated. Antennas function as transducers, transforming electrical signals into electromagnetic signals and vice versa. They serve as a link between unguided and guided media, facilitating the transmission of signals from the transmitter to the receiver [108]. The antenna performance parameters like wide bandwidth, high gain, high radiation efficiency, low losses, and compactness are desirable for TVWS technology. In TVWS main desirable parameter is compactness with all performance parameters.

1.7 Type of Antennas

The antenna is the main element of any communication system for transmission and reception. Different varieties of antenna are present in today's communication era, as given in Figure 1.4. The analog TV signals were received by the traveling wave antennas, especially the Yagi-Uda antenna. A Log-periodic antenna is also designed at TVWS frequency but again compromises in the size [167]. The frequency of the TV band is small as compared to most of the available wireless devices, so the biggest challenge at this frequency is the larger dimensions. The use of planar technology in antenna design is one method for reducing size [90].

In this thesis, microstrip patch antennas and fractal antennas are used for the TVWS band. The detailed literature survey of microstrip patch and fractal antennas for wideband, reduced size, and high gain is discussed further.
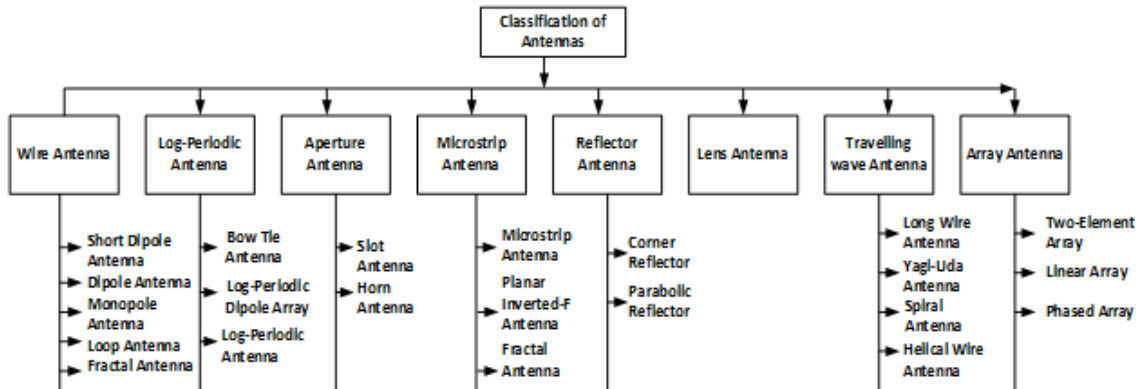
Fig. 1.4 Classification of Antennas

1.8 Microstrip Patch Antenna

A microstrip patch antenna is a popular antenna design utilized in wireless communication systems for its compact size and ease of fabrication. It consists of a thin metallic patch, typically made of copper or gold, that is suspended above the ground on a dielectric substrate. The basic geometry of the antenna is given in Figure 1.5. The patch is typically in the shape of a rectangle, but can also be in other shapes such as circular or elliptical. The diagram also shows the dimensions of the patch, ground, substrate, and the location of the feed line in relation to the patch.
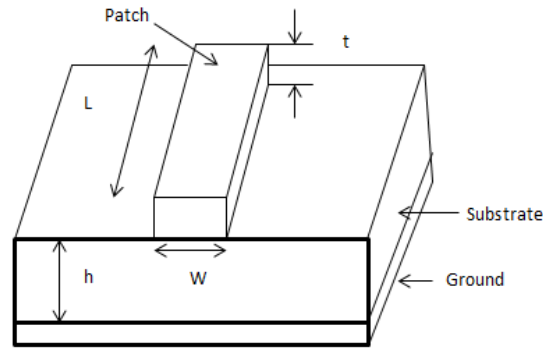
Fig. 1.5 Patch Antenna Geometry

One of the main advantages of microstrip patch antennas is their low profile and ease of fabrication, making them suitable for integration into portable devices and other compact systems. They also have a wide bandwidth and high gain, which makes them suitable for a variety of wireless applications such as mobile phones and Wi-Fi.

1.8.1 Working of Microstrip Patch Radiator

The working of a microstrip patch antenna can be understood by looking at the way it radiates electromagnetic energy. The patch is excited by an electromagnetic wave that travels along the microstrip feed line and is then radiated by the patch in the form of an electromagnetic field. The patch is designed such that it acts as a resonant element, which means that it resonates at a specific frequency. The patch's size, shape, and substrate's dielectric constant should be carefully selected to match the appropriate resonance frequency. The patch is also designed for maximum transfer of power which can be done by proper impedance matching with feed.

The radiation mechanism of an antenna is based on the resonant element. When an electromagnetic wave travels along the feed line and reaches the radiator, it induces surface currents on the radiator. These currents then radiate an electromagnetic field in the form of an electromagnetic wave. The patch antenna's design features a standing wave pattern in the surface current distribution, leading to a specific resonant frequency. The patch also behaves

as a resonant cavity, which means that it has a specific resonant frequency that is obtained by the patch's size, shape, and dielectric constant of the substrate.

1.8.2 Advantages of Microstrip Patch Radiator

The microstrip patch antenna offers several benefits compared to other antenna types:

1. **Low profile and compact design:** Microstrip patch antennas are relatively thin and have a low profile, making them ideal for applications where space is limited.

2. **Lightweight:** The lightweight construction of microstrip patch antennas makes them suitable for use in portable and mobile devices.

3. **Low cost:** Microstrip patch antennas are relatively inexpensive to manufacture, making them suitable for mass-produced consumer devices.

4. **Easy to fabricate:** The widely used and inexpensive printed circuit board (PCB) technology makes it simple to create microstrip patch antennas.

5. **Adaptable:** Microstrip patch antennas can be easily modified to meet the requirements of different applications by changing the size, shape, and material of the patch.

In conclusion, microstrip patch antennas are favored for their low profile, compact design, cost-effectiveness, ease of fabrication, and adaptability, making them suitable for a variety of applications

1.8.3 Drawbacks of Microstrip Patch Radiator

Microstrip patch antennas also have some drawbacks:

1. **Limited operating frequency range:** Microstrip patch antennas are typically only able to operate within a narrow frequency range.

2. **Low power handling capability:** Microstrip patch antennas are not able to work at high power levels which makes them less appropriate for some applications.

3. **Low efficiency at higher frequencies:** Microstrip patch antennas have lower efficiency at higher frequencies, which can lead to reduced performance.

4. **Sensitivity to substrate properties:** Microstrip patch radiators are sensitive to the substrate selected on which they are mounted, which can affect their performance.

5. **Low radiation resistance:** Microstrip patch antennas have low radiation resistance, which means they can transmit and receive signals with minimal loss.

6. **Limited radiation pattern:** Microstrip patch antennas have a limited radiation pattern, which means they can only transmit and receive signals in a specific direction.

7. **Coupling effect:** Microstrip patch antennas are prone to the coupling effect which leads to reduced performance.

8. **Low Gain:** Microstrip patch antennas are having low gain because of their small size, small aperture, small active area, low profile, and shape of the patch.

9. **Narrow bandwidth:** Microstrip patch antennas have a relatively narrow bandwidth compared to other types of antennas due to their small size, high Q-factor, and simple structure.

In summary, microstrip patch antennas have a limited operating frequency range, low power handling capability, low efficiency at higher frequencies, sensitivity to substrate properties, low radiation resistance, limited radiation pattern, and coupling effect.

Overall, microstrip antennas are a common choice in wireless communication systems due to their versatility and positive impact on antenna performance. They have a proven track record of success in a variety of wireless applications and continue to be an important area of research and development in the field of antenna design.

1.9 Fractal Antenna

Fractals are shapes that repeat themselves in a given space by the method of iterations. The study of natural patterns served as the primary inspiration for the creation of fractal geometry. Benoit Mandelbrot, a renowned Polish mathematician known as the father of fractal geometry, recognized that traditional Euclidean geometry was not sufficient in describing the complex shapes and structures found in nature. He suggested that fractal geometry, which allows for non-integer dimensions and can be used to quantify the space occupied by a fractal, could be used to better understand real-world objects. While fractals can be observed in nature, they can also be generated through mathematical formulas. These shapes cannot explain with the help of any conventional mathematical equations. These geometries can be solved by iterative function methods (IFS). Fractals are having numerous advantages that why this type of structure catches the interest of antenna designers. Fractal properties are utilized by antenna designers to increase the gain and bandwidth of the antenna. When the number of iterations of any fractal antenna is increased its electrical length increases which gives a size reduction of the antenna geometry. Multiband and wide bandwidth can also achieve through fractal. In this thesis, fractal design is used to get multiband and size reduction.

Antenna design is constantly evolving, with engineers constantly looking for ways to improve performance. Maximizing bandwidth and gain while reducing antenna size is a key objective in antenna design. This requires engineers to think creatively and explore new ideas to push the boundaries of what is possible with antenna technology. A detailed literature survey of fractal antennas has been done in the next section of the chapter Fractals properties can be used to design a compact, multiband, and high gain antenna. elements.

1.9.1. Properties of Fractal Antenna

Fractal antennas are a type of antenna that are characterized by their fractal geometry, which is a type of geometry that is characterized by self-similarity, meaning that the same patterns repeat at different scales. Fractal antennas are appreciated for their versatility, as they can effectively work across a broad spectrum of frequencies, thus making them a suitable choice for a variety of applications.

1. **Wide Bandwidth:** Fractal antennas have a wide bandwidth, meaning that they can operate over a wide range of frequencies. This is due to their fractal geometry which allows them to radiate energy over a wide range of frequencies, as the fractal element resonates at multiple frequencies.

2. **Compact Size:** Fractal antennas are typically smaller in size compared to other types of antennas, which makes them suitable for use in portable devices and other applications where size is a constraint.

3. **Multi-Frequency Operation:** Fractal antennas are created with the capability to function at multiple frequencies, which makes them a suitable option for applications where there is a need for frequency hopping, such as in wireless communication systems.

4. **Low Profile:** Fractal antennas have a low profile and can be integrated into a variety of devices, which makes them suitable for use in applications where the antenna needs to be hidden or embedded.

5. **High Gain**: Fractal antennas have a high gain, meaning that they can direct and amplify the radio frequency (RF) energy that they transmit or receive.

6. **Low Cost**: Fractal antennas are relatively low-cost to manufacture, which makes them

suitable for use in a variety of applications where cost is a constraint.

In summary, Fractal antennas are known for their wide bandwidth, compact size, multi-frequency operation, low profile, high gain, and low cost. They are suitable for many different types of applications, such as wireless communication systems and portable devices

1.9.2 Types of Fractal

Fractal antennas can be classified based on their geometry, dimension, and generation method. Some of the main types of fractals include:

- ✓ Sierpinski Gasket
- ✓ Sierpinski Carpet Geometry
- ✓ Koch Fractal
- ✓ Cantor Set Geometry

1.9.2.1 Sierpinski Gasket Geometry

Sierpinski gasket fractal geometry is shown in Figure 1.6. This structure is constructed by dividing the geometry in the same fashion. In Sierpinski first, a triangle is taken. After the middle point, all the sides of a triangle are joined to form a triangle in the middle as shown in the figure. Now this triangle is removed from the main triangle. The final geometry is formed by performing this iterative process number of times [152].
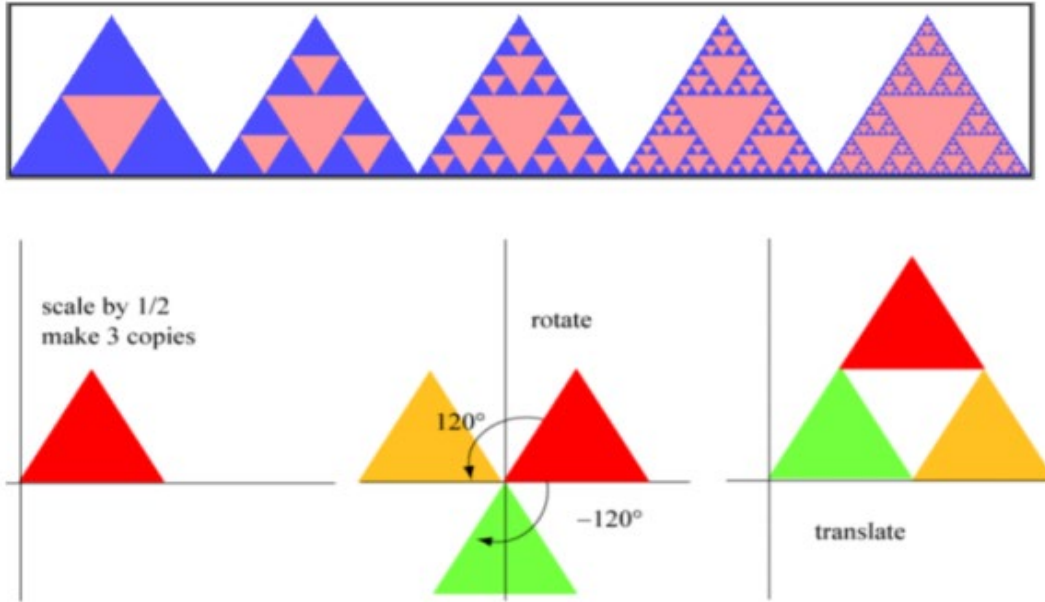
Fig, 1.6 Iteration steps of Sierpinski gasket

1.9.2.2 Sierpinski Carpet Geometry

The Sierpinski carpet is depicted in Figure 1.7. It is similar to the previous fractal. The difference is the shape only. In Sierpinski gasket, iteration starts from a triangle but this iteration starts from a square. This method of dividing a square into smaller congruent squares, subtracting the center square, and repeating the process is a fractal pattern known as the Sierpinski carpet. It is a famous example of a fractal and can be generated by a process of recursive division and subtraction. The pattern can be visualized by starting with a large square, dividing it into smaller congruent squares, and then repeatedly removing the center square at each level of division. As the process continues, the remaining squares will form a fractal pattern.
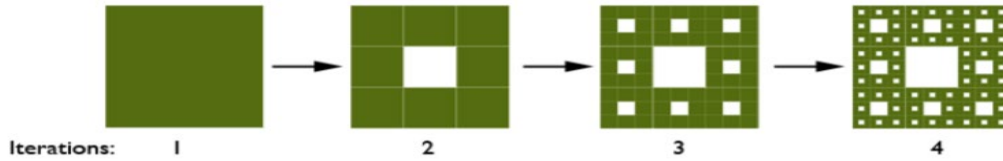
Fi, 1.7 Iteration steps of Sierpinski Carpet

1.9.2.3 Koch Curves

The Koch snowflakes geometry is shown in Figure 1.8. It is a fractal pattern that starts with a straight line and then repeatedly replaces the middle third of each line segment with a triangular "bump" made up of four smaller line segments. This creates a fractal pattern that is characterized by an infinite perimeter with a finite area. The fractal has a Hausdorff dimension of log4/log3, which is greater than its topological dimension of 1, meaning it takes up more space than a one-dimensional object.
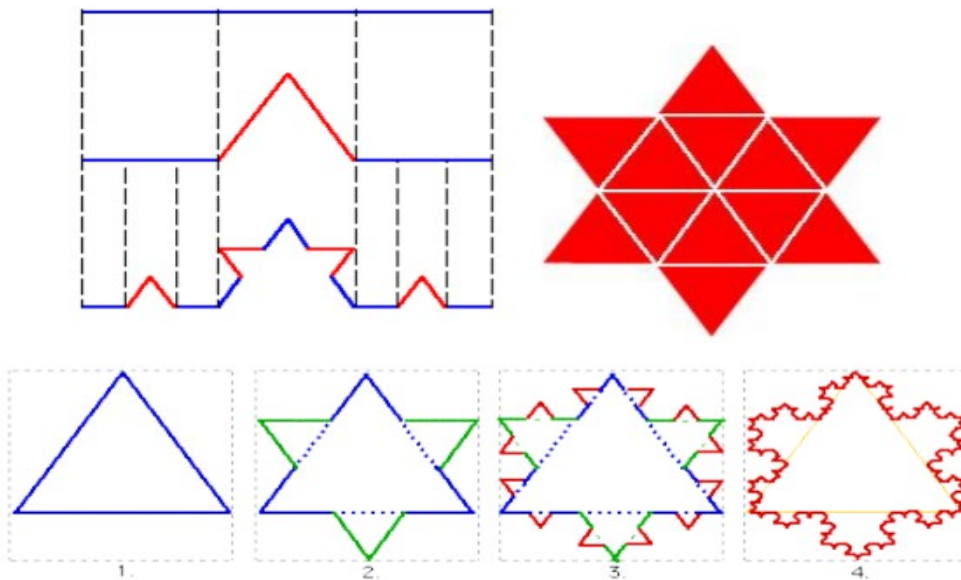
Fig.1.8 Iteration steps of Koch Fractal

1.9.2.4 Cantor Set Geometry

The Cantor Set is shown in Figure 1.9. It is a fractal pattern that starts with a simple straight line and repeatedly removes the middle third of the remaining segments. This is done by dividing the line into three equal parts and removing the middle one, then repeating the process on the remaining segments. It is one of the first fractal sets to be described and studied, and it has many interesting properties including being a perfect set and having a Hausdorff dimension of log2/log3.
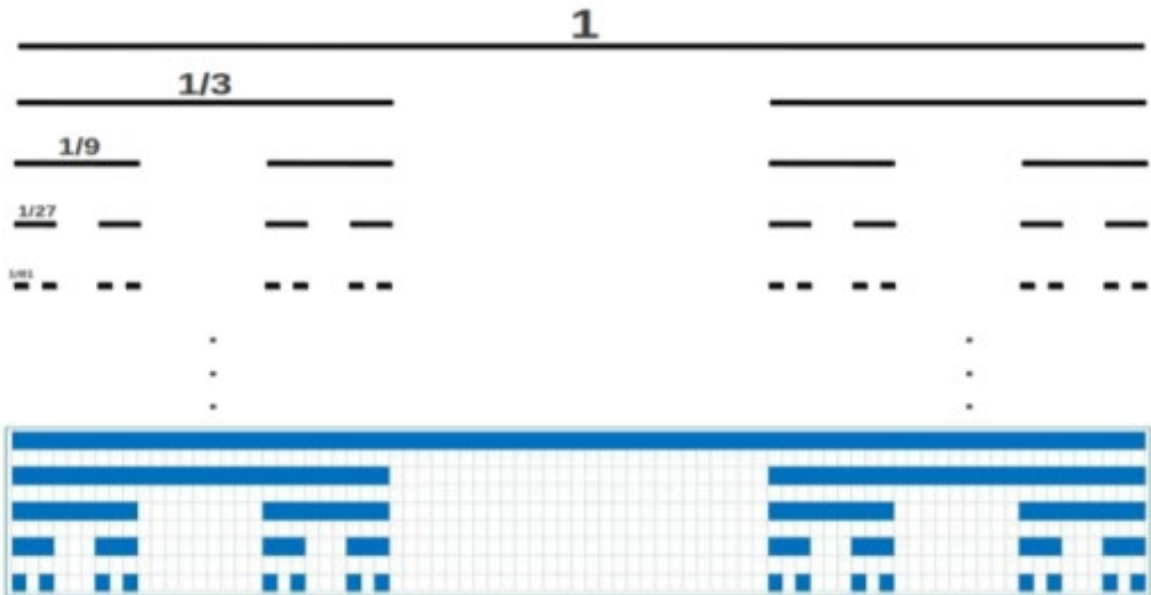
Fig. 1.9 Iteration steps of Cantor Set

1.10 Literature Survey

S. A. Long and M. D. Walton [97], 1979 have experimentally investigated the behavior of two stacked circular disk antenna. Coaxial feed is given to the lower dish to get desired dual frequency and the upper circular patch is connected electrically with the lower one. Practically two circular patches are photo-etched on separate PCB and then carefully aligned. The size of both discs and their spacing are varied and noted down their impact on resonant frequency.

B. B. Mandelbrot [104], in 1983 described that sometimes it is impossible to describe any object using mathematical equations. All the shapes cannot explain using Euclidean geometry. So, he proposed fractal geometry to describe such types of objects.

J. S. Dahele, K. F. Lee, et al. [41,110,98,191,53,142,197], in 1987-1997 proposed a dual frequency operated circular patch antenna, a square microstrip patch antenna, and a slotted patch antenna that can work on two frequencies. The first resonance frequency and radiation pattern are not affected by these slots, but new resonance frequencies with similar radiating properties are introduced by them. This new resonance is dominated by the slot length, which is equal to the patch length. A small circular patch antenna with a shorting post, a slotted patch antenna with a short at the ground, a rectangular and trapezoidal microstrip patch antenna with a short at one end, and a circular, compact meander patch antenna were also proposed by the authors. An increase in the slot length has been demonstrated to decrease antenna resonance. The author's findings indicate that the trapezoidal patch antenna is more compact than a conventional rectangular patch antenna, as determined by their comparative performance.

N. Cohen [40,71,38,39], in this series [1995-1996] of a paper first wire antenna is designed using fractal shapes. An innovative method being investigated is the implementation of fractal

shapes to traditional dipole or loop antennas. The procedure entails carefully converting the wire into a fractal shape, without changing the total wire length while decreasing the size through each iteration. Studies have demonstrated that this technique, when executed accurately, results in the creation of highly efficient and compact antenna designs.

C. Puente et al. [134,132,135,131,172,147,22,126,73,10,170,173,193,78,11,119,130], in 1996-2001 a multi-band fractal monopole Sierpinski gasket and its radiation characteristics at the on-flare angle were documented. A further performance was enhanced using perturbations in the fractal geometry. The multi-hand approach was discussed using Mod-P Sierpinski gaskets. The concept of utilizing fractal geometry in antenna design has been explored in various studies. This approach involves bending the wire of a standard dipole or loop antenna in a fractal pattern, resulting in efficient miniaturized designs. Computationally efficient methods, such as iterative network models and the method of moment formulation, have been developed to predict the performance of fractal antennas, including the Sierpinski fractal. Dual-band designs and specific applications to emerging technologies such as GSM and DECT have also been presented. Additionally, novel configurations such as the shorted fractal and bowtie patch antennas based on the Sierpinski-gasket techniques have been discussed in the literature.

Sir J. B. Pendry et al. [124], in 1998 Veselago's idea was used for the first time in the form of an artificial material with negative permeability. After that, work was started in this direction to observe the material properties. The first artificial material of this type was fabricated using a split ring resonator (SRR) with wires. When light passed through a prism made of metamaterial, the light showed a bend. The materials made with the help of SSR and copper wire, which showed negative permeability and negative permittivity, are called metamaterials. Pendry demonstrated that a medium formed by a periodic structure of copper wire behaves as

a homogeneous material, whereas a medium formed by a split ring resonator has negative permeability.

C. Puente et al. [124,166,194,171,96,133], in this series [1999] of work fractal trees were designed for multi-band operation. In this property, fractal tree antennas were created and analyzed. It was investigated that tree fractals were better than Sierpinski in terms of multi-band operations. The impedance of the tree fractal antenna was investigated using numerical simulation methods and results were compared with measured results. After that stacking was used in the Sierpinski carpet to get a wide band. The results gave a better impedance match over the 1-20GHz band.

C. Puente et al. [23,177,146,55,192,74,183] in 2000-2001 the Koch fractal monopole was discussed in this work. It was observed that the Koch fractal antenna had a good electrical performance as compared to other straight fractals. As the number of iterations increased, the Koch fractal electrical length increased along with the size reduction. A method for enhancing the multi-frequency nature of the antenna's gain by reducing the impact of higher-order modes was introduced. The ability to achieve high levels of directivity in a fractal patch antenna using the Koch-island design was also demonstrated.

Shelby Smith and Schultz [161], in 2001 invented the split ring structure that has been used to prove the existence of metamaterial. The authors proposed the first left-handed metamaterial and demonstrated the property of the negative reflection coefficient. In a parallel plate waveguide the authors have placed a prism-shaped metamaterial structure.

J. Anguera et al. [9], in 2002 a unique approach to designing a shorted fractal Sierpinski gasket antenna was discussed. In this way hand ratio of less than 2 was achieved between the 1st and

2nd iterations. For compact radiators space-filling properties of the Hilbert curve were investigated. The feeding affects the input impedance of the proposed design. Careful consideration of the feeding method is crucial when designing and evaluating the performance of the proposed antenna.

Chakravarty, T., & De, A. [32], in 2002 presented an empirical formula for the impedance of metallic post. The accuracy of a circular microstrip patch antenna with shorting post depends on the exact position of shorting post in the radial guide. The proposed empirical formula considers the edge effects into account and gives an accurate formula for all the eigenmodes of shorting posts. The earlier analyses failed to predict the significant decrease in resonance when the shorting post is located near the periphery of the patch. Integral equation/FDTD methods are very accurate but numerically intensive. This results in a simplified and quite accurate model of a shorting-pin-loaded circular patch, which can predict the resonance for all cases within reasonable limits.

Richard W. Ziolkowski [209], in 2003 a new way of creating a metamaterial with a negative index of refraction was suggested. The material consists of a substrate with capacitive loaded strips (CLSs) and square split ring resonators (SRRs) embedded in it. The CLSs offer a strong dielectric response, leading to negative permittivity, while the square SRRs provide a strong magnetic response, contributing to negative permeability. The result is a frequency range where both the effective permittivity and permeability are negative, producing a negative index of refraction.

Guo, Y.-X., et al. [66], in 2004 proposed a circular patch antenna having a conical pattern with an L-shaped probe feeding technique and which can be used for wide-band operation. Bandwidth was limited if the coaxial cable is used with a thick substrate due to cable inductance. This inductance can be compensated by using an L-probe feed with the patch which acts as a short circuit stub. But the proposed antenna is having a large size.

R. Moussa et al. [109], in 2005 triangular array structure of rectangular bars was used with a photonic crystal. The experimental results show the negative refraction and support super lensing property of metamaterial.

D. R. Smith et al. [153], in 2006 realized the first real invisibility cloak at microwave frequencies. However, only a very small object was imperfectly hidden. The cloak structure was designed using artificial metamaterials. These structures reduce the scattering of signals and their shadow and by doing so cloak and object combined begin to resemble free space.

Guha, D., & M. Antar, Y. M. [64], in 2006 a unique design for a circular microstrip patch antenna was introduced. This design featured two shorting pins, positioned at the center of the patch to increase the impedance bandwidth without negatively impacting the gain or radiation characteristics of the antenna.

Raghava, N. S., and A. De [137], in 2006 proposed a stacked microstrip antenna for road vehicle communication. The antenna featured a shorting post on the slotted ground and was made up of two stacked rectangular patches on the substrate. The ground plane was etched with a rectangular hole, which acted as an EBG structure. This structure improved the antenna's efficiency by suppressing surface waves and increasing gain. It was found that this PBG structure significantly improved the antenna's efficiency.

M. J. Facchine & D. H. Werner [56], in 2006 research was conducted on fractal spheres and their effect on backscattering cross-sections. These fractals' self-similar geometrical structure was found to provide a distinctive multiband response. This was attributed to the fractal geometry, in which the structure's various self-similar components resonated at various frequencies. Additionally, it was discovered that fractal spheres have backscattering characteristics that are comparable to both solid spheres and linear dipoles. Furthermore, it was shown that fractal spheres of the same physical size have a lower resonance frequency than solid spheres of the same size. In particular, it was discovered that the third iteration of the fractal sphere exhibited low-frequency resonance behavior resembling that of a solid sphere half its size.

Bhattacharya, M. [27], 2007 describes the use of a slot patch antenna for compact and broadband operation. The band frequency is adjusted by altering the position of the shorting pin. It was discovered that the first resonant frequency increases but the second resonant frequency decreases with the movement of shorting post from the edge to the center of the patch.

R. Abdullah, D. Yoharaaj, and A. Ismail [4], in 2008 air as a substrate is chosen in the proposed design with a lower relative permittivity. With IDMA and an air gap, a bandwidth of 287.77 MHz (11.794%) with an S_{11} value of -15 dB is measured. However, employing a single-layer microstrip antenna, a bandwidth of 41 MHz (1.4699%) (measured) with an S_{11} of -26 dB is produced. The IDMA's VSWR value is less than 2. The IDMA-obtained bandwidth can be applied to WLANs.

N. S. Raghava and Asok De [138], in 2008 proposed a unique, two-layer, extremely efficient patch radiator in the shape of an E. The size of the initial rectangular patch is decreased by

changing its shape and adding two slits. By stacking E-shaped patches, the size is further reduced. This redesigned antenna has a 16% boost in efficiency and gain. Additionally, it has been found that adding an EBG structure increases the antenna's bandwidth by about 10.5%.

U. B. Yeo, and J. N. Lee [200], in 2008 proposed a trapezoid Sierpinski sieve fractal for ultra-wideband application. This antenna may be employed for UWB applications due to its wide frequency range and excellent impedance matching. Over the whole frequency range, the pattern of the suggested antenna is like a figure of eight, and gain varied from 2-4dBi.

Dalia Nashaat, Hala A. Elsadek [111], in 2009 proposed an antenna layout with two cells etched out in a spiral pattern from the ground plane and an antenna that resonates for five different frequencies resulting in a 50% size reduction.

Al-Zoubi, Asem, et al. [7], 2009 proposed a patch antenna with an annular ring coupled with a circular patch. The coaxial cable at the center is used for feeding. The proposed antenna gives monopole radiation in a complete operational band and has a low profile.

Yong-Xin Guo, & Tan, D. C. H. [201], in 2009 proposed a wideband single-feed CP patch antenna. The radiation pattern of the antenna is conical. The impedance bandwidth of less than 10dB is 63.91%, and less than 3 dB bandwidth is 10 %.

 Prombutr, N., Kirawanich, P., & Akkaraekthalin, P.[129], in 2009 a technique for boosting bandwidth was presented for the design of small antennas employing a changed ground plane. The main patch is introduced with an L-shaped slot, with parasitic patches electromagnetically coupled with it.

Asok De, N.S. Raghava [50], in 2010 different substrates have been used to study various CSSMA properties. It is discovered that specific antenna requirements can be satisfied by

choosing an appropriate substrate. Among the seven dielectrics used in CSSMA, Roger's 4350 is the most effective, and it also has a good gain and directivity value for usage in WLAN and road vehicle communications.

G. Konstantatos, C. Soras [86], in 2010 revealed a brand-new monopole antenna element that was printed on a wireless device's circuit board. The suggested antenna is a combination of Minkowski fractal curve and folding techniques which give wider bandwidth and compactness. To ensure antenna variety under all combining methods, it can be employed in portable devices operating in the 2.4 GHz band because of its small size. Finite element simulations, which were more computationally intensive than their moment method counterparts, were used to forecast the performance of the tested configurations.

Chen, S., Yang, X., & Sun, H. [35], 2011 proposed a circular microstrip patch antenna for satellite application. The proposed antenna is fed by an arc network. A circular parasitic patch is placed over the driven patch. A circular slot in the center of the parasitic patch is made and two convex rectangular slots on the edge are also placed on the driven patch to improve impedance matching, bandwidth, and axial ratio.

M. Ali, H. Jaafar, and A. Yusof [6], in 2012 the effect of air in the substrate between the ground and the radiating patch is explained. Thus, a gain of 14.62 dBi, suitable for 5G applications, is attained. The air gap approach also increases bandwidth.

Patel, Jigar M., et al. [120], 2012 proposed an S-shaped slot on a patch. By introducing an S-shaped patch Antenna starts to resonate for 3 different frequencies. The proposed antenna will now start working for multi-frequency and hence bandwidth is increased.

Shivkant Thakur, Rajesh Kumar Vishwakarma [180], in 2013 a new design of an antenna featuring L-shaped slots on a patch was proposed. This design resulted in a 6% increase in bandwidth and is suitable for use in C-band applications,

Gupta, Sakshi, et al. [67], in 2013 H-shaped slot antenna design, when paired with a defective ground structure (DGS), offers a wide frequency range, making it suitable for use in radar systems is proposed.

Sabapathy, T., et al. [150], in 2013 proposed a CMSA with infinite ground plane. A parasitic ring is used beside the patch and coaxial feed is used for feeding. The author investigates the performance of the proposed antenna with a conventional circular patch antenna. It found that gain enhancement is achieved by the introduction of a parasitic ring. The suggested antenna can be used in point-to-point communication.

Sergey S. Kurk et al [169], in 2013 metamaterials with three different symmetries—square lattice, hexagonal lattice, and quasi-crystalline Penrose tiling were shown both physically and conceptually. We establish a connection between the symmetry characteristics and the far-field optical response, including ellipticity and circular dichroism, when the incidence angle changes by using an advanced Jones calculus.

J Kandwal and S. Khah [79], in 2013 a unique design suggested that bandwidth improvement might be attained by angling the patch 45 degrees outward. It is demonstrated that even if numerous resonance frequencies are produced, the patch bandwidth acquired in the stationary situation is 1.6%. By relocating the patch 20 mm with a return loss value of -17 dB, bandwidth increased from 1.6% to 12.6%. However, by shifting, the side lobe has decreased to -15 dB while the patch directivity has increased to 15 dBi. When the patch is moved farther than 20

mm from the center, the radiation efficiency decreases. Wideband wireless applications can use this antenna.

Ke Li et al. [95], in 2014 two innovative metamaterial antennas for WLAN and WiMAX were proposed. Antenna 1 is made up of an electric monopole radiator, and Antenna 2 is integrated with an EBG structure with good impedance matching. The suggested antennas' easy fabrication, downsizing, and compactness make them suitable for use in wireless mobile communication systems.

Wang, B., Zhang, F., Li, T., Li, Q., & Ren, J. [187], 2014 developed a planar antenna for mobile communication that comprises four pairs of arc dipoles. A balun is used to change an unbalanced signal into a balanced one, and a ground conductor is used to improve gain. Antenna prototypes are constructed and measured. According to the measurement results, the suggested antenna can cover the GSM, PCS, and UMTS bands with a bandwidth of 34.1%. and a return loss of more than 10 dB. Additionally, the suggested antenna has a radiation efficiency of over 81% and a peak gain of 3.4–4.2 dBi during the operational bandwidth.

Tej Raj Sharma, and Arjun Singh [160], in 2015 proposed to create a patch with double U and H slots that resonate at triple band frequencies and have superior impedance matching for WiMAX and WLAN applications.

Dawar, Parul, et al. [47], in 2015 a unique metamaterial called Closed Ring Pair is described (CRP). Designing and analysing the MTM with Mylar (r = 2.89) as the substrate material was done using Ansoft HFSS. The Nicolson Ross Weir (NRW) method was used to recover μ_r and ε_r from S_{11} and S_{22} coefficients to mathematically depict the negative permeability area using

CRP MTM's magnetic properties. The resonance frequency was determined through modeling to be 30.55 THz.

Parul Dawar , Asok De, and N. S. Raghava [44], in 2016 a design for a brand-new μ_{-ve}, Split Ring Resonator antenna has been presented. Ansoft HFSS version 13 is used to develop the microstrip patch antenna. MATLAB programming based on CAD formulas was used to compare the results with patch antenna equivalent circuit analysis. The material properties have been retrieved using the NRW method from the transmission and reflection coefficients. A microstrip patch antenna based on metamaterials has then been created. This research proposes a novel design that offers notable improvements in bandwidth, directivity, and front-to-back lobe ratio but at the expense of a lower antenna gain.

Yoo, Sungjun, et al. [202], in 2016 Patch antennas with parasitic elements were proposed to modify the polarisation characteristics. The number, length, and angular positions of the parasitic elements that surround the circular radiating patch of this structure were changed to change the axial ratio and orientation angle. The outcomes show that tweaking the parasitic elements allowed the suggested antenna to change the orientation angle and axial ratio.

Anuradha, K., & Karmugil, M. [13], 2016 proposed a circular microstrip patch antenna with a partial ground technique. By introducing partial ground in the design, the design can be used for enhanced radiation characteristics and it gives three resonant frequencies.

Pragya Shilpi, and Dharmendra Upadhyay [164], in 2017 proposed a patch antenna with five slots at the ground plane has five slots. Antenna resonance is detected in the C band and X band frequencies; at 8.9 GHz, a 95% bandwidth enhancement is noted.

T. Ara Nayna, F. Ahmed, and E. Haque [112], in 2017 it was observed that due to a defective ground structure, it is now evident that the bandwidth has increased from 478 MHz to 512 MHz in 2017. The VSWR value for the ground structure with the flaw is almost 1, compared to 1.125 for the ground structure without the problem. The directivity of this antenna was good at the resonance frequency of 10.25 GHz. This antenna can be used for UWB purposes,

S. Kulkarni and V. Kasabegoudar [199], in 2017 multiple antenna designs with different shape slots have been presented. A single ring with a defective ground structure is used. Here, it is shown that the resonance frequency for such designs is falling. Although the proposed design's resonance frequency is the lowest, its bandwidth and VSWR are superior to those of other designs. Due to a flawed ground structure, the final bandwidth of 9.2 GHz—which is higher than the original design—was achieved. This antenna is appropriate for use with UWB technology.

R. Shah and P. Prajapati [157], 2017 proposed that bandwidth is a function of the number of slots introduced in the patch. But when the number of slots increases, the radiation efficiency falls. Therefore, there is a trade-off between the number of slots and radiation efficiency. Due to the slot antenna's lower radiation efficiency, the gain is also lower. This antenna can be used with WLAN and Wi-Fi apps.

Lai, H. W., Xue, D., Wong, H., So, K. K., & Zhang, X. Y. [94], 2017 proposed a 3D M-Probe feeding system for the substrate-integrated antenna. This feeding method offers broadband circular polarisation and wide impedance bandwidth. The author also discusses the array's construction and the proper sequential rotation-feeding method. The techniques can provide some helpful references for the circular polarisation multi-layer PCB array design. The

proposed antenna array can accommodate the Ku-band satellite TV application and the OTM antenna system's applied bandwidth.

Abdullah- Al- Mamun, M., Datto, S., & Rahman, M. S. [3], 2017 presented a study of performance parameters of different shapes of the patch antenna. The designed antenna is fabricated on FR4 with coaxial feed. The antenna is designed for C-band frequencies with resonance at 5 GHz. The antenna is simulated on HFSS for the parametric study of different shapes. It is found that all patches' resonance peak is exactly at 5GHz. It is found that the elliptical patch is better than the two other patches except for bandwidth. The bandwidth of rectangular patches is higher than that of circular and elliptical patches.

M. Harinath Reddy, R. Joany, and M. Reddy [144], in 2017 the effects of parasitic patch on the bandwidth and VSWR was explained. The bandwidth was improved from 299MHz to 557MHz and VSWR remained less than 2 for a gain of 5.35dBi due to parasitic patches. The designed antenna is suitable to work in X-band frequencies.

Kaul [120] in 2018, it was hypothesized that the growth of parasitic patches was causing the bandwidth to expand. It is demonstrated that a single parasitic patch increases bandwidth by 197 MHz with a VSWR value under 2. When four parasitic patches were employed with VSWRs under 2 and gains of 9.02 were achieved, the bandwidth was raised to 944 MHz Even though using the parasitic patch increases radiation efficiency, it also causes the antenna to grow in size, which is a drawback. Higher radiation efficiency led to a higher gain.

Xu, Kai D., et al. [198], in 2018 demonstrated two unique triangular patch antennas with shorting vias. By adding short vias, more resonance can be attained, resulting in a wider bandwidth. The proposed antenna takes advantage of several parasitic patches to provide an

effective far-field radiation pattern. Inserting two shorting vias will enhance bandwidth even more.

Fangzhou Guo et al. [65], in 2018 a metamaterial transmission line (TL) with improved design freedom is presented. The top and bottom metal plates are etched with interdigital fingers and rectangular slots, which provide series capacitances and shunt inductances to create the composite right- or left-handed (CRLH) attribute.

Parul Dawar, Asok De, and N. S. Raghava [45], in 2018 a S-shaped metamaterial incorporated in an antenna substrate is shown for optimizing antenna parameters. The suggested metamaterial array is included in the antenna substrate, increasing the antenna's bandwidth by 74% and its directivity by around 11%. The development of the "S-shape" has been detailed, starting with the one SRR. When the suggested structure was built, an almost 6-percent departure from the simulation results was recorded. By achieving 81% downsizing, this metamaterial antenna overcomes the patch antenna's limited bandwidth restriction and aids in keeping a low profile.

Parul Dawar, N. S. Raghava, and Asok De [48], in 2019 a 2-segment SRR Labyrinth metamaterial implanted inside the antenna substrate of a unique patch antenna inspired by metamaterials. It is noted that the antenna is 400% smaller, and the VSWR improves by about 1.5% after inclusion. The bandwidth also widens by about 600%. From the transmission and reflection coefficients, the material parameters have been retrieved using the Nicolson-Ross-Weir (NRW) method.

A. Bakhtiari, R. A. Sadeghzadeh & M. Naser. Moghadasi [48], in 2019 suggested a magnetic material substrate and superstructure for a high-gain miniature microstrip patch

antenna. An engineered magnetic material with electric-LC resonators in the substrate layer and a second kind of Hilbert fractals in the substrate was employed to achieve high permeability and permittivity. According to simulation and test data, the shrunk antenna at 534 MHz has a gain enhancement of 8.1 dB and a miniaturization factor of 4.8. Additionally, employing superstrate results in patch size being less than resonance frequency, and antenna size is reduced to 170 X 170 X 37 mm3. Due to the loading impact of these layers, a modest shift in the resonance of the antenna with superstrate layers has been seen in the improved design.

Xiufang Wang et al. [190], in 2019 for effective wireless power transfer (WPT) using magnetic resonant coupling, a spiral superconducting metamaterial with an effective negative permeability is presented. The simulated results demonstrate that the superconducting metamaterials can significantly increase the system's transfer efficiency through enhanced evanescent wave coupling and lower loss characteristics.

Sindhu Kotla et al [87], in 2019 a circular polarization compact patch antenna is recommended for S-band. Circular polarization is accomplished using metamaterial and defected ground structures (DGS). In comparison to a standard CP antenna, the suggested antenna is 44.7% smaller and exhibits good circular polarization at 2.36 GHz.

M. K. Verma, Binod K. Kanaujia [182] in 2019, the circularly polarized, gap-coupled wideband microstrip antenna is given a revolutionary ground structure design. This antenna has orthogonally placed slits in the ground plane. The suggested antenna's impedance bandwidth of less than 10dB and axial ratio bandwidth of less than 3dB are 8 GHz (57.33 %) and 13 GHz (28.64 %), respectively. The peak gain is 4.08 dBi, and it varies over the entire axial bandwidth from 3.83 to 3.76 dBi.

Mohd Gulman Siddiqui et al. [165] in 2019, to lessen the impact of surface currents, a design was presented that applies the combination of the Koch fractal and Sierpinski gasket concept to its outer and interior segments respectively. The suggested antenna covers applications in the C, X, and Ku-band. The Fr4 substrate produced the greatest results when compared to the results of the proposed antenna when three different substrates (Rogers RO 4003, Rogers Ultralam, and Fr4) were used. The simulation and the results of the experiment were in good agreement.

Nigar Berna Teşneli et al. [179], 2020 introduced a small microstrip patch antenna with DGS on the back and EBG on the front. With EBG on the front and regularly etched DGSs on the back, the microstrip patch antenna's gain and directivity values are increased by around 23%, and its bandwidth is increased.

Sonal Gupta, Binod Kumar Kanaujia [68] In 2020, a square patch with inclined fractal defected ground structure patch with circular polarization was proposed. An angled fractal-shaped slot implanted along the ground plane's diagonal axis produces the CP radiation. The third iteration of the IFDGS in the CP antenna is constructed and measured. The suggested antenna's overall dimensions were 41 by 41 by 1.6 mm3, and it produced CP radiation at 2.61 GHz. It displays axial bandwidth of less than 3 dB at 1.14% at the resonance frequency of 2.61 GHz and an impedance bandwidth of less than 10 dB at 5.53% at the resonance frequency of 2.6 GHz. The peak gain is obtained as 4.12 dBi.

Ashwini Kumar and Amar Partap Singh Pharwaha [88], in 2020 presented a modified Hilbert antenna with the parasitic patch for multiband applications. The dual-layer substrate for the fractal antenna has dimensions of 50 x 60 x 3 mm, and feed is provided by the modified coplanar waveguide. The proposed design exhibits four resonance peaks at 0.315 GHz, 3.220

GHz, 2.955, and 1.94 GHz. At all resonant frequencies, the suggested antenna shows a greater level of impedance matching and a consistent omnidirectional radiation pattern.

Kattimani, B., Patil, R.R [181], in 2021 a Sierpinski gasket fractal concept for a microstrip antenna is proposed. It is based on an iteration algorithm with up to three iterations and uses the self-similar quality of fractal geometry. It is possible to increase bandwidth to 980 MHz with a decrease of return loss from -31.97 to -23.4 dB. Feeding is provided by microstrip line feed. In the antenna, a fractional bandwidth of up to 27% has been attained. This antenna can be utilized for several wireless applications.

1.11 Antenna Design Methodology

The design methodology followed in this thesis is shown in Figure 1.10. Following are the steps used to design an antenna:

➢ Study the literature on various microstrip configurations with a mathematical design. After that, depending on the application, resonance frequency, the substrate used, and the height of the substrate, a decision is made.

➢ Mathematical modeling of a patch antenna is done to calculate design parameters.

➢ Different gain and bandwidth enhancement techniques are employed with the basic design.

➢ The designed antenna is analyzed using the simulation software HFSS.

➢ Parametric analysis is done to find the optimized dimensions of the antenna.

➢ If results are desirable, fabrication of the design is done in the fabrication lab.

➢ Testing and measurement of the proposed design are done using a network analyzer.

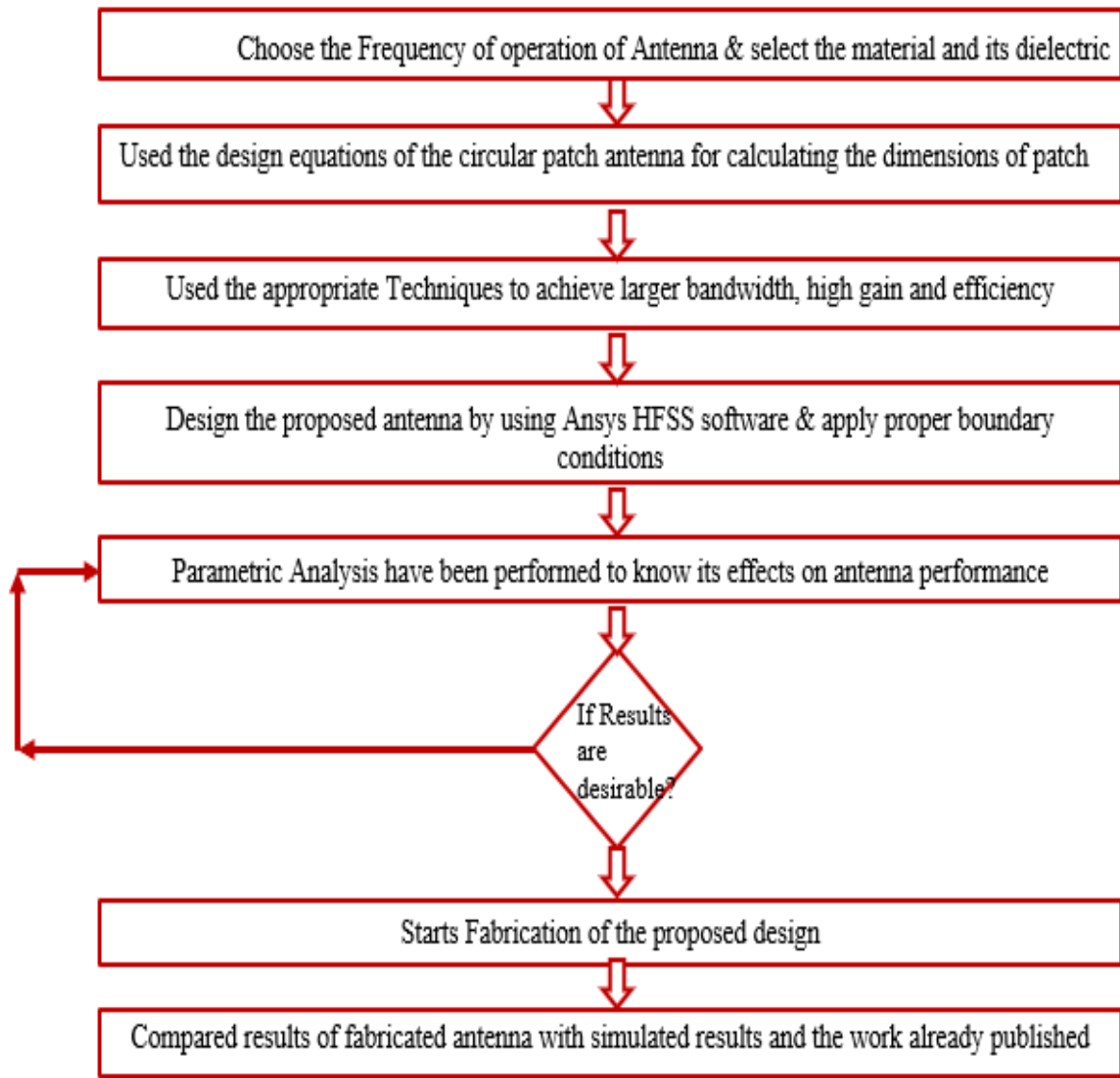➢ In the last, results have been compared with fabrication results.

Figure 1.10 Antenna Design Methodology

1.11.1 Organization of Thesis

This thesis is divided into six chapters. A brief description of each chapter is given below:

Chapter 1: In the first chapter of the thesis, the concept of the white space TV band and the TVWS technology is briefly introduced, including the rationale behind the need for TVWS and the specific spectrum requirements for a TVWS antenna. The chapter also provides a short overview of the antenna design approach used in the thesis, along with a review of existing research on enhancing gain, and bandwidth, and reducing the size of antennas. This introductory chapter sets the foundation for understanding the work presented in the rest of the thesis.

Chapter 2: In Chapter 2, a compact circular patch antenna was designed for RFID applications for India, where the frequency band is 865-867 MHz with 2MHz bandwidth. The proposed antenna, built on FR4 substrate, had four concentric rings and a shorting pin connecting the patch to the ground. The antenna had a gain of 7.5dBi and a directivity of 9.9 dB. It operated on two bands, 479-492MHz, and 643-653MHz, with bandwidths of 13MHz and 10MHz respectively, and return losses of -29dB and -14 dB. The proposed antenna had the lowest VSWR of 1.07 compared to other commercially available RFID antennas and an increased bandwidth of 13 MHz compared to 3MHz. The compact size, gain, bandwidth, VSWR, front-to-back ratio, and limited ground size made the proposed design a good candidate for RFID applications.

Chapter 3: Building on the previous chapter, another circular microstrip patch antenna with three circular rings was designed. The first design had desirable gain and multiband capability but limited bandwidth. Adjusting the ring position and ground plane size improved the antenna for use in the entire TV band with low gain. The three rings, with frequencies of 500 MHz, 700 MHz, and 900 MHz, combine to provide wide bandwidth when embedded in a patch with a finite ground plane. Although this increased bandwidth, it reduced the gain value to 1.3 dBi. The antenna's performance was compared to previous work in the TV white space spectrum and found to have good bandwidth, efficiency, and low gain. The antenna's lumped parameters were calculated and an equivalent circuit was simulated in ADS, with good agreement between the results.

Chapter 4: The chapter covers the study of a two-layer inverted-stacked parasitic patch antenna. The antenna has two layers stacked with coaxial feed at the driven patch and two upper parasitic patches inverted and electromagnetically connected to the lower patch, made of FR4 material. It has a gain of 5.6dBi and operates in a 499-650 MHz frequency range with 98% efficiency. A parametric analysis was conducted to optimize size, gain, and radiation pattern, which showed that elliptical top patches gave the smallest size with the highest gain. Optimal top patch eccentricity was found to be 0.5 for an enhanced gain of 5.6dBi and compactness. Can be used as a user terminal or base station depending on the scenario. Low frequencies in the TVWS region between active channels are suitable for various applications like IEEE 802.11 and can penetrate obstacles like walls and trees better than high frequencies. The antenna's lumped parameters were calculated and an equivalent circuit was simulated in ADS, with good agreement between the results.

Chapter 5: A fractal patch antenna design is presented in this chapter. The effects of fractal slots on patch and cross slots in the ground are investigated. The Koch snowflake patch is used to obtain a dual band in the proposed design iteration. 4th iteration Koch snowflake patch is placed 18mm above the air. FR4 is placed 65mm above the ground plane as the superstrate. As the number of iterations increased, the antenna size decreased. In the patch, additional 4th iteration Koch snowflakes slots has been added to get three bands. The last two bands were combined to increase bandwidth by forming a defective ground structure using the fourth iteration cross slot in the ground plane. The axial ratio bandwidth (<3dB) for 1st band is 78MHz. The electric field polarization of the designed antenna is circular in the first band and linear in the last band. The antenna is working in multi-polarization in the received bands. The physical dimensions of an antenna have been decreased by 38 millimeters with a gain of 4.5dBi. The equivalent circuit of the proposed antenna was simulated in ADS with the help of lumped parameters.

Chapter 6: In the end, the sixth chapter consists of the overall conclusion and future scope of the thesis. In this thesis, we designed a circular microstrip patch antenna with circular rings, parasitic circular patch antenna, and Koch fractal patch antenna to achieve high gain and considerable bandwidth in white space TV band with reduced size. These antennas can be used as RFID applications, IEEE 802.11, and any application used in TV band.

In this way, this thesis will discuss size reduction, bandwidth and gain enhancement using slots, stacking, and fractal shapes.

List of Publications

Journals

1. **Sharma, R.,** Raghava, N.S. & De, A., " Design and Analysis of Circular Microstrip Patch Antenna for White Space TV Band Application", in *Wireless Pers Commun,* Vol.126, June 2022, pp. 3333–3344, doi:10.1007/s11277-022-09867-9.

2. **Richa Sharma and** N. S. Raghava and Asok De, "Design of Inverted Stacked Parasitic Patch Antenna for Communication in White Space TV Band", in *IETE Journal of Research*, Oct 2022, pp.1-12, doi: 10.1080/03772063.2022.2127942.

3. **Richa Sharma**, Asok De, Srinivasa Nallanthighal Raghava, "Multi-Band Multi Polarized Fractal Antenna for White Space TV Band", in *International Journal of Electronics* (Review submitted).

4. **Richa Sharma**, Asok De, Srinivasa Nallanthighal Raghava, "Circular RFID antenna for White Space TV Band" in *Wireless Pers Commun (Under Review)*

Conferences

1. **R. Sharma**, R. S. Nallanthighal and A. De, "Design and Analysis of RFID Antenna for White Space TV Band," in 2022 International Conference for Advancement in Technology (ICONAT), 2022, pp. 1-4, doi: 10.1109/ICONAT53423.2022.9725975**.**

2. **R. Sharma**, N. S. Raghava and A. De, "Design of Compact Circular Microstrip Patch Antenna using Parasitic Patch," in 2021 6th International Conference for Convergence in Technology (I2CT), 2021, pp. 1-4, doi: 10.1109/I2CT51068.2021.9418104.

CHAPTER 2

Compact RFID Antenna for White Space TV Band

2.1 Introduction

There is an endless demand for wireless spectrums but due to limited supply, it leads to a spectrum crunch. Ironically, out of the 100% spectrum allocated, the actual utilization is only 5 to 15%. The main reason for such a low utilization rate is that spectrum is allocated fixedly. If we could use the underutilized spectrum dynamically without interfering with the incumbents, this will open up huge opportunities to serve user needs. TV White Space (TVWS) is the first wireless technology to use spectrum in a dynamic manner utilizing unused TV bands. TVWS technology is compared with other communication technologies in Chapter 1. There are lots of advantages of TVWS technology over other communication technologies as discussed in the previous chapter. But, the main interest of antenna designers is the compactness of the antenna in this technology. The solution to this problem is to design a microstrip patch antenna in the TVWS band. However, these antennas have major operational disadvantages as mentioned in Chapter 1. But mainly low gain, low efficiency, and very narrow frequency bandwidth [1, 17,99] are the main concern. In this chapter, we are discussing one of the applications of the TVWS band as a radio frequency identification (RFID) antenna. RFID antenna requires better coverage, non-line of sight communication, and better penetration which can achieve with the TVWS technology. However, compactness is also the main desirable factor for RFID antenna. Various compact RFID antenna design techniques are presented by many researchers, which are working on different frequencies varying from low

to high frequency [2]. RFID antennas are designed for two frequency ranges in the UHF band i.e. 433MHz and 860-960MHz. Manufacturers do not use the frequency range 433-860MHz for commercial use because this TV band was formerly used for the transmission of television signals.

RFID techniques have become increasingly widespread in various industries today, including inventory control, asset monitoring, container tracking, proximity cards, and so on, to track the delivery position. [102]. RFID works in the same fashion as a barcode or magnetic strip on credit cards does. In barcode or magnetic strip scanners and readers should have a very specific position for functionality but in the case of RFID tags, this is not necessary as RFID tags should be in the range of the reader in any orientation [15]. The increasing growth of RFID technology provides antenna designers with new chances to create various types of RFID antennas [162,14]. When an RFID tag gets within the range of an RFID scanning antenna, electromagnetic waves (EM) trigger it. The antenna picks up these EM waves and sends them to an RFID reader, which decodes them. With the progress in anti-collision aspects, RFID technology has introduced safety and security characteristics [208]. Low Frequency (30-300KHz) tags have been used since 1979 all over the world. For very small range passive tags are used which are working in Low Frequency. High Frequency (3-30MHz) tags are also passive and have a short reading range of approximately 3 feet. High-frequency (HF) tags are having a higher data rate as compared to low-frequency (LF) tags, anti-collision facilities are also employed in them. Ultra-high frequency (300-1000MHz) tags are active tags and have a read range of about 15-20 feet. The data rate of UHF tags is high and its multiple tags can be scanned simultaneously. UHF tags will be unidentified if any conductive material comes in between the RFID reader antenna and the RFID tags. Various radio channels with different power levels were used by each county. The available bandwidth for RFID applications is

divided by government rules around the world. Each country can divide its allocated bandwidth into different channels. 865–867 MHz band is used for RFID applications in Indian regions with 2MHz bandwidth [145]. Different types of antennas are available for RFID application in the literature [163]. Different slots can be further printed as a microstrip antenna to take benefits of the FR4 substrate which is best suited for RFID technology [58].

Besides the benefits of the substrate, microstrip techniques have concerns about bandwidth, gain, and efficiency. The solution to these problems is available in the literature [178]. One of the methods is to change the dielectric constant of the material [123]. When such a material is used, the antenna efficiency will be poor and the bandwidth will be narrow due to surface wave excitation. Hence, one can modify the shape of the antenna geometry [77,122,5,28,123,26,33] instead. Initially, a conventional circular antenna is studied for one frequency [49,51,19,21,128]. This conventional microstrip antenna with any standard shape will not give better results, such as high gain, efficiency, and physical size. Hence, the geometry of the antenna is modified in different methods to improve the values of these above said parameters. Some of them are changing the dielectric constant [59], finite ground [151,17], the introduction of different slots [199,110,189], changing substrate height [70,21], use of meander-lines [149] or shorting pins [155,103,30,31,19,72,195], etc. Planar antenna technology can also be utilized in small wireless systems, such as RFID [72].

In this chapter, a circular microstrip radiator has been proposed. The microstrip patch considered here is simply circular. As mentioned above, first a circular patch is designed with the standard equations and its parameters have been studied. A simple circular patch is not so efficient to radiate all the power fed to it. Hence, to improve the performance parameters of this simple circular patch effect of circular ring slots, the finite ground plane on its performance parameters has been studied.

2.2 Design Procedure and Parametric Study of RFID Antenna

Here antenna design steps and analysis of parameters' effects (effect of ground size, the thickness of ring slots, and distance between ring slots) design performance are explained.

2.2.1 Antenna Design

The design flow chart of an antenna is presented in Figure 2.1. The design of the antenna being discussed is shown in the figure referred to as Figure.2.2. The circular microstrip patch antenna (CMSA) has a defined radius, which is represented by the letter "r." The patch antenna's radius is calculated using the supplied equation. (2.1).

$$r = \frac{F}{\left\{1 + \frac{2h}{\pi \varepsilon_r F \left[\ln\left(\frac{0.5\pi F}{h}\right) + 1.7726\right]}\right\}^{1/2}}. \tag{2.1}$$

The resonant frequency of the antenna can be calculated using the formula $F = \frac{K_{nm}c}{2\pi a_e \sqrt{\varepsilon_e}}$ [143], where K_{nm} is the mth root of the derivative of the Bessel function of order n and 'c' is the velocity of light. The ε_e and a_e are the effective dielectric constant and the effective radius of the patch antenna, respectively. The influence of the fringing fields along the boundaries of the CMSA is taken into consideration by replacing the radius "r" with the effective radius a_e as described in the following equation: [168]

$$a_e = r\sqrt{\left[1 + \frac{2h}{\pi r \varepsilon_r}\left\{In\left(\frac{0.5r}{h}\right) + \frac{1}{\sqrt{2}}\varepsilon_r + \frac{1}{0.564} + \frac{h}{r}\left(\frac{1}{3.73}\varepsilon_r + 1.65\right)\right\}\right]} \tag{2.2}$$

The value of ε_e is obtained by using the ratio of the total capacitance of the dominant mode of CMSA with and without a dielectric substrate [93] as given in equation (2.3)

The value of ε_e is obtained using

$$\varepsilon_e = \frac{C(r,h,\varepsilon_o \varepsilon_r)}{C(r,h,\varepsilon_o)}, \tag{2.3}$$

where $C(r, h, \varepsilon_o \varepsilon_r)$ and $C(r, h, \varepsilon_o)$ are the total capacitance of TM$_{11}$ mode of CMSA with and without a dielectric substrate, respectively. The capacitances can be calculated using the given equation

$$C(r, h, \varepsilon_o \varepsilon_r) = \frac{0.8525\varepsilon_o \varepsilon_r \pi r^2}{h} + 0.5C_f. \qquad (2.4)$$

Equation (2.4) combines the main capacitance of the disc with the fringing capacitance, as stated in reference [72]. The fringing capacitance can be determined using the following relation:

$$C_f = 2r\varepsilon_o \left[In\left(\frac{0.5r}{h}\right) + \frac{1}{\sqrt{2}}\varepsilon_r + \frac{1}{0.564} + \frac{h}{r}\left(\frac{1}{3.73}\varepsilon_r + 1.65\right) \right], \qquad (2.5)$$

where $C(r, h, \varepsilon_o)$ is calculated by putting $\varepsilon_r = 1$ in equations (2.4) & (2.5) [195,168].

The antenna is designed in three steps: In the first step basic circular patch is designed and different parameters have been studied. In the second step, rings are etched on the circular patch with an infinite ground plane. As a final step, a center-shorted circular patch that includes four etched rings and a finite ground plane has been designed, and various parameters of this design have been analyzed. High-Frequency Simulation Software (HFSS) is used for simulation and microstrip line feed is chosen as the excitation of the antenna.

The design process for the microstrip patch has been outlined step by step using the flow chart presented in Figure 2.1. The first step in the design process is to determine the frequency, dielectric material, and substrate height based on the intended application. Using relevant design formulas, the dimensions of the circular patch are then finalized. In this design, the frequency of operation is chosen as 480 MHz, for FR4 substrate. The height of the substrate has been set at 1.6mm. Using these values in equations (2.1) to (2.5), the size of the patch can be calculated.

In the 2nd step, circular rings are etched on the circular patch. By etching all rings on the patch resonant frequency shifted from 480 MHZ to 608 MHz. Each ring has its resonance frequency. When all four rings are embedded simultaneously on the patch, the resonance at 608MHz is dominant, and all resonance combine here.
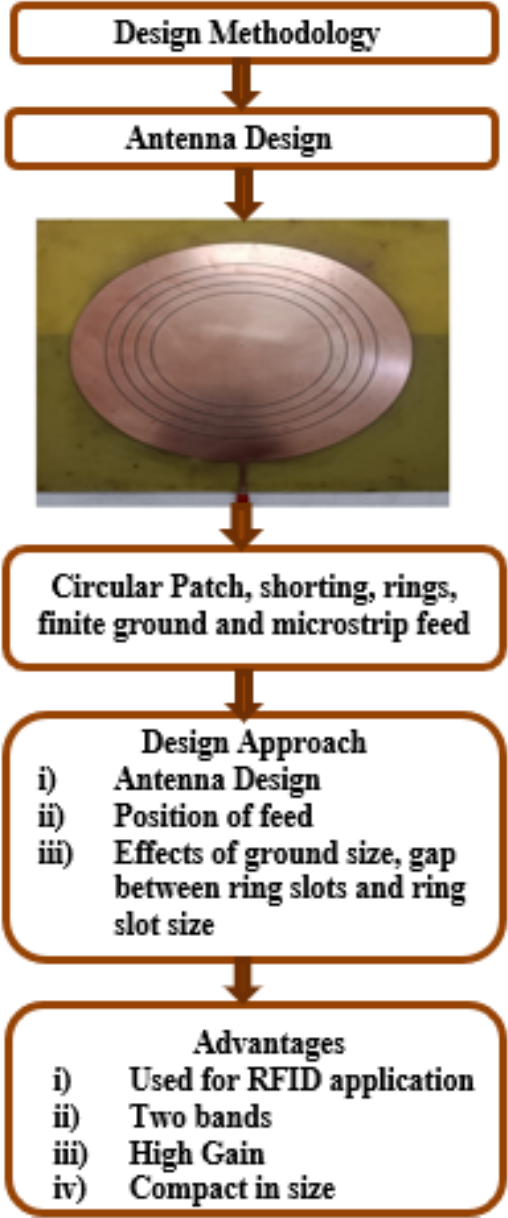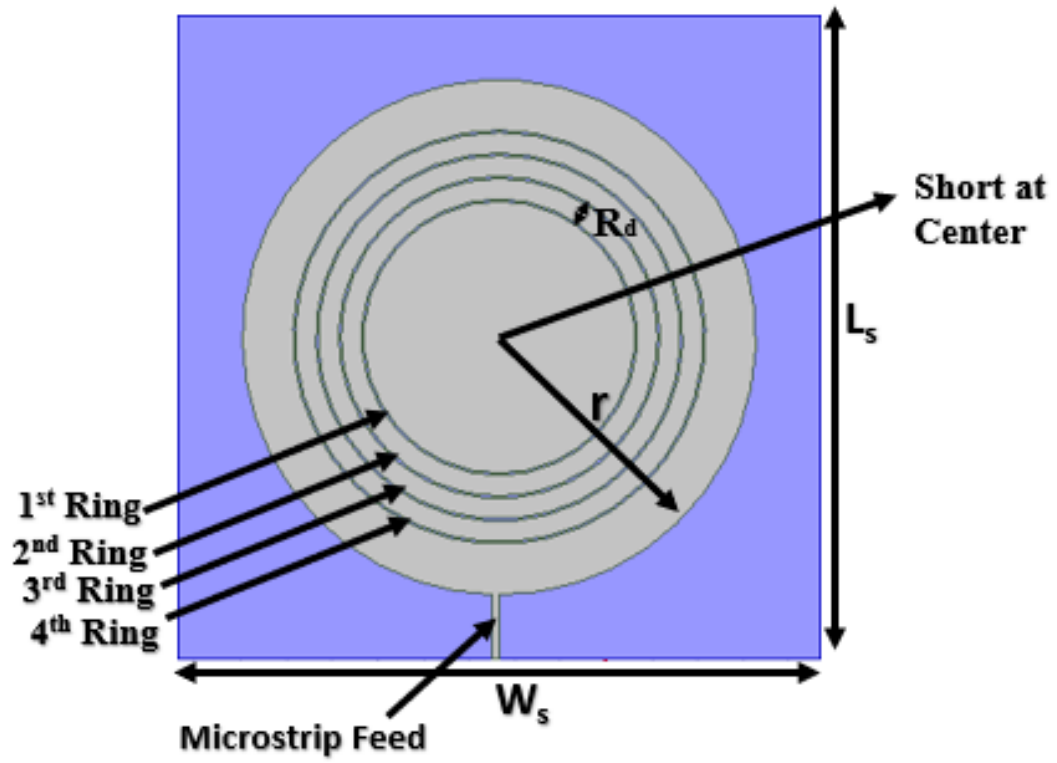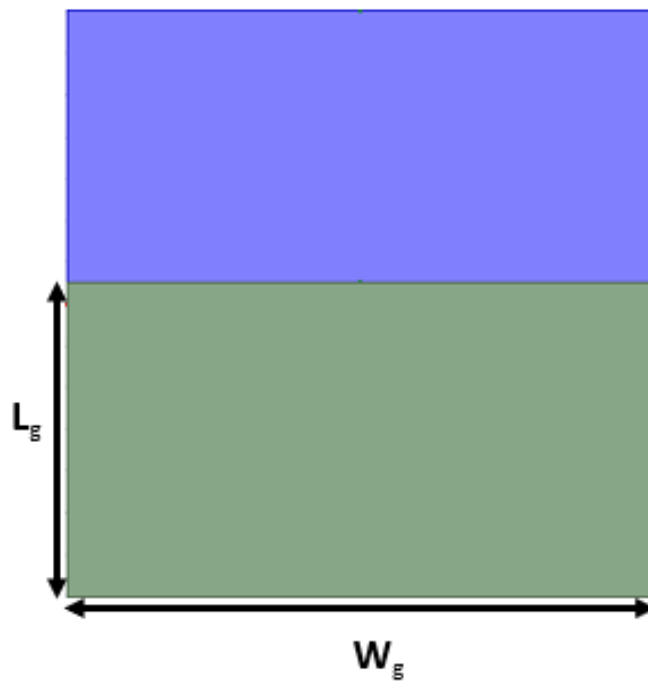

Fig. 2.1 Flow Chart of Antenna Design

Fig. 2.2. The antenna has two views: (a) Front and (b) back view.

In 3rd step: the size of the ground is varied to get desired bandwidth of the RFID antenna. Here 'L$_g$' and 'W$_g$' denotes the length and width of the ground plane. 'W$_s$' and 'L$_s$' is the width and length of the substrate. The distance between rings is denoted by 'R$_d$' and the size of the ring slot is denoted by 'R$_s$'. In this work, a patch antenna is designed on which four rings are etched from the copper patch. The size of each ring is 1mm and each ring is separated from the other ring by a 10mm distance. The antenna is energized by a microstrip feed, which is located at the center of the substrate's width. The addition of rings and a finite ground gives desired results of bandwidth and gain. After optimization the proposed design parameters are: r= 112 mm, W$_s$ = 280 mm, L$_s$ = 280mm, W$_g$ = 280mm, L$_g$ =150mm, R$_d$ = 1mm, R$_s$ = 10mm.

2.2.2 Parametric Analysis

This section explores the impact of L$_g$ (ground size), R$_s$ (ring size), and R$_d$ (distance between rings) on the performance of the proposed RFID antenna.

2.2.2.1 Effects of ground size L$_g$

Parametric analysis has been done to find out the optimum size of a ground plane. The size of L$_g$ is varied from 280mm to 150mm. The resonant frequency and S$_{11}$ are dependent on the ground dimensions, as depicted in Figure 2.3. It is found that the return loss drops from -10.4 dB to -29 dB, and the resonance shifted from 480 MHz to 487 MHz when L$_g$ decreased. When the ground size is reduced up to 210mm, S$_{11}$ improved but resonance shifted to the higher side. After 210mm resonance starts shifting towards the lower side with better return loss. The optimum value of L$_g$ obtained is 150mm. Due to finite ground, bandwidth has increased from 3MHz to 13MHz.
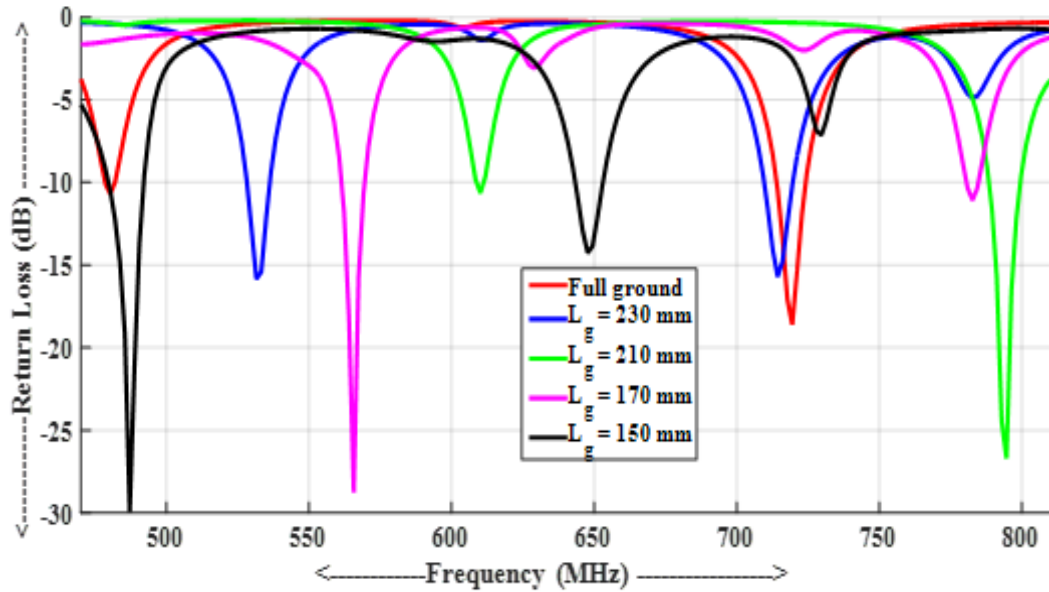
Fig. 2.3 Simulated S-parameter of proposed antenna as a function of L_g

2.2.2.2 Effects of gap between ring R_d

To find out the optimum gap between rings, R_d is varied for desired results. The effects of the gap between rings are depicted in Figure 2.4. The gap between rings is varied from 5mm to 15mm. As the gap between rings is increased multiple resonance is received but resonance at desired frequency is achieved at a gap of 10mm.
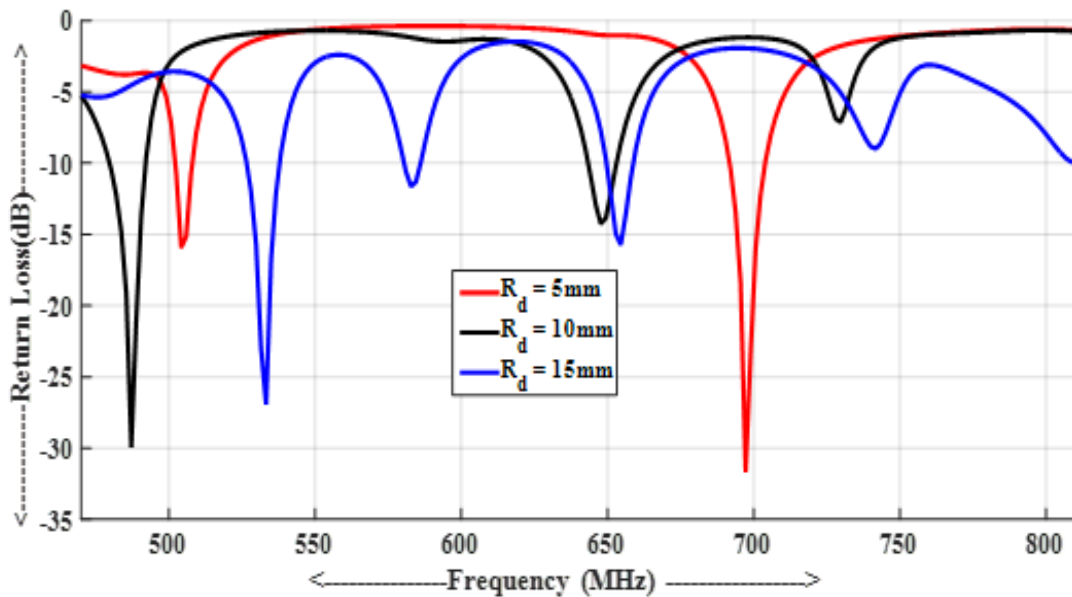

Fig. 2.4 Simulated S-parameters of proposed antenna as a function of R_d

2.2.2.3 Effects of ring slot size R_s

The effects of the size of the ring slot are shown in Figure 2.5. The size of the ring slot (R_s) is varied from 0.5mm to 1.5mm. It is observed that the optimum value for R_s is 1mm for the best matching of S_{11}. The change in the size of ring slots is less sensitive in this design because after changing the ring size only return loss is going to change. There is no change in the resonance of the antenna. The return loss is changed from -12 dB to -30dB with a change of 2MHz in resonant frequency.
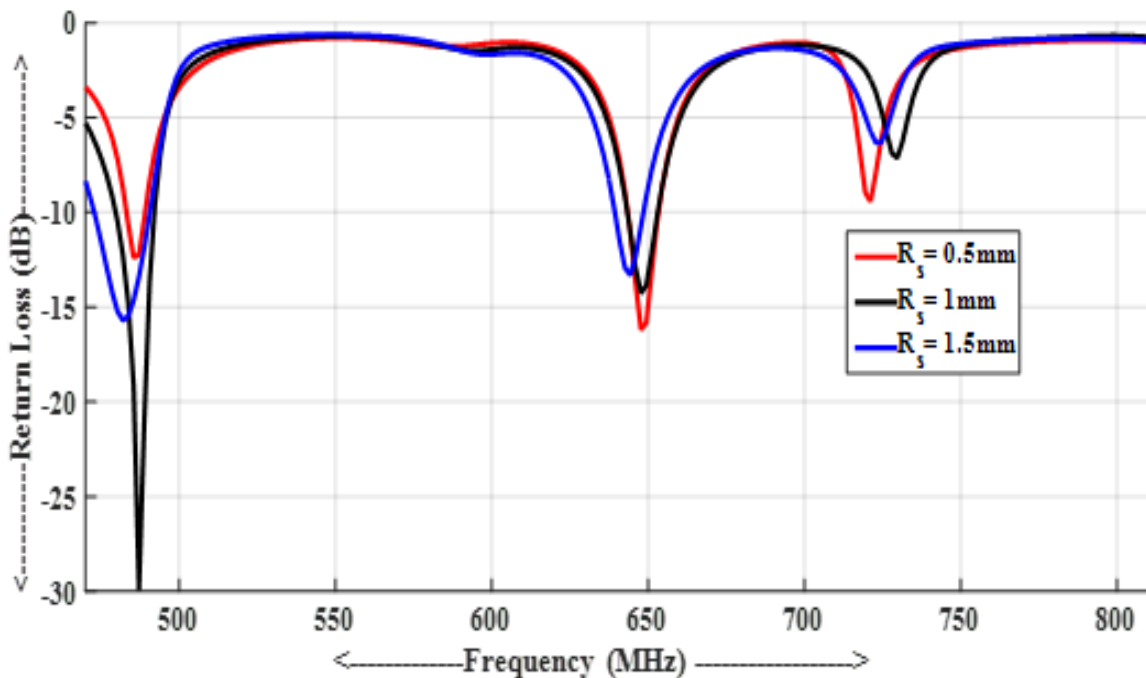

Fig. 2.5 Simulated S-Parameter as a function of R_s

2.3 Simulated and Measured Results

The suggested work demonstrates that by reducing the ground plane dimensions, the antenna bandwidth can be increased. Due to a shorting pin connecting the patch to the ground, two frequency bands are received. Figure 2.6 it is depicted that the S_{11} is improved from -10.4 dB

to -29 dB and bandwidth improved from 3 MHz to 13 MHz due to a change in ground plane size.

The proposed antenna has been manufactured and hardware results have been compared with simulated results. The fabricated design is shown in Figure 2.7. It is clear from Figure 2.8 that bandwidth is more than 2MHz which is used for RFID operation in the Indian region that is why the proposed antenna is suitable for RFID applications with a return loss of -29dB. The antenna is designed at a frequency of 480MHz, but due to the ring structure on the main patch, the operational frequency is moved from 480MHz to 487MHz in simulation. In terms of the resonant frequency, there was an error of 1.4 % in simulated results. The comparison between simulated and experimental results reveals that the experimental results exhibit a higher resonant frequency. The S_{11} of the fabricated design is -23dB at 482MHz frequency. The identical antenna may be used at 647 MHz frequency for a bandwidth of 10 MHz and return loss of -14 dB.
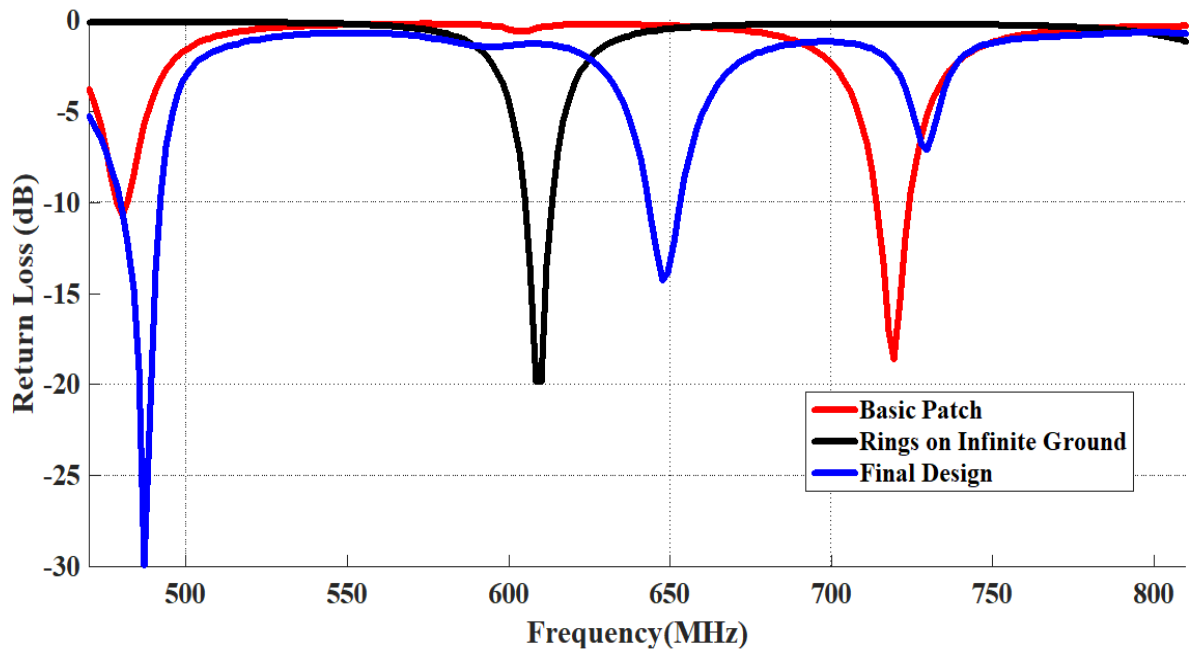

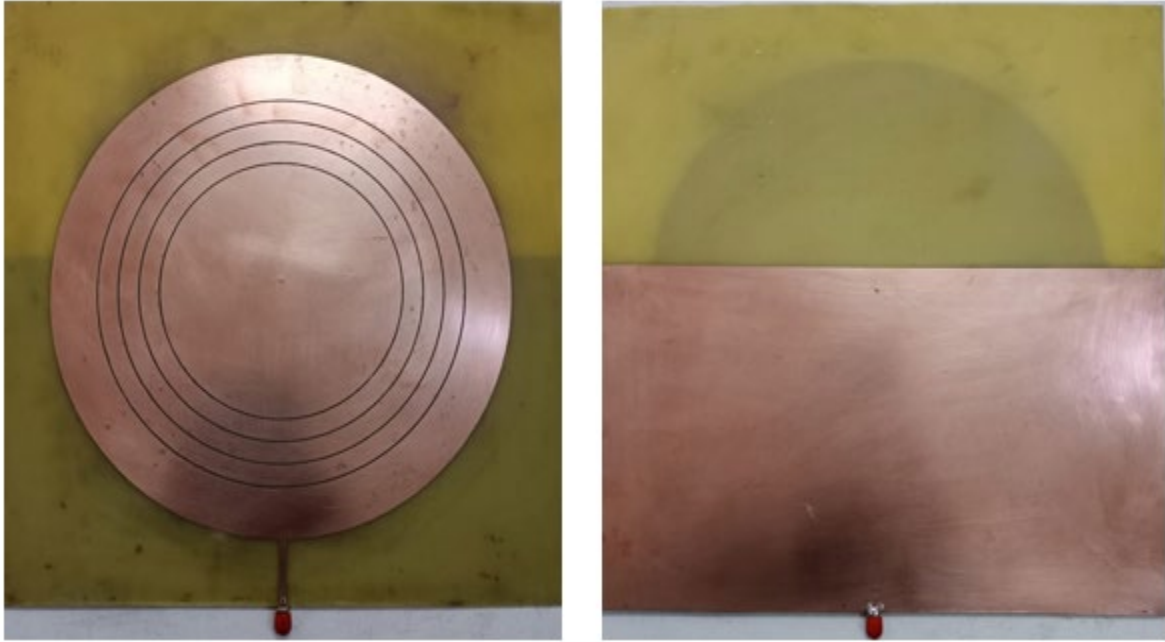Fig. 2.6 Simulated return loss of proposed antenna for three stages

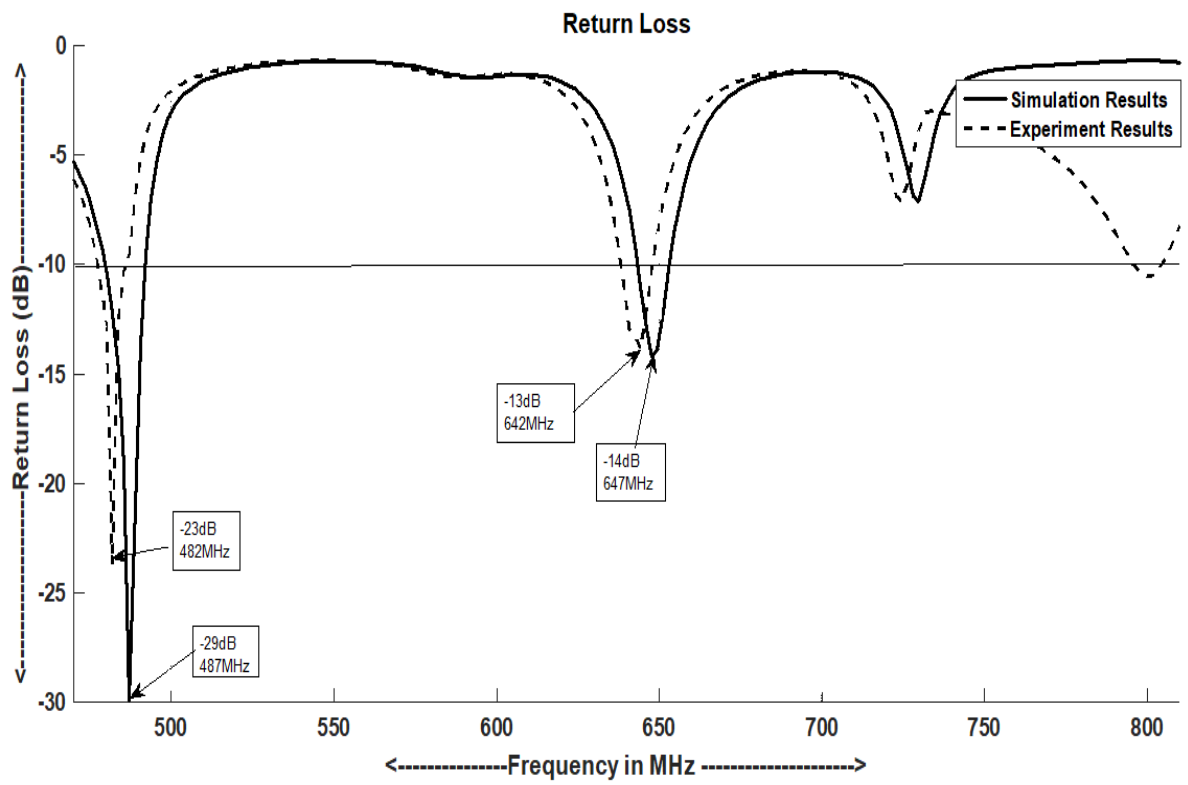Fig. 2.7 Fabricated Design (a) Front View and (b) Back View

Fig. 2.8 Simulated and Experimental S-parameter

The efficiency of an antenna design can be determined by its voltage standing wave ratio (VSWR). Furthermore, VSWR is a reliable indicator of how much power an antenna reflects. From Figure 2.9 it is indicated that the antenna is adequate for practical use as the simulated VSWR value is 1.07 while the experimental VSWR is 1.13.
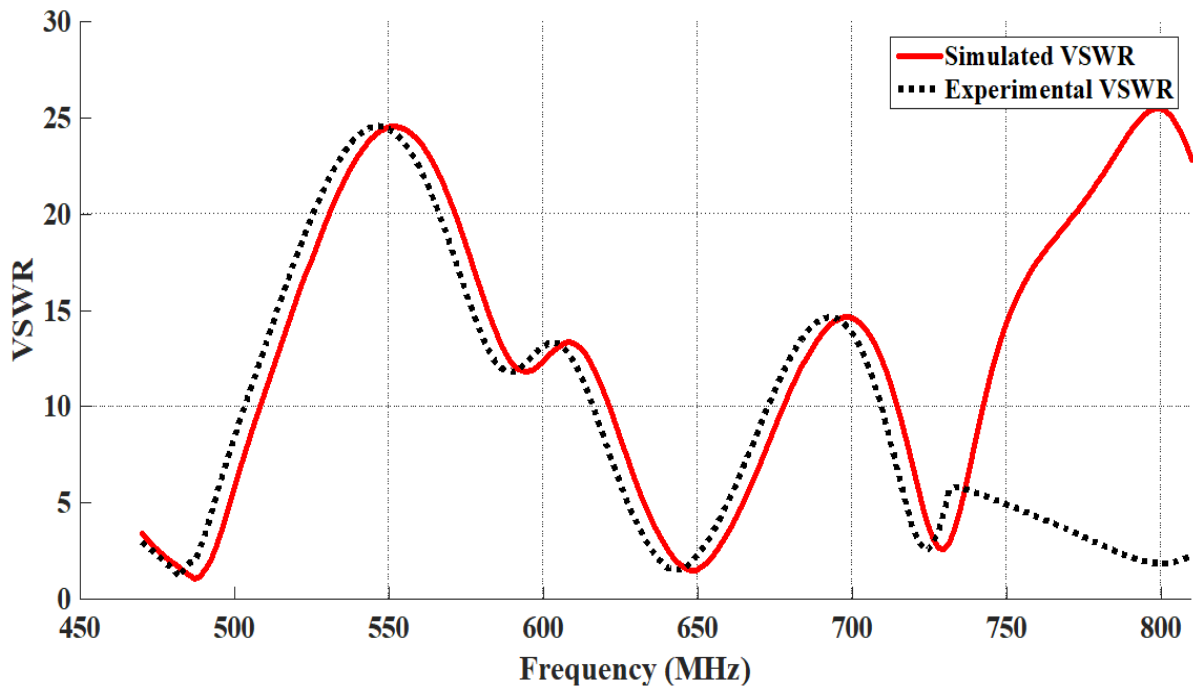

Fig. 2.9 VSWR plot for proposed design

Figure 2.10 depicts the radiation plot of the presented antenna. Most of the signals are only transmitted in one direction. The directivity of the antenna is 9.9dB at 480MHz frequency. Figure 2.11 displays the antenna's radiation pattern at phi=0^0 and 90^0, at a resonant frequency of 480MHz. The gain magnitude in the main lobe is 8.11dBi. As indicated in the graph, maximum gain is directive. Figure 2.12 shows the total gain for the antenna at phi=0^0 and 90^0 at 647 MHz in the 2nd band. Figure 2.13 shows the comparison of measured and simulated gain versus frequency. There is some variation between measured and simulated gain. The measured gain achieved is 7.5dBi while the simulated gain is 8.11dBi over the desired

frequency range. In a given direction, the phase and amplitude of the co-polarization and cross-polarization components are entirely coupled. The real and imaginary impedance is plotted with frequency and its impedance is matching at a resonant frequency. The impedance plot is depicted in Figure 2.14.
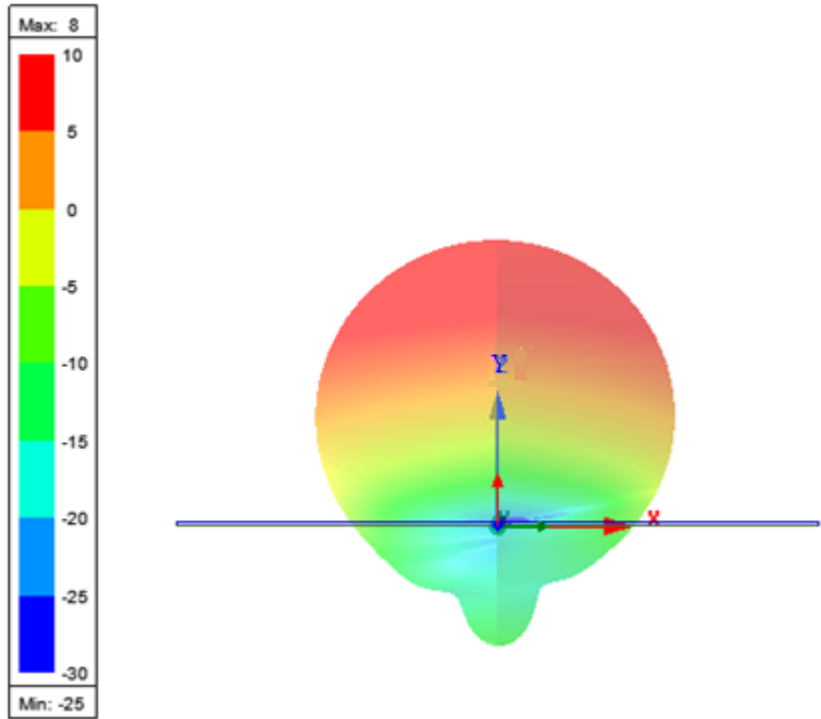

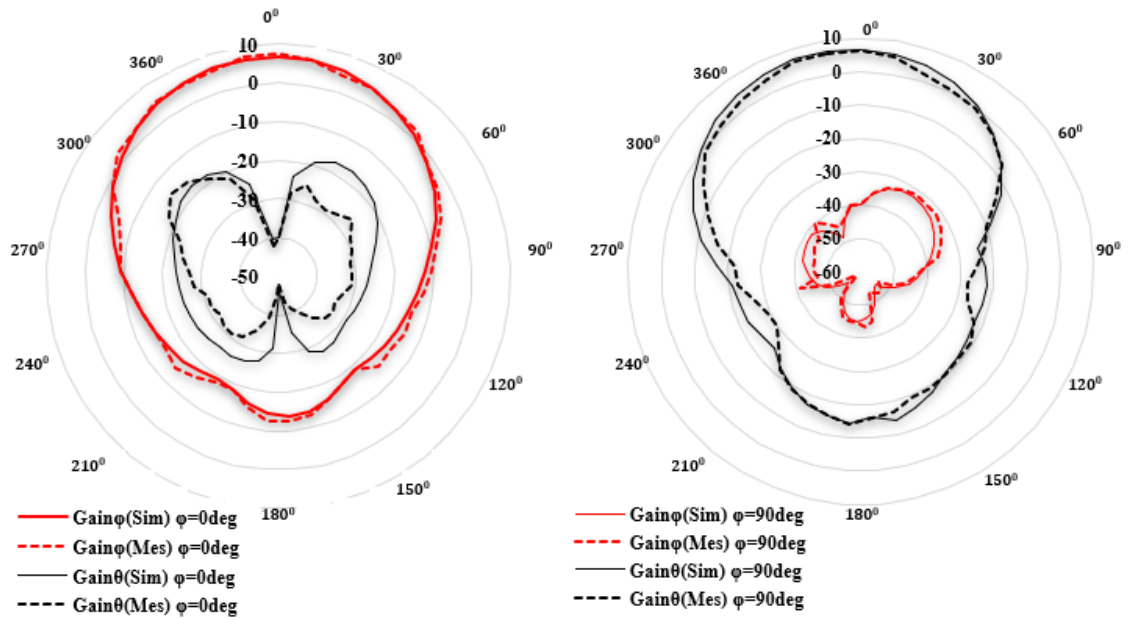Fig. 2.10 Radiation plot of proposed antenna

Fig. 2.11 Simulated and experimental radiation patterns of the proposed antenna at 487 MHz
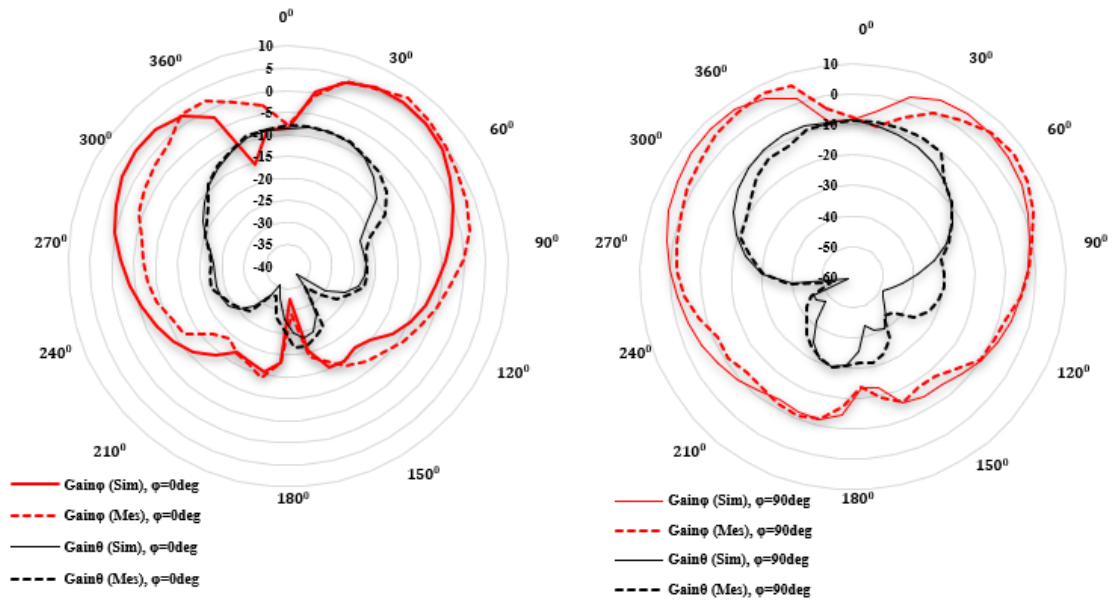
Fig.2.12 Simulated and experimental radiation patterns of the proposed antenna at 647 MHz
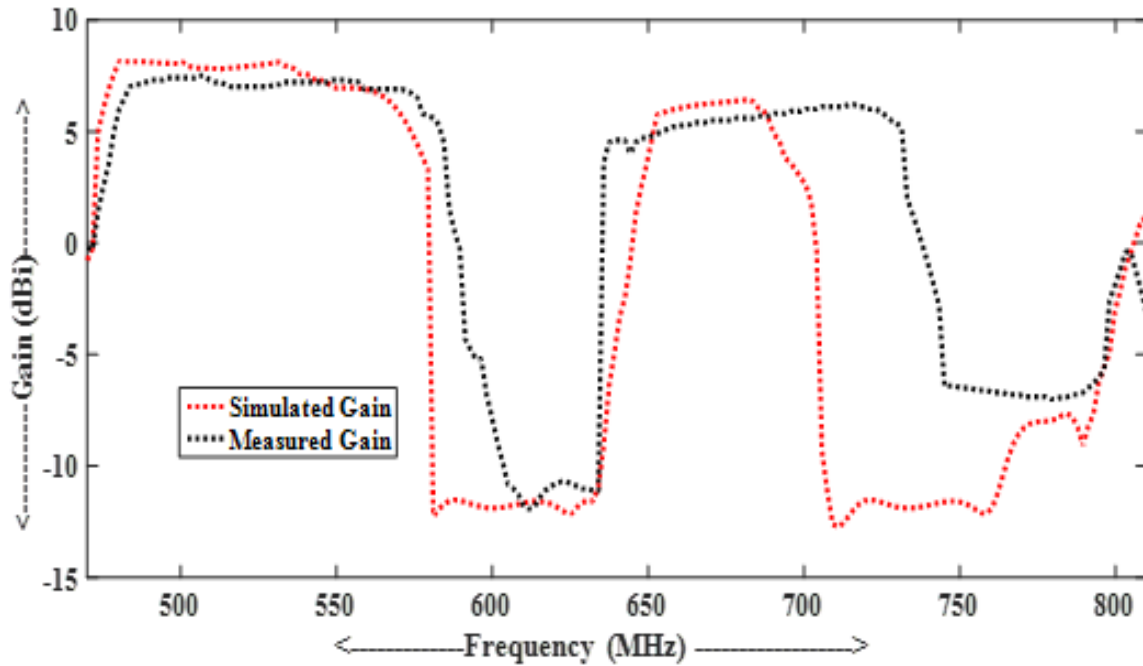
Fig. 2.13 Simulated and experimental gain vs frequency

The surface current density of the proposed antenna is shown in Figure 2.15. Surface current density is maximum at a phase angle of 90^0. The Electric filed is shown in Figure 2.16. From the electric field, it is clear that all four rings are radiating. The outer ring radiates less as compared to the inner ring corresponding to 480MHz.

Fig. 2.14 Real and imaginary impedance of proposed design

Fig. 2.15 Surface current density of proposed design

Fig. 2.16 Electric Field of proposed design

2.4 Antenna Observations and Comparisons with Existing Designs

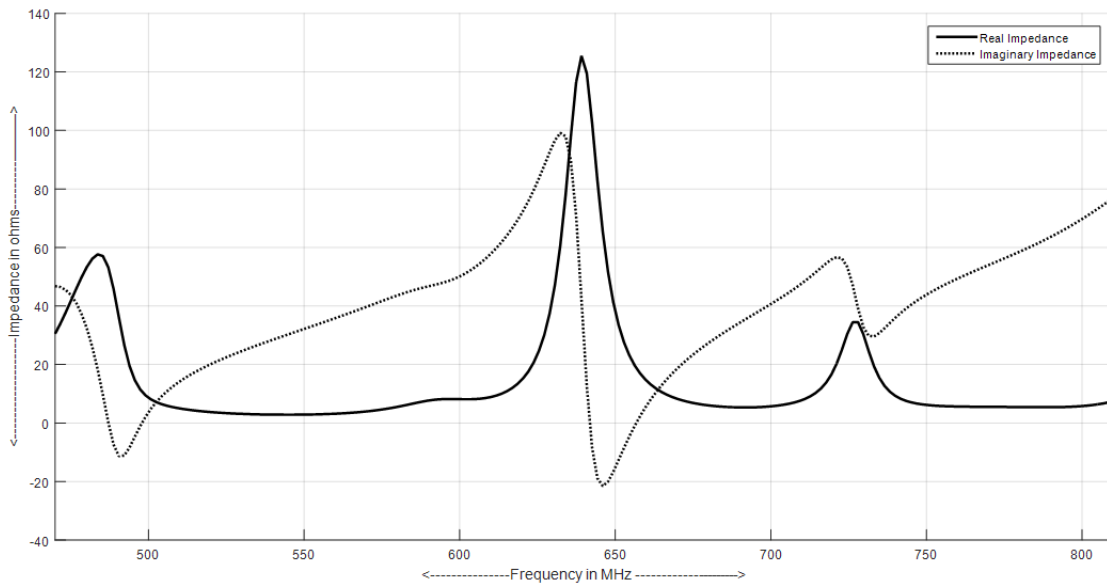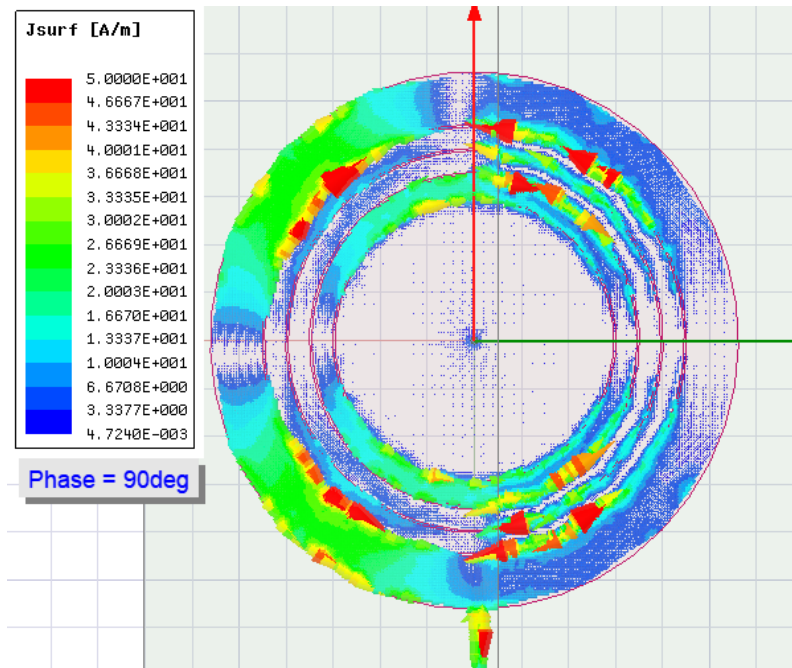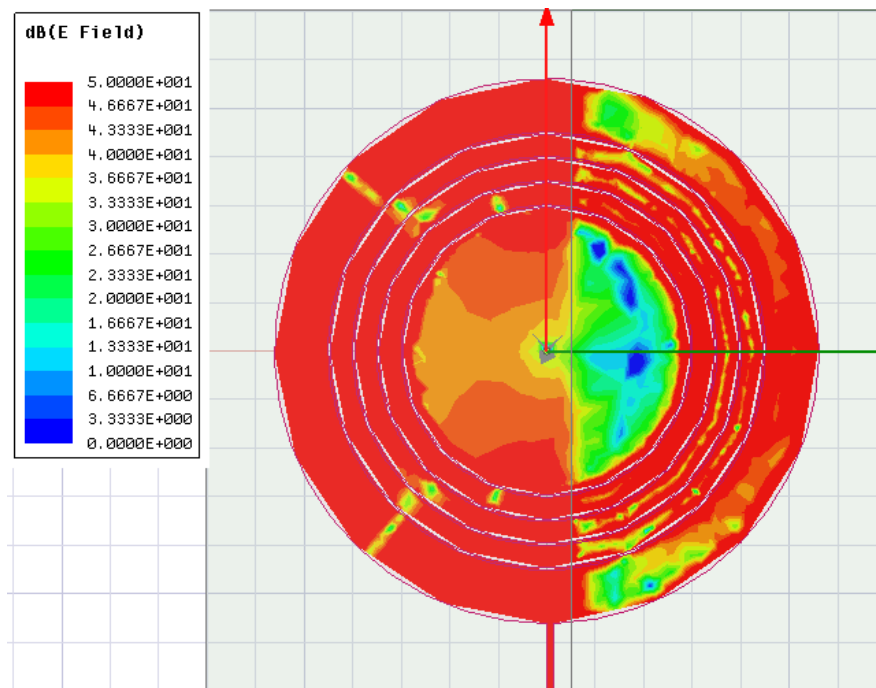The parameters of the designed antenna have been compared with the commercially available RFID antenna in Table 2.1. The proposed design is having the lowest VSWR of 1.07 as compared to 1.4 for all compared antennas. Bandwidth is also increased from 3MHz to 13MHz. It was observed that the proposed design has a compact size with a good agreement of gain, bandwidth, VSWR, front-to-back ratio, and limited ground size.

Table 2.1

Comparison of proposed design with commercially available RFID antenna

Model No	Size (mm)	Freq. (MHz)	Gain	FBR	weight	HPBW
ETS-RA 02	260 x 260 x 45	865-868	8dBi	≥ 20	1.2kg	$65^0/65^0$
ETS-RA 03	140 x 120x 20	865-868	5dBi	$\geqq 23$	0.4kg	$65^0/55^0$
ETS-UFMAS 15	900 x 500 x 25	865-868	5dBi	$\geqq 24$	1.5kg	$95^0/84^0$
CP11 RFID UHF	180 x 180 x 17.5	865-868	0.2 dBi		485g	120°/120°
p11 RFID UHF	230 x 230 x 25	865-868	3.2-3.4 dBiC	<-15	545g	100°/100°
p13 RFID UHF	417 x 137 x 3.3	865-868	1.1 -3.2 dB	< -20	350g	40°/90°
p14 RFID UHF	557 x 137 x 3.3	865-868	8.0-8.1 dBiC	< -18	460g	30°/90°

p16 RFID UHF	837 x 137 x 3.3	865-868	9.4-9.5 dBiC	< -20	725g	20°/ 90°
p22 RFID UHF	277 x 277 x 3.3	865-868	0.5- 2.5 dB	< -20	470g	60°/60°
p33 RFID UHF	417 x 417 x 3.3	865-868	10.7- 10.8 dBiC	< -20	1050g	40°/40°
SP11 RFID UHF	207 x 207 x 11.7	865-868	7.7-8.0 dBiC	< -15	1055g	70°/70°
SP12 RFID UHF	417 x 207 x 11.7	865-868	9.3 -9.5 dBiC	< -20	2520g	40°/70°
Proposed Design	280 x 280 x 1.6	479 -492	8.11 dBi	> 21	280g	40º/40º

2.5 Conclusion

In this chapter, an RFID antenna is proposed to use 470MHz to 806MHz (white space T V frequency band) frequency band which is now available for commercial use as the transmission of television signals has transferred from the TV to the satellite band. An antenna is fabricated on FR4 substrate which is a fairly common and durable substrate. The design consists of four concentric rings cut from a circular microstrip patch, connected to the ground via a shorting pin. In this design finite ground is used. The proposed antenna experimental gain is 7.5dBi. The antenna may operate on two bands in the intended frequency spectrum, namely 479-492MHz and 643 -653MHz. The bandwidth obtained in these bands are 13MHz and 10MHz,

individually, which is higher than the commercially available UHF RFID antenna. The bands have a return loss of -29dB and -14dB, respectively. The impact of ground plane changes is also discussed, and return loss and bandwidth have been increased from -10.4dB to -29dB and 3MHz to 13MHz respectively. In comparison to the currently existing RFID antenna in India, the proposed antenna is compact in dimensions. An effective low-profile compact design with restricted ground size and circular ring slots has been modeled for the bandwidth of 13MHz and S_{11} of -29dB.

CHAPTER 3

Circular Microstrip Patch Antenna for White Space TV Band

3.1 Introduction

As MMIC technology has advanced, microstrip patch antennas (MSA) are the most popular antenna structures. Due to their many benefits, including low profile planar layouts, lightweight, simple manufacture, etc., these antennas have gained popularity. Due to the resonant nature of the patch structure, its primary drawback is an inherent bandwidth restriction. Compact and affordable antennas are necessary for modern communication systems like wireless local networks, direct broadcast satellites, global positioning satellites, etc., making planar technology helpful and occasionally inevitable [156]. These antennas are suited for deployment on aerial platforms because of their small weight. For these applications, a fresh justification is provided for the study of creative remedies that get beyond bandwidth restrictions and the microstrip antennas' downsizing [83, 128]. As a result, bandwidth increment has emerged as one of the key design factors for microstrip antennas' practical uses. In Chapter 2, it is seen that a simple circular patch was studied, and also circular ring slots were embedded in the patch to reduce size with a good gain. By observing the results, it was achieved to a greater extent. But in this case, bandwidth was very narrow. In this regard, bandwidth enhancement techniques have received much attention [34,184]. High efficiency, enough bandwidth, good impedance matching, little deterioration due to the presence of nearby objects, etc., are the electrical criteria for such applications.

The techniques of bandwidth enhancement are discussed in this chapter. Different methods are employed to increase the bandwidth. These methods include:

1. Modifying the shape of the patch using slots

2. Shorting posts, shorting pins, and short circuits

3. Using defective ground

4. Using metamaterial

5. Using fractal shapes in the patch

6. Using a combination of the above techniques

In the first method, by modifying the basic shapes of the antenna significant bandwidth enhancement may be obtained. The slots in the patch give rise to different bands and the correct position of the slots helps to combine these bands to get higher bandwidth. By adding various kinds of slots to the antennas' typical forms, modifications may be made. These slots can be of any shape like- a rectangle, circular, ring, arithmetical sign, alphabet, etc. [52,37,57,120,180,160, 25, 54,188,42]. It was discovered that while the bandwidth of the radiating patch increases due to the addition of different slots, radiation efficiency drops. Due to the introduction of slots lower radiation efficiency causes a gain reduction [157]. To overcome the microstrip antenna's many drawbacks, without drastically affecting the resonance, choosing the right substrate for its manufacture is one of the effective ways [50].

The second method, shorting post or shorting pin or short circuit [196], is regarded as a more efficient technique and is used at different locations to minimize the overall dimensions. By using shorting pin, size is reduced as well as bandwidth is enhanced but with a compromise in gain.

In the third method, defected ground plane (DGS) is used as a new way to enhance the many characteristics of microwave circuits, such as their bandwidth [121], cross-polarization [63], gain [148], and other properties. DGS has been created on the ground with the help of planner techniques. A defect on the ground plane disrupts the current distribution, altering the properties of the antenna [84]. The use of a DGS raises the fringing field, leading to an increase in parasitic capacitance. The increase in parasitic capacitance between the patch and ground plane results in enhanced bandwidth due to increased coupling [89].

The fourth method uses metamaterials to improve antenna performance parameters [100]. Metamaterials are synthetic materials not found in nature. When metamaterials are used with an antenna it creates a resonant circuit which increases the bandwidth of the antenna. [46].

In the fifth method, fractal shapes are used to increase antenna performance parameters. Fractals are fun-loving shapes [176,158] which repeat themselves by reducing their size. Microstrip patch antenna's disadvantages can be overcome by fractal design. The fractal antenna's resonant frequency has been seen to drop as the order of iterations rises. [85].

The sixth method is a combination of one, two, or more so that the effect of all the methods [117,141,81] can be obtained in one. As the first and second methods are discussed in this chapter. The last four methods will be discussed in the subsequent chapters.

Initially, a conventional circular patch with infinite ground is considered. By using the first method, i.e. by introducing the slots in the geometry, this simple microstrip patch antenna can be modified in two ways:

- A slot can be cut within a simple microstrip patch

- A microstrip patch itself can be changed to a particular shape by cutting the slots

In the first method, any type of slot is embedded in a simple radiating patch. By embedding such suitable slots compact operation of the antenna may be obtained. In the literature, there are many antennas with slots cut in them, which have been explained in Chapter 1.

In the previous chapter circular patch radiator with the finite ground is used for the RFID application. In the last design, two bands were obtained with smaller bandwidths and good gain. In this chapter same design is used at different places of concentric rings to achieve 100% bandwidth but with a compromise of gain.

3.2 Antenna Design

The design methodology is depicted in Figure 3.1 and the circular patch radiator with finite ground is shown in Figure 3.2. The design equations described in Chapter 2 are used for the calculation of the dimensions of the proposed antenna. The radius of the proposed design 'a' comes out to be 86.6mm for 480MHz frequency. In the design L_g and W_g are the length and width of the ground plane. L_s, W_s, and R_s are substrate length, substrate width, and ring slot size respectively.
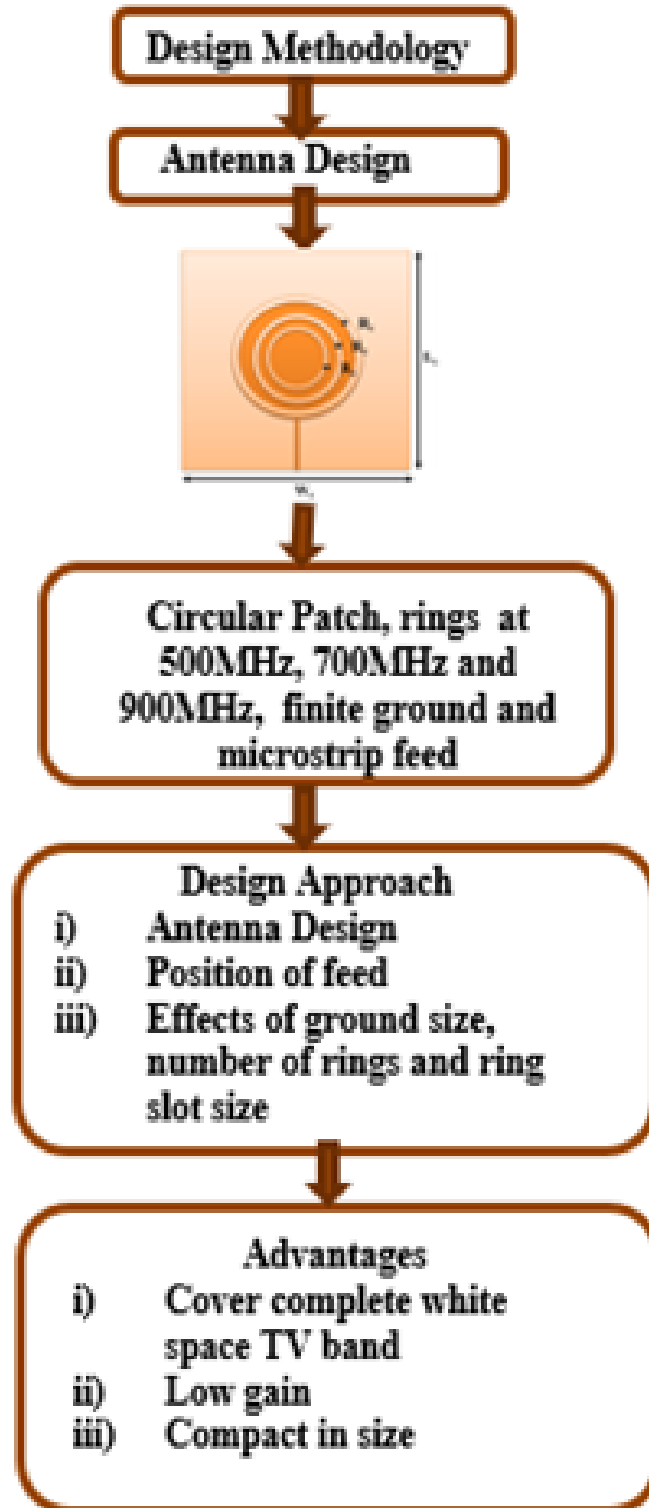
Fig.3.1 Design Methodology of Proposed Antenna

This chapter extends the work of the last chapter. Here three rings are etched on the circular patch to get desired bandwidth. Three rings are added on different frequencies to get desired resonant frequency after that all rings are combined on the patch to find out the results. FR4 substrate is used for the fabrication of the antenna. The first ring is added at a frequency of 900 MHz. The second and third rings are added on 700 MHz and 500MHz frequencies respectively. The size of rings is taken as 0.5 mm after optimization which will be discussed in further sections of the chapter. Due to the etching of circular rings efficiency of the design reduces. The distance between rings is optimized to 10 mm. The designing process of an antenna uses two steps as shown in Figures 3.2 and 3.3.

In the first step, circular rings are etched one by one on the infinite ground as depicted in Figure 3.2 (a) to (e). If the size of the ground is taken six times the substrate height as compared to patch dimensions it, behaves as infinite ground. It was found that when rings were etched on an infinite ground plane desired bandwidth did not achieve. Figure 3.2 (a) is the basic circular shape patch on an infinite ground plane.
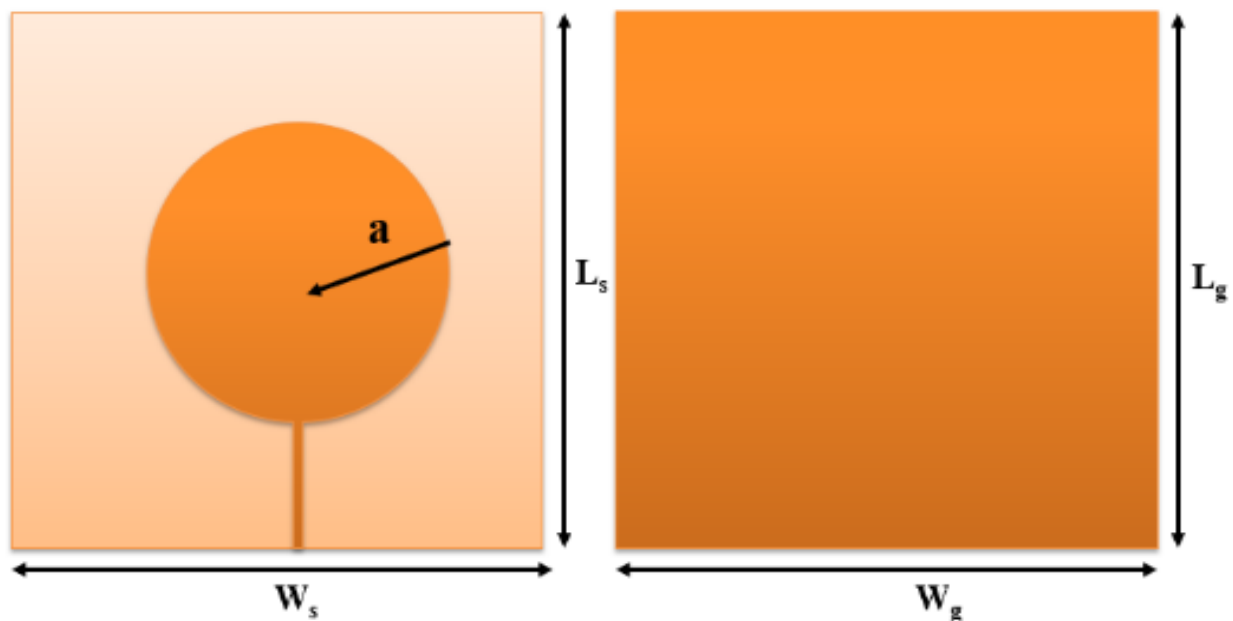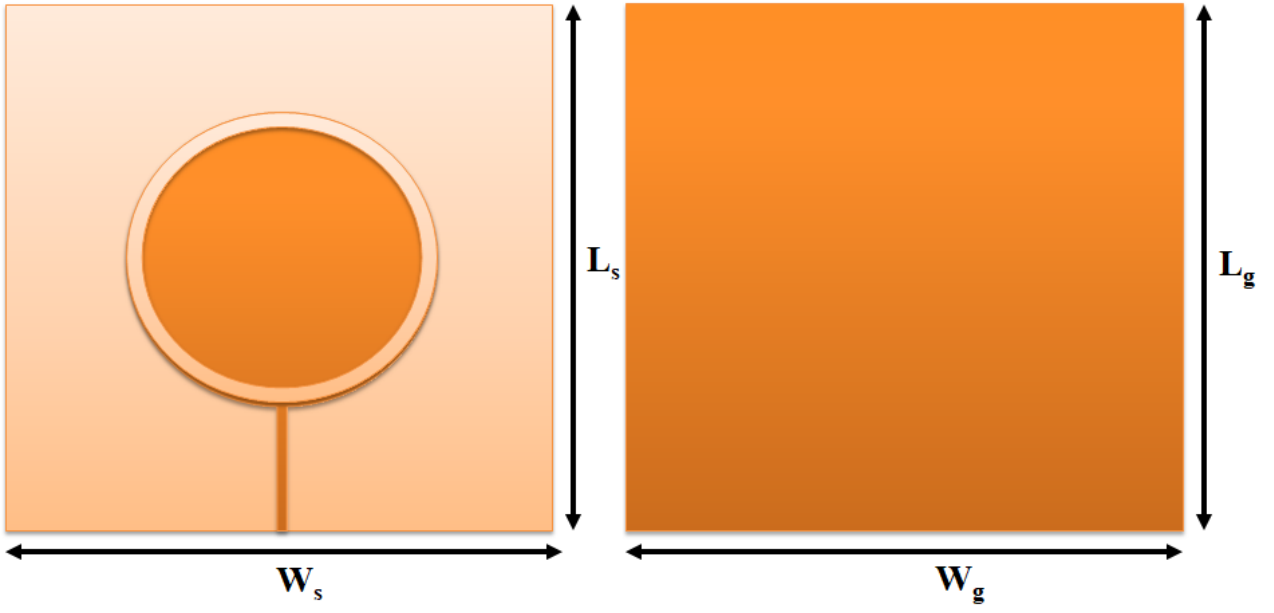

(a) Basic Patch
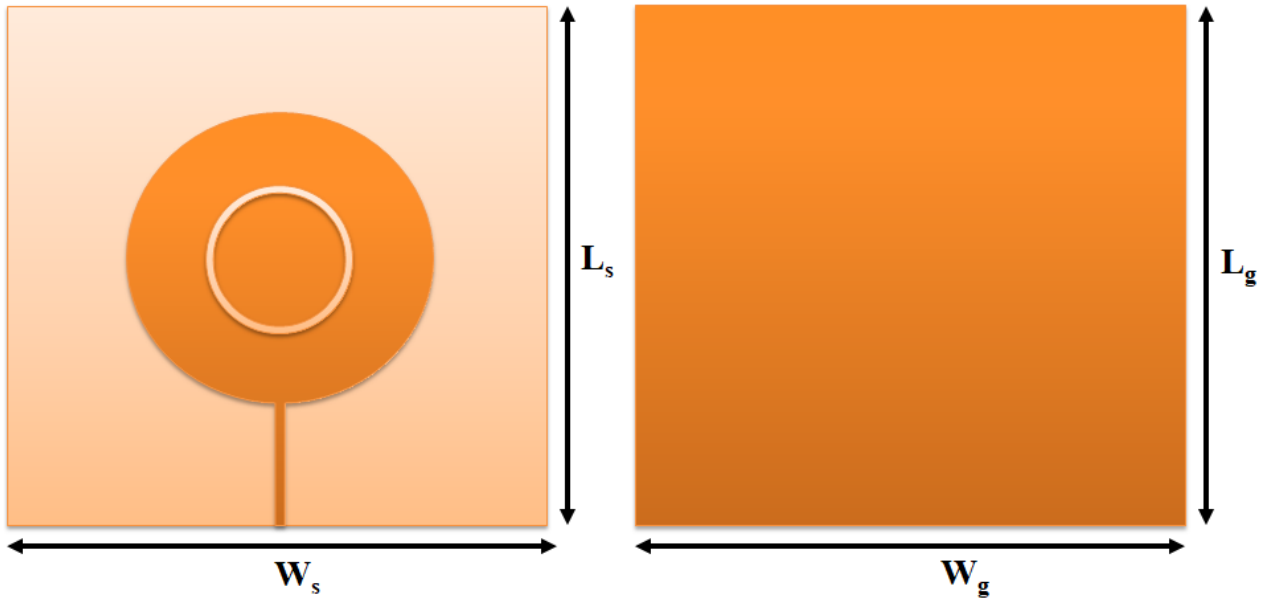
(b) Ring at 900MHz
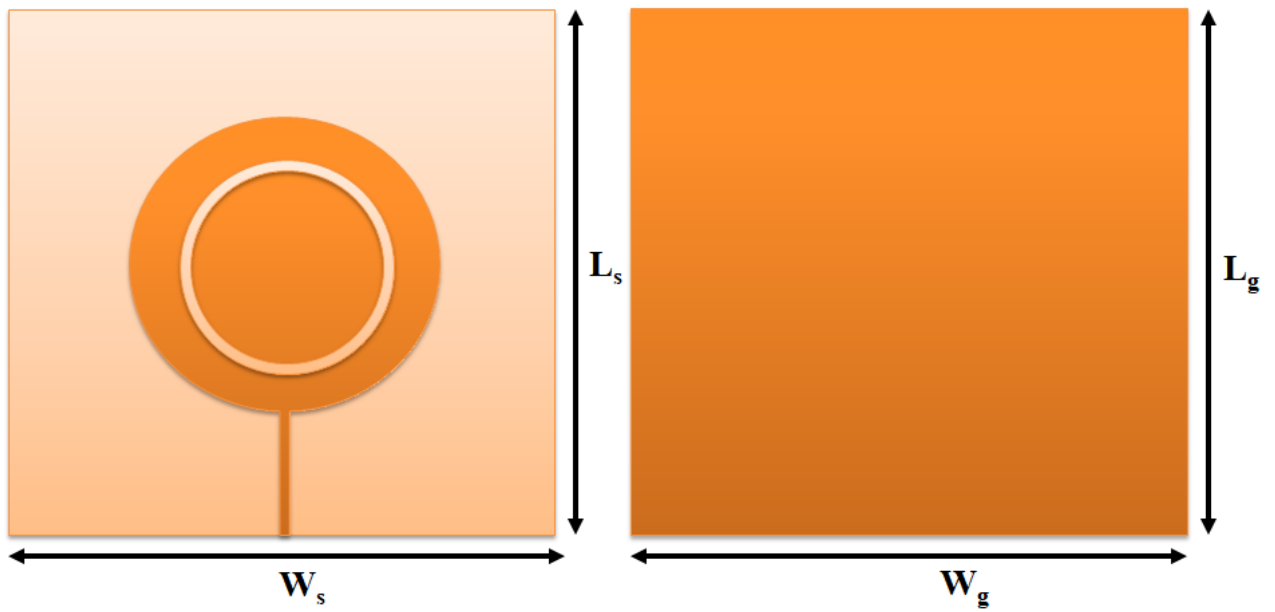
(c) Ring at 700MHz

(d) Ring at 500MHz
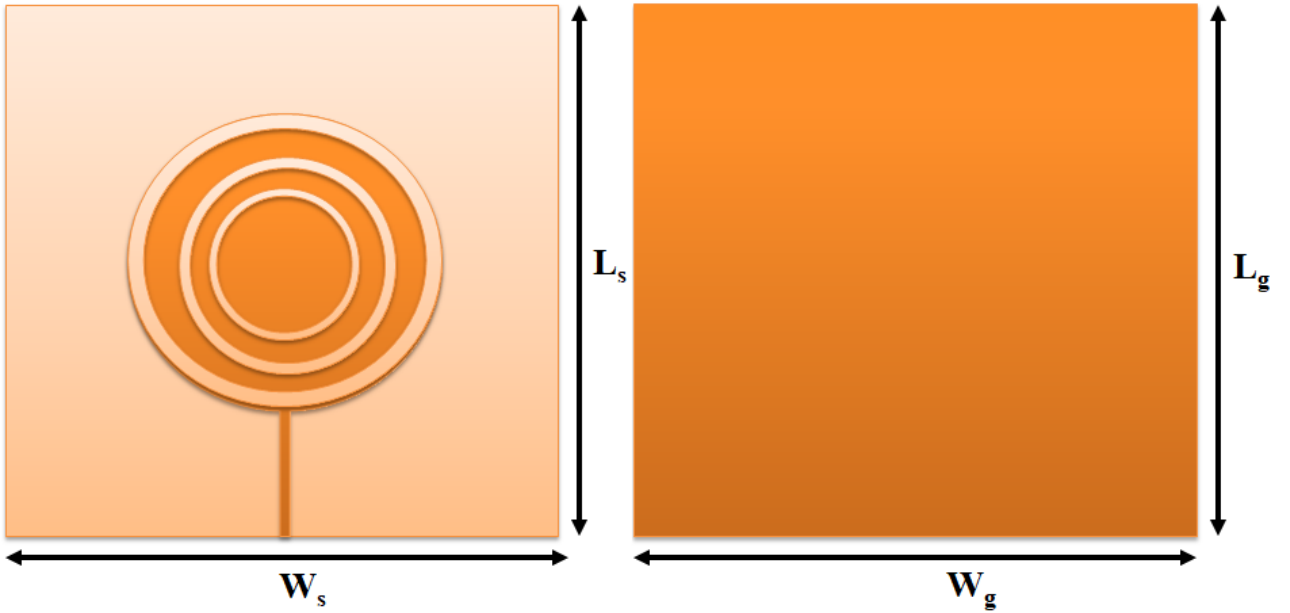
(e) All Three Rings

Fig. 3.2 Front and Back view of Antenna with Infinite Ground Plane

In 2nd step, the ground was reduced from infinite dimensions to some finite dimensions. After size optimization of ground plane rings were added. In this way, desired bandwidth is received with low gain. Antenna 1 presented in Figure 3.3(a) is a basic antenna of circular shape with

finite ground. Bandwidth is enhanced by etching three rings on finite ground step by step which

is shown in Figure 3.3 (a) to (e).
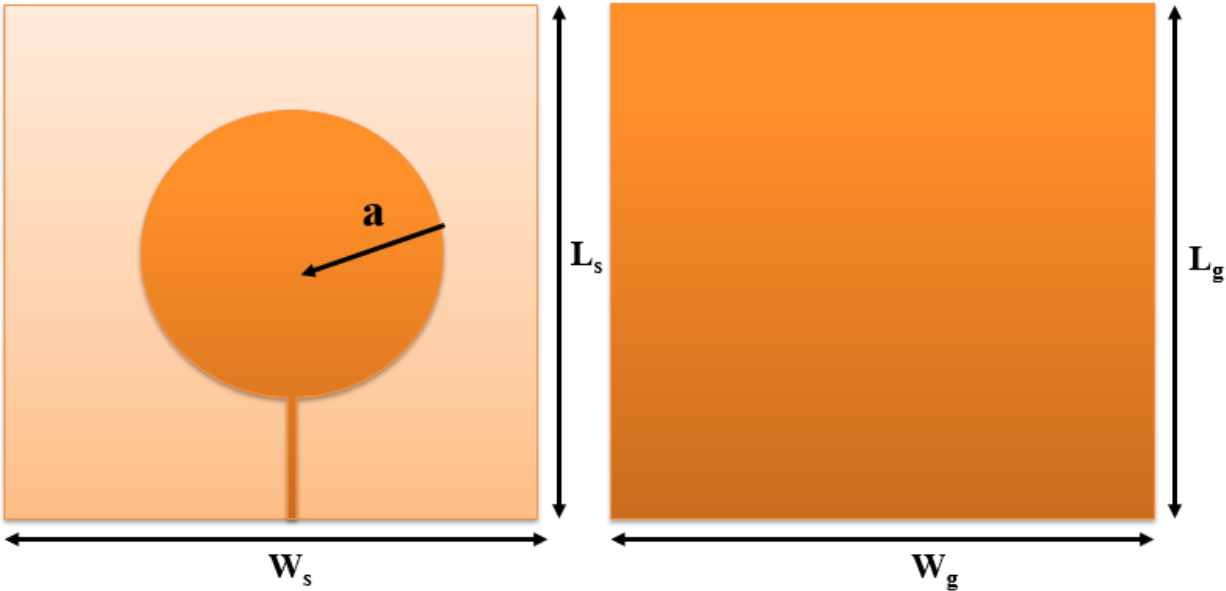
(a) Antenna 1
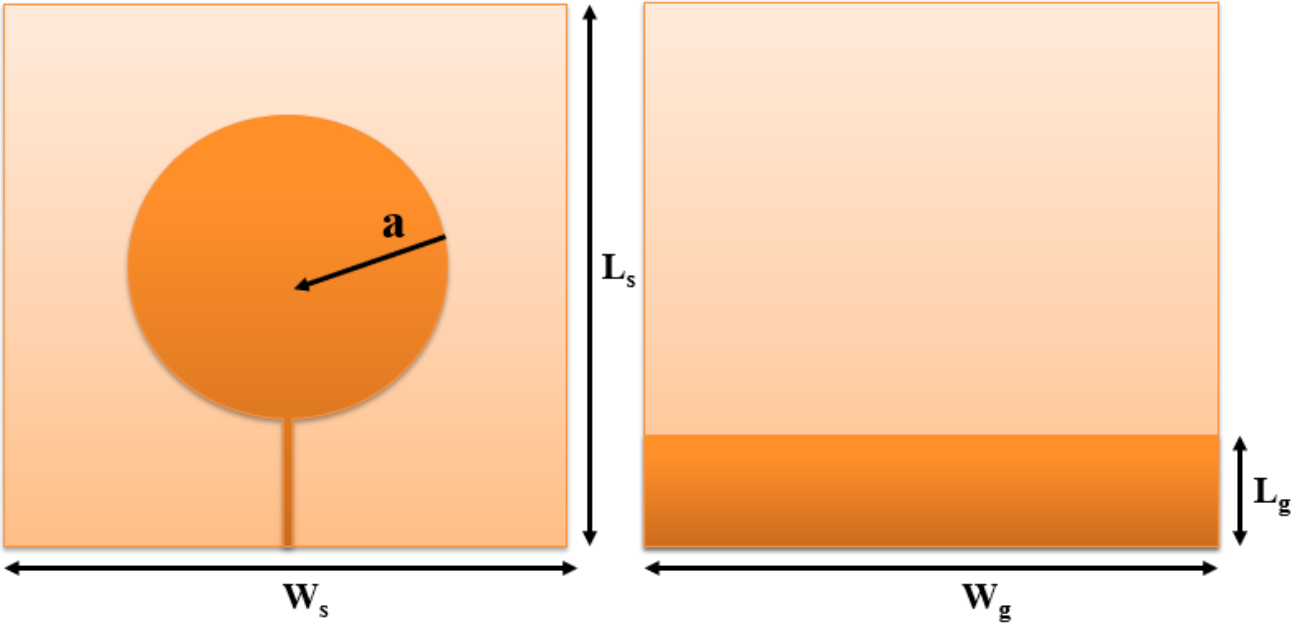
(b) Antenna 2

(c) Antenna 3

(d) Antenna 4
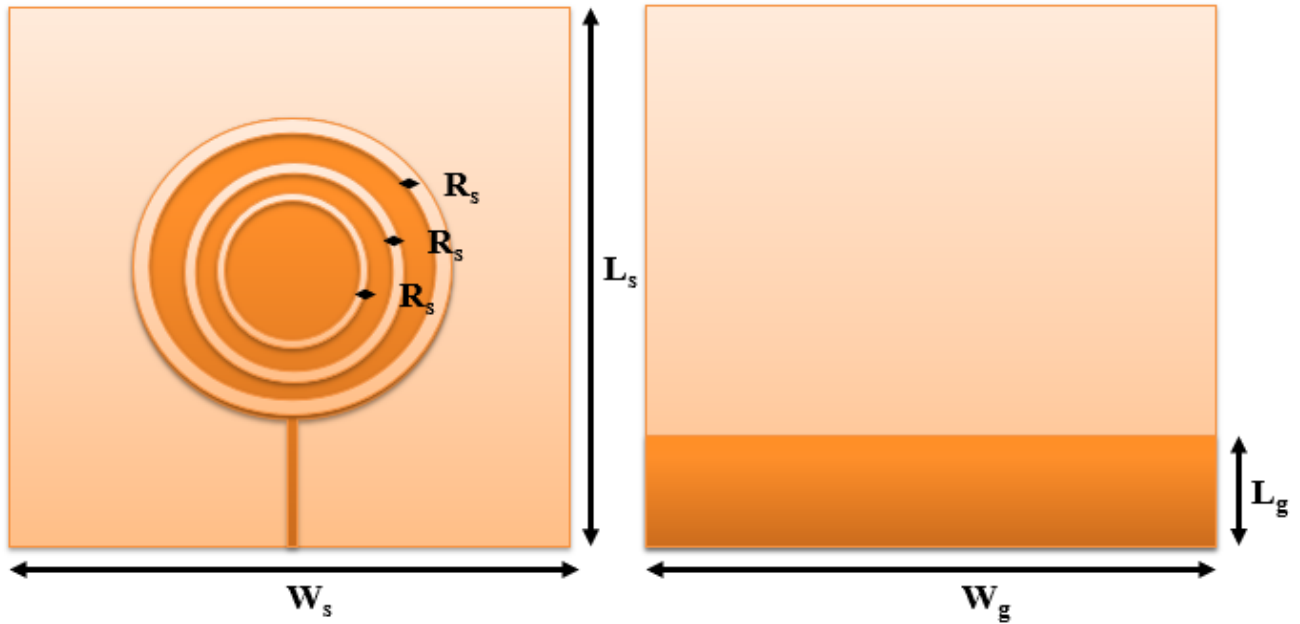
(e) Antenna 5

Fig. 3.3 Front and Back view of Antenna with finite Ground Plane

3.3 Parametric Analysis

The effects of L_g (ground length), R_s (ring size), and adding rings on the finite and infinite ground of the proposed design step by step are discussed in this section.
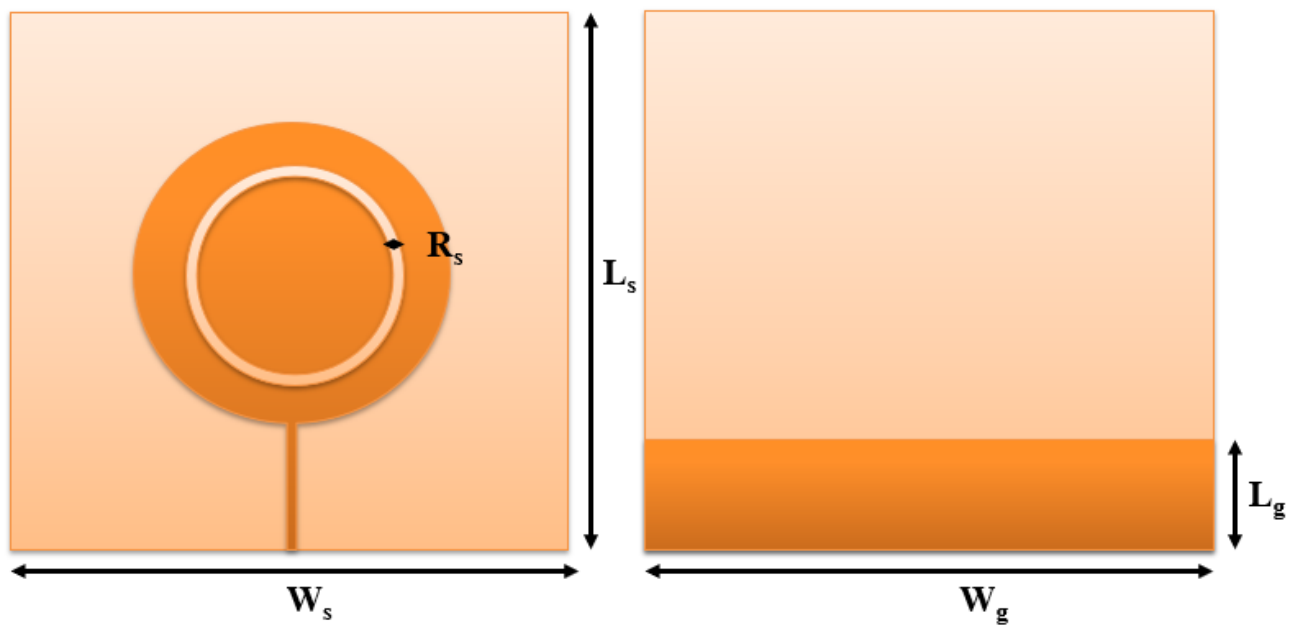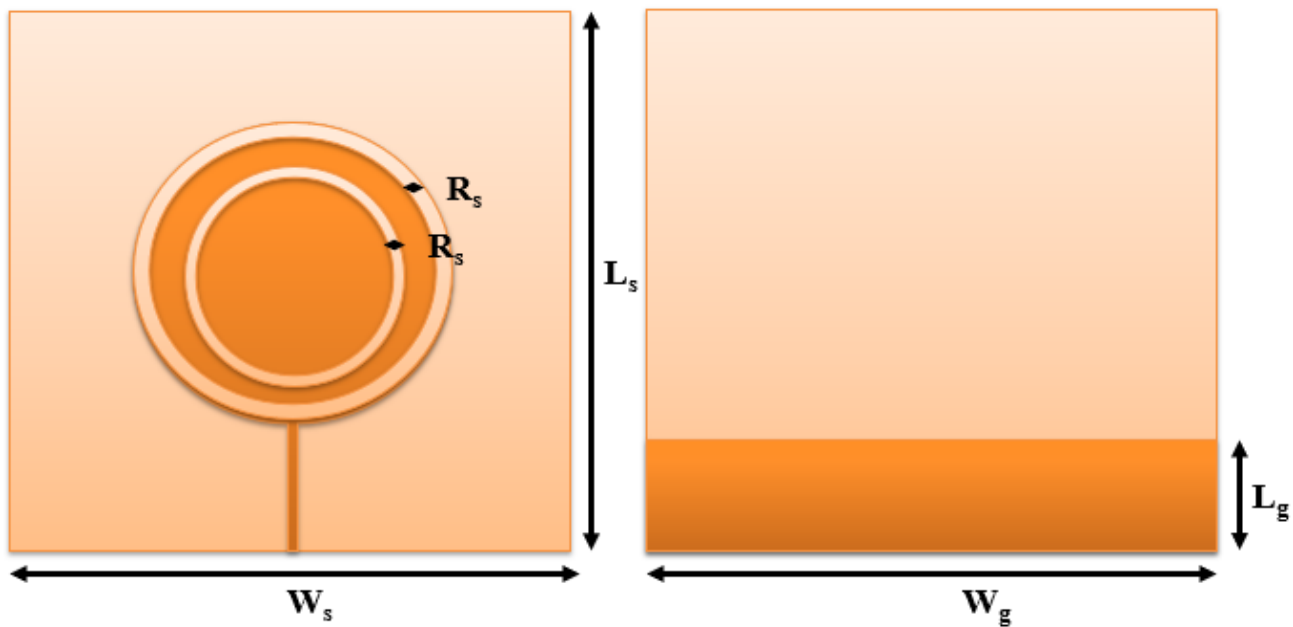
3.3.1 Effects of each ring with infinite ground

Effects of the number of rings on the s-parameter with an infinite ground plane are depicted in Figure 3.4. The resonance of the basic circular patch is 485MHz with a return loss of -22dB. After that 1st ring for 900MHz is etched. The resonance has been shifted from 485MHz to 747MHz with a return loss of -28dB. If only the 2nd ring for 700MHz is etched on the patch resonant frequency shifted to 672MHz. When only the 3rd ring for 500 MHz is added on the outer side of the patch the resonant frequency shifted to a lower frequency of 472MHz. One higher mode is also generated with the effect of 3rd ring at a frequency of 782MHz. When all three rings are added together the resonant frequency is received at 655MHz. It is clear from

Figure 3.4 that after adding all rings resonance is shifted without change in the bandwidth. Bandwidth will be increased when we will play with the ground size. The effect of rings with finite ground size will be explained next.
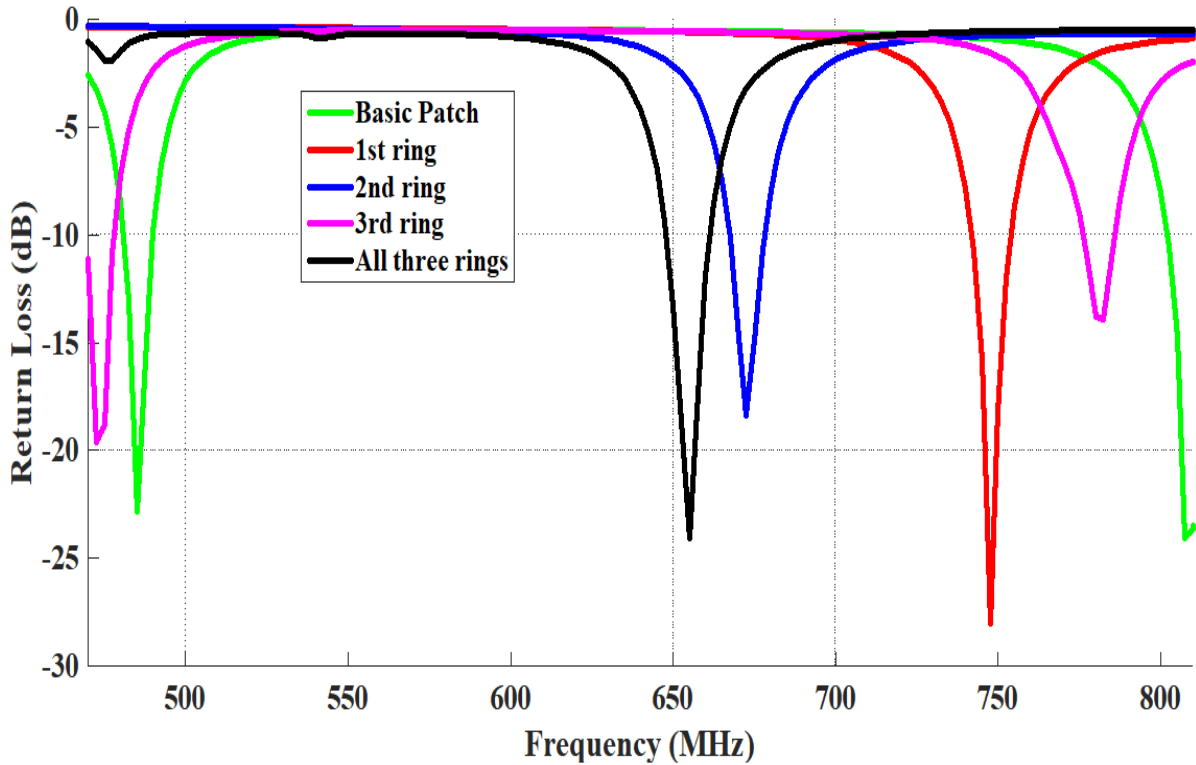
Fig. 3.4 Simulated S_{11} for each ring with infinite ground

3.3.2 Effects of ground size L_g

It was found that after etching rings on the patch, resonant frequency shifted but there is no increment of bandwidth. Parametric analysis has been done to find out the optimum size of the ground plane. The size of L_g is varied from full ground to 80mm. The bandwidth and resonant frequency varied as the length of the ground changed, as depicted in Figure 3.5. A 7MHz bandwidth is achieved at a frequency of 485MHz with a full ground plane ($L_g= W_g$) and 28MHz bandwidth at a frequency of 860MHz with half ground ($L_g= W_g/2$). When $L_g= W_g/4$, the bandwidth achieved is 100% but the resonant frequency is out of the required band i.e. at

1.2GHz. The optimum value of L_g obtained is 80mm with a lower resonant frequency of 220MHz.
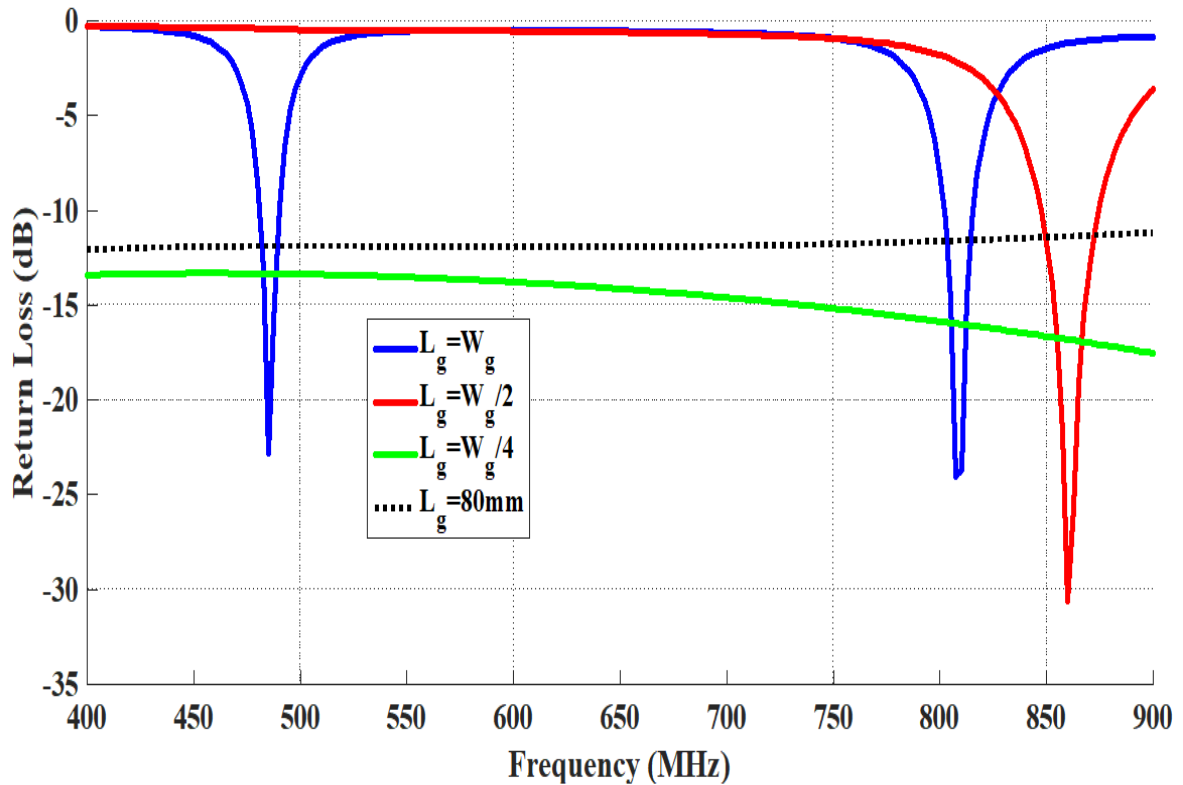
Fig. 3.5 Effect of changing L_g on S_{11} of proposed antenna

3.3.3 Effects of number of rings

Now the effect of the number of rings on the finite ground is studied. It is clear from Figure 3.4 that the number of rings only changed the resonant frequency. Bandwidth will be increased when ground size is reduced. The return loss is improved when the number of rings is etched on the finite ground. In the basic design, the return loss is -22dB at 485MHz. The resonant frequency of the basic patch is 485MHz. In antenna 2, the ground size of the basic patch has been reduced and we found that resonant frequency vanishes from the desired band. In antenna 3, 1st ring is etched on finite ground and the resonant frequency achieved is 512MHz. In antenna 4, when 2 rings are etched on the patch resonant frequency changes to 417MHz. A higher mode is also received at 847MHz which is out of the desired band. In the final design, two resonance

75

has been received at 552MHz and 735MHz with a 100% bandwidth in the desired band of frequencies due to the introduction of the 3rd ring slot as shown in Figure 3.6.
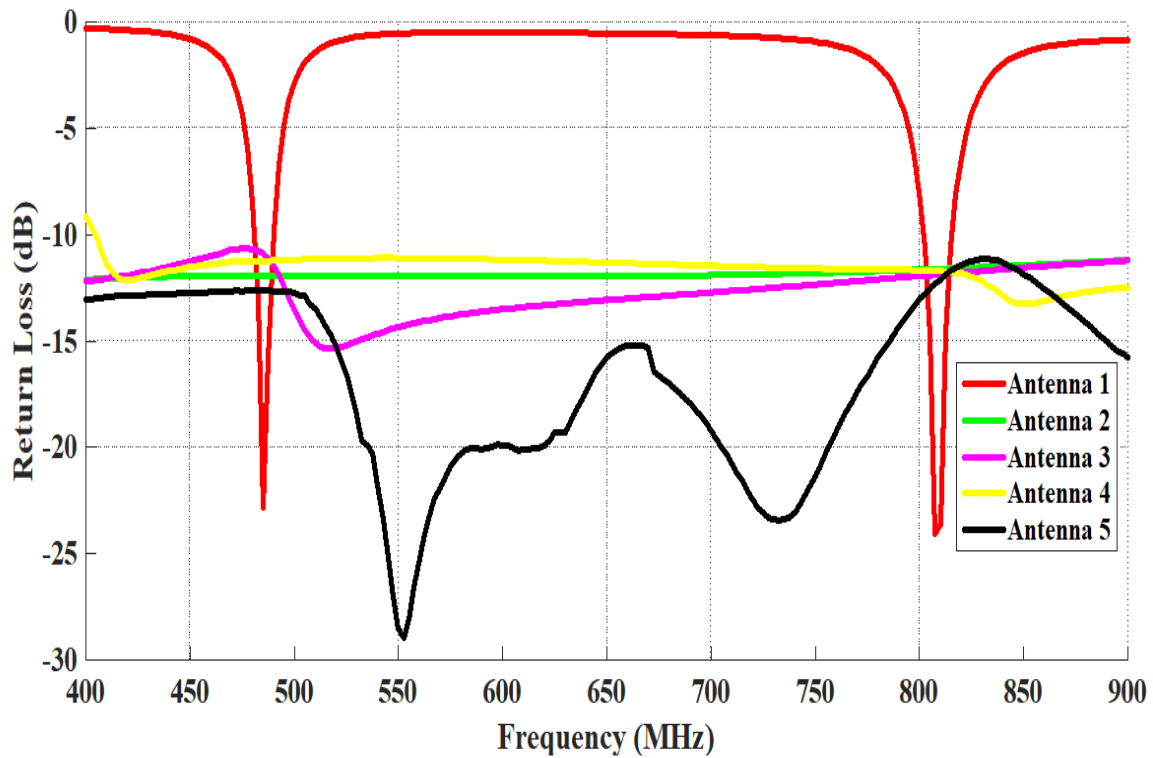
Fig. 3.6 Simulated S-Parameters of etching no of rings step by step.

3.3.4 Effects of ring slot size R$_s$

The effects of the size of the ring are shown in Figure 3.7. The size of the ring (R$_s$) is varied from 0.25mm to 1mm. The bandwidth of the proposed design is increased as the ring size is reduced. For R$_s$ =0.25mm and 0.5mm bandwidth is 100% but in the case of R$_s$ =0.25mm resonant frequency is less than desired with a low value of S$_{11}$. It is observed that the optimum value for R$_s$ is 0.5mm for the best matching of S$_{11}$.
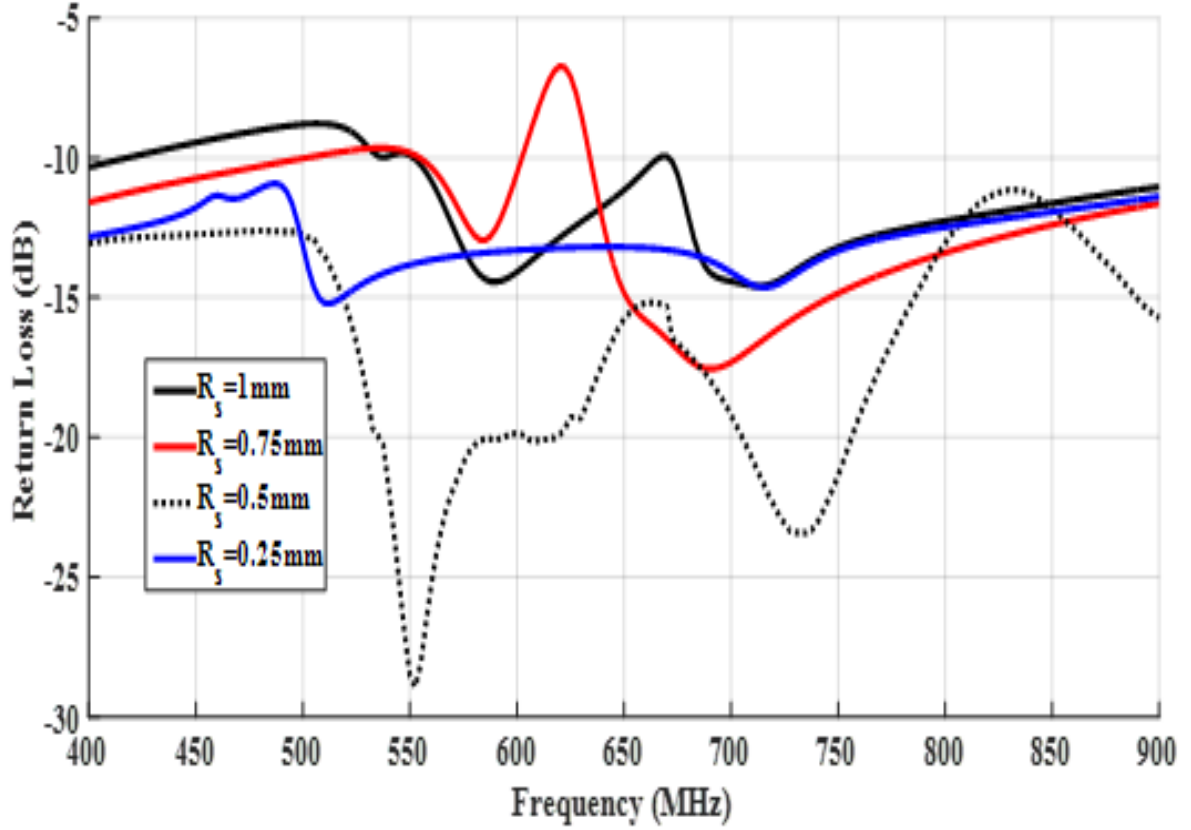
Fig. 3.7 Effect of changing R_s on S_{11} of proposed antenna

3.4 Equivalent Circuit

Figure 3.8 displays the equivalent circuit of the proposed design, which was developed using the S_{11} graph. The real impedance corresponding to resonant frequencies of 552 MHz, 630 MHz, and 735 MHz is noted down. From the following equations, the value of L and C is calculated to make a resonant circuit.

$$C = \frac{Q}{2\pi F_r} \qquad (3.1)$$

$$L = \frac{1}{C(2\pi F_r)^2} \qquad (3.2)$$

77

Where Q denotes the quality factor that is the ratio of F_r and bandwidth. F_r is the resonant frequency. After calculating L and C for three resonant frequencies, the equivalent circuit is designed in the ADS software.
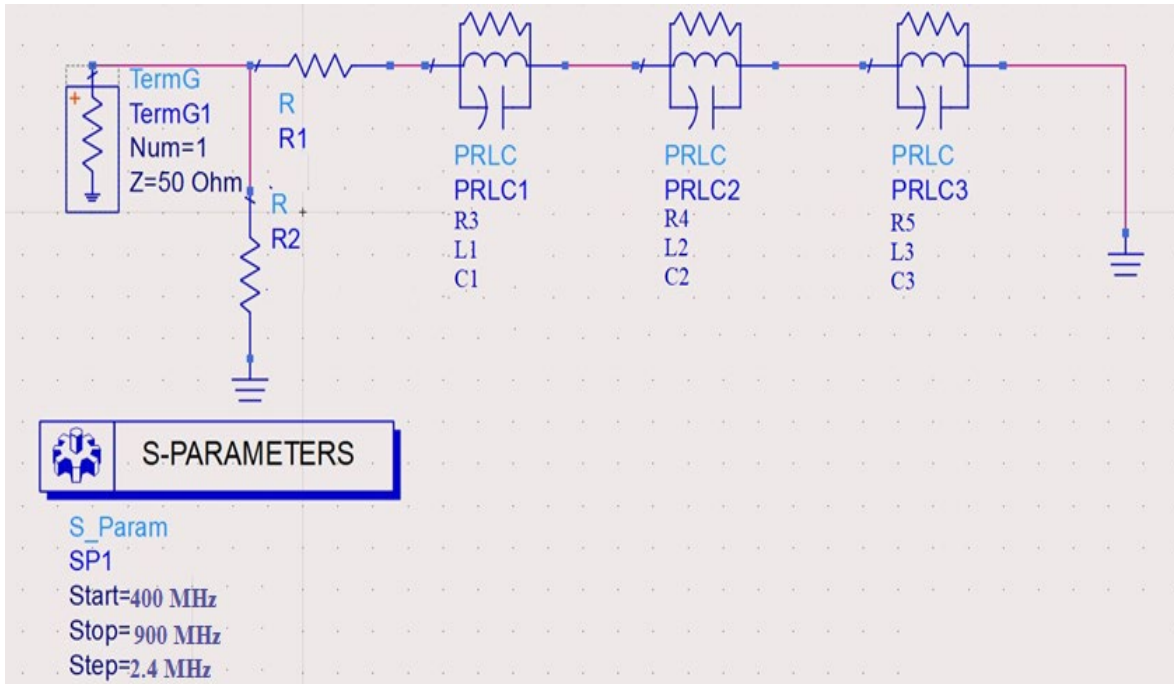
Fig. 3.8 Equivalent Circuit

After optimization the values of components are R1=35Ω, R2=85Ω, R3=54.23Ω, R4=22.81Ω, R5=49.94Ω, L1=2.189nH, L2=1.266nH, L3=1.472nH, C1=0.037nF, C2=0.0504nF and C3=0.0318nF. The S_{11} graph from ADS software is shown in Figure 3.9. There is a minor shift of the resonance but again bandwidth received is 100%. Figure 3.10 compares the S11 of the circuit with the antenna simulation results
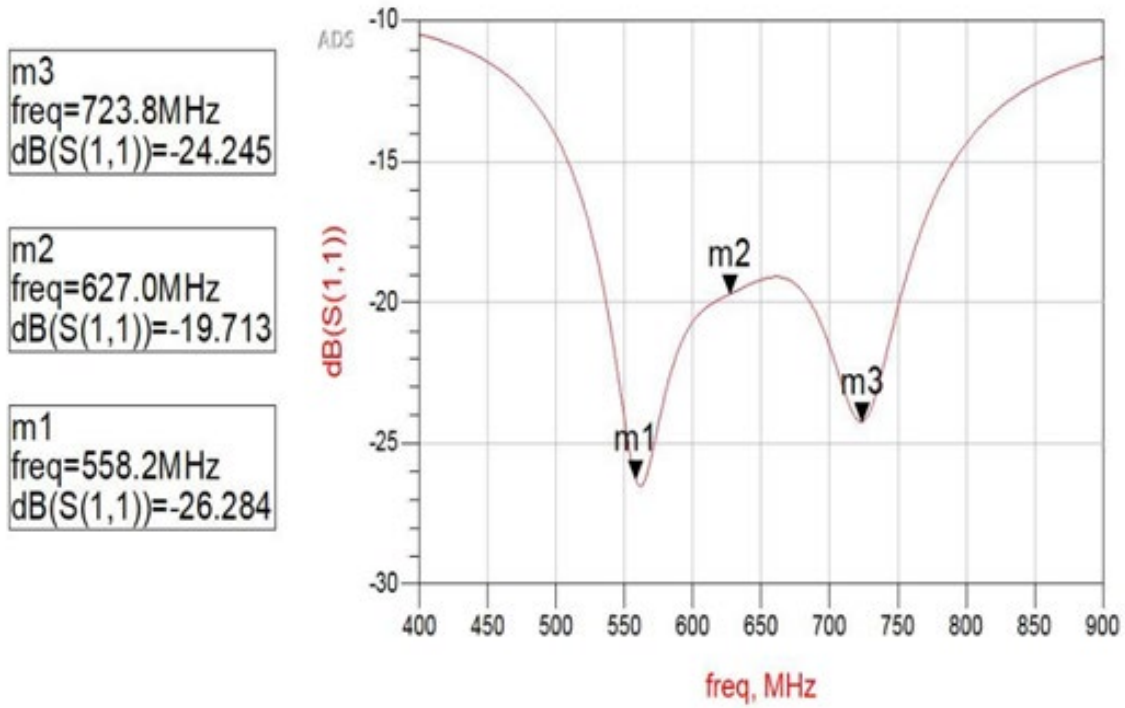
Fig. 3.9 S_{11} plot of equivalent circuit
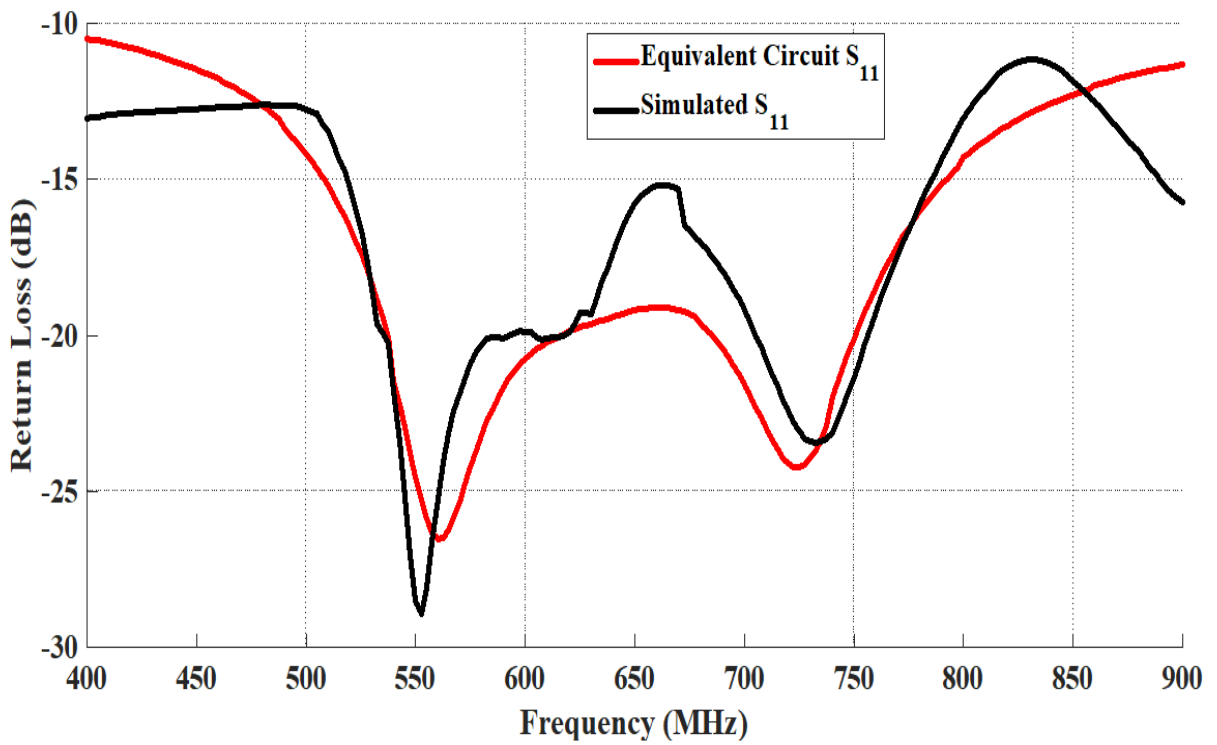
Fig. 3.10 Comparison between equivalent circuit and antenna simulation S_{11}

79

3.5 Simulated and Measured Results

This section compares the simulation results with the hardware measurement. The design was manifested as shown in Figure 3.11, with improved return loss compared to simulation results. Figure 3.12 depicted that the resonance of the fabricated design is at 553 MHz with a return loss of -31dB

Fig. 3.11 Fabricated Antenna

Fig. 3.12 Experimental Return Loss

The simulated and experimental return loss is depicted in Figure 3.13. The resonance of experimental design is 553MHz which is 1MHz greater than simulation result. So, the 0.54 % variation in observed in simulated and experimental results.
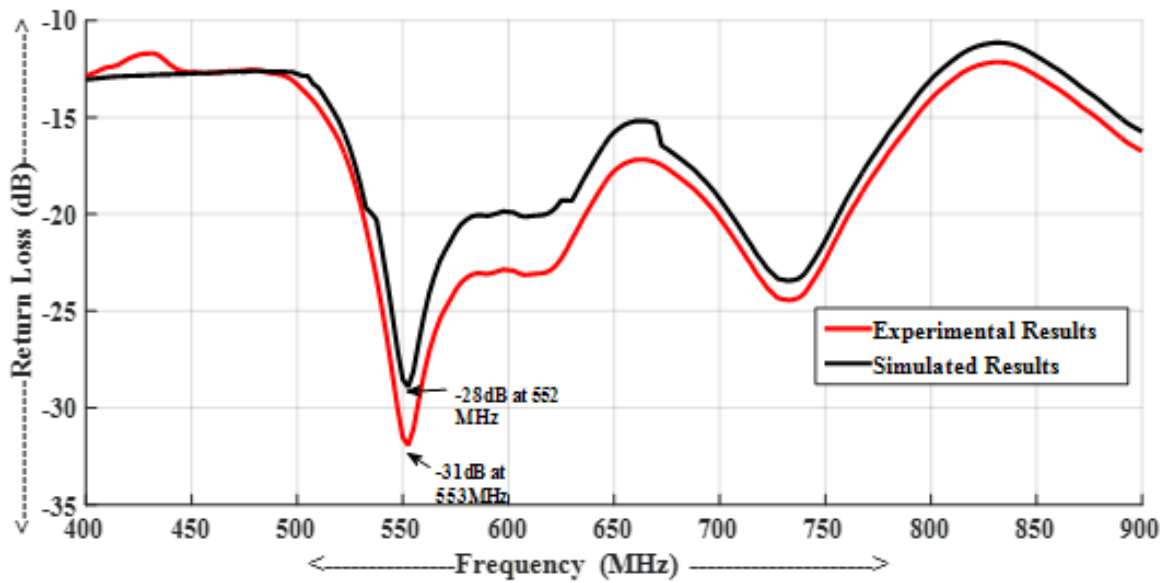
Fig. 3.13 Experimental and Simulated Return Loss

The measured and simulated voltage standing wave ratio is shown in Figure 3.14. The complete desired band (TV band) is received for the impedance bandwidth of $|S_{11}| < 10dB$. The VSWR is below 1.2 for the complete band.
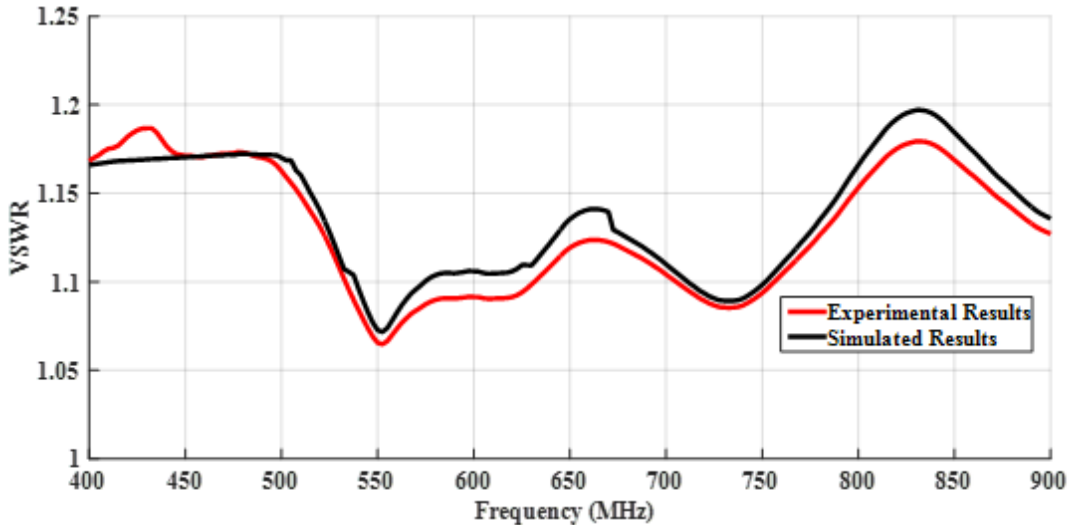
Fig. 3.14 Voltage Standing Wave Ratio of Experimental and Simulated Results

Figure 3.15 depicts the fabricated antenna in the anechoic chamber at the Advance Microwave Lab of the Indian Institute of Technology, Roorkee. The gain and radiation pattern were measured at the lab.
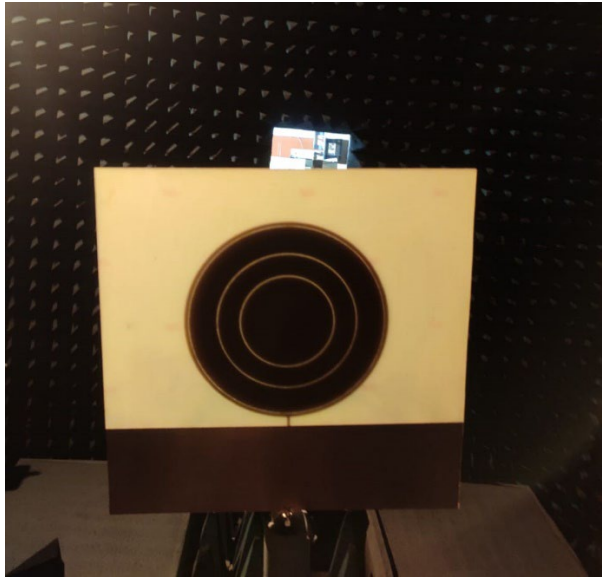
Fig.3.15 Fabricated Antenna in Anechoic Chamber

The experimental and simulated radiation pattern of the proposed design at 553MHz frequency at different phi cuts are shown in Figure 3.16.
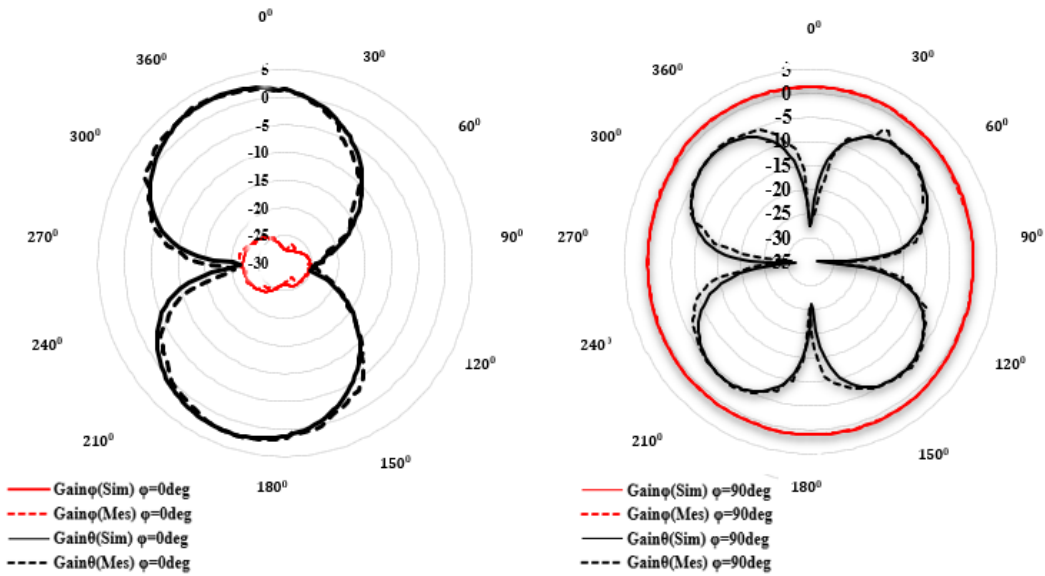
Fig. 3.16 Simulated and measured radiation patterns of the proposed design at 553 MHz

The agreement between simulation and experimental results suggests that the proposed antenna design has been successfully implemented and its performance is consistent with the expected results. The high cross-polarization levels indicate that the antenna is highly directional, radiating less power in undesired directions.

From Figure 3.16 it is clear that the electric field is maximum at 553 MHz frequency as impedance matching is best at this frequency. The electric field intensity at 630 MHz and 735 MHz are shown in Figures 3.18 and 3.19 respectively. The electric field intensity is less at 630MHz as impedance matching at this frequency is low compared to the other two resonant frequencies. But still, all three rings contributed to radiation. The patch is radiated because of three rings etched on it.
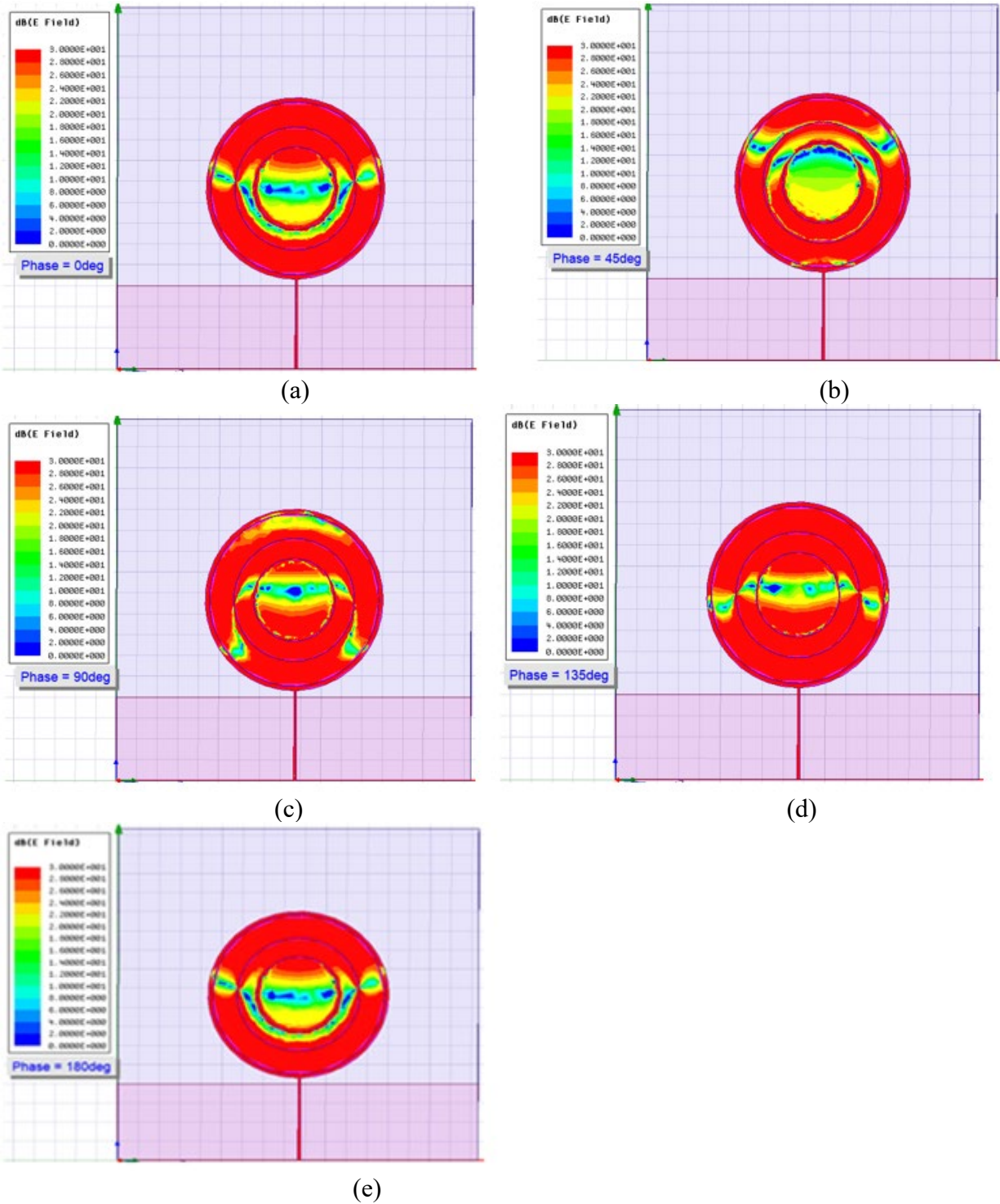
Fig. 3.17 Electric field intensity at (a) 0^0, (b) 45^0, (c) 90^0, (d) 135^0 (e) 180^0 for 553 MHz
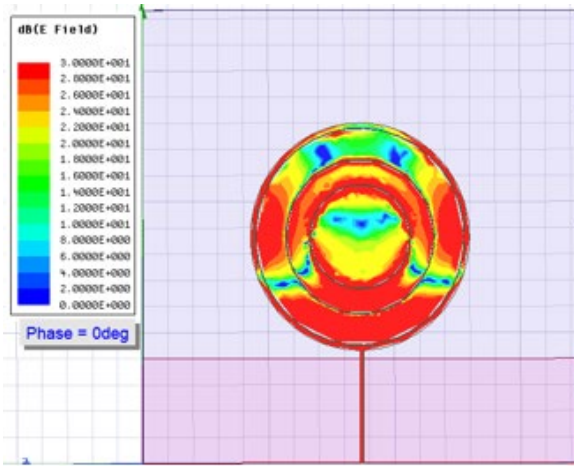
(a)
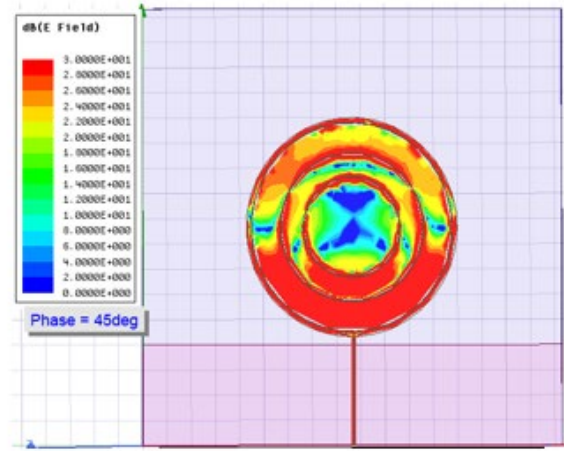
(b)
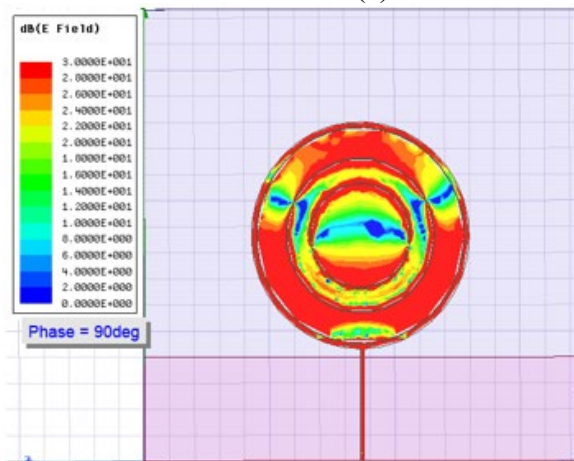
(c)
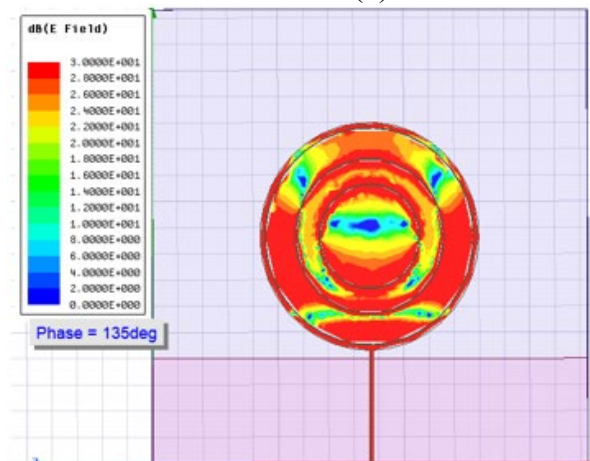
(d)
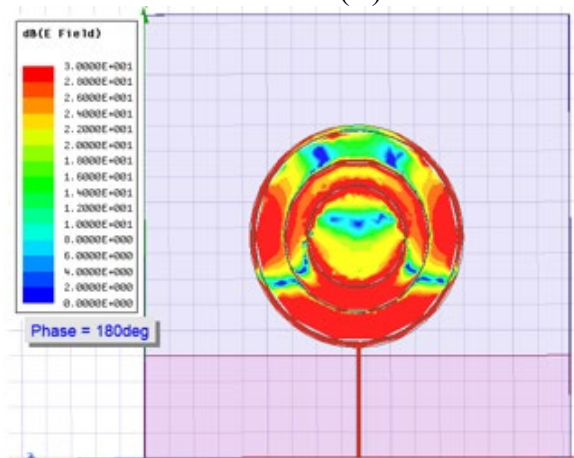
(e)

Fig. 3.18 Electric field intensity at (a) 0^0, (b) 45^0, (c) 90^0, (d) 135^0 (e) 180^0 for 630 MHz
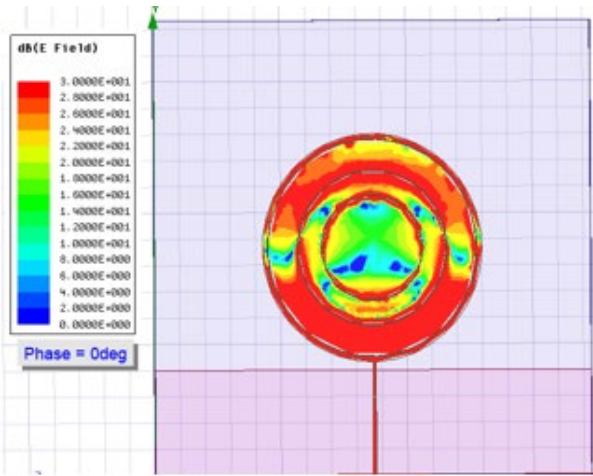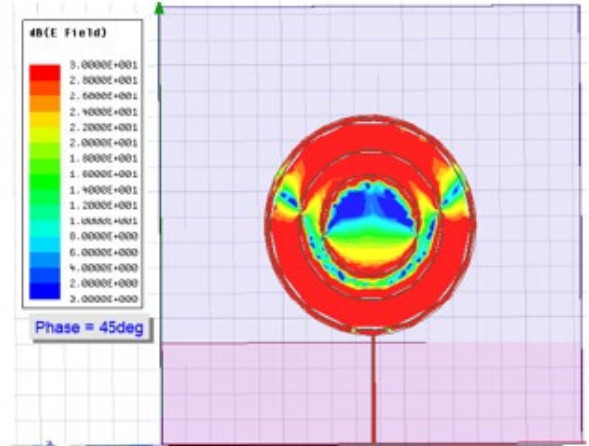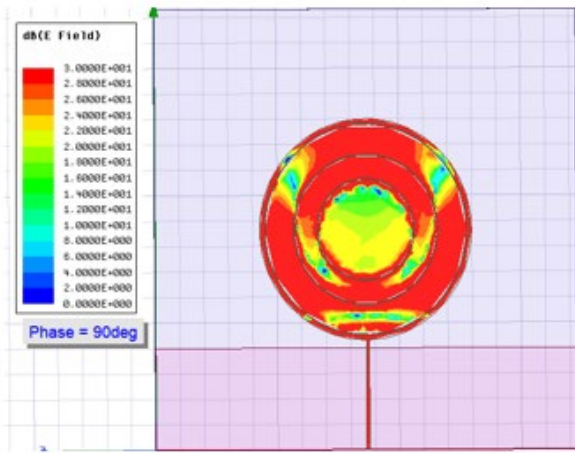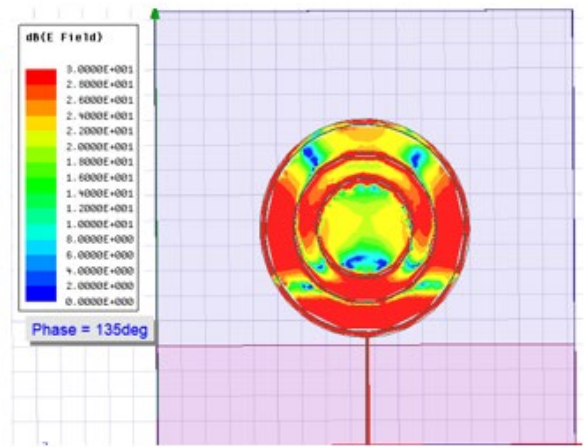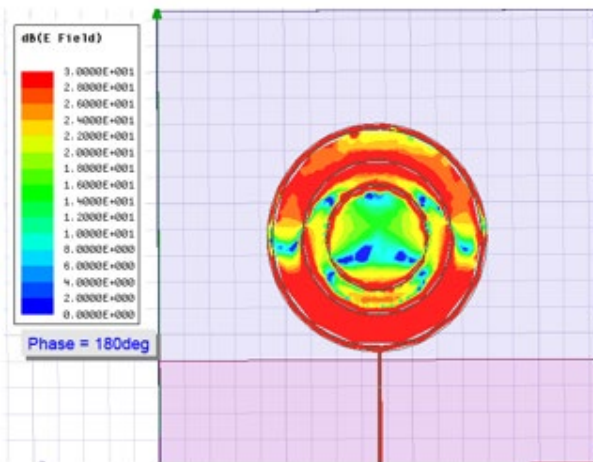
Fig. 3.19 Electric field intensity at (a) 0^0, (b) 45^0, (c) 90^0, (d) 135^0 (e) 180^0 for 735 MHz

3.6 Comparisons of Proposed Antenna with Existing Designs

The parameters of the designed antenna have been compared with already published work in Table 3.1. The proposed antenna is having comparable gain and radiation efficiency with 100% bandwidth. It is found that the designed antenna has a good agreement of gain, bandwidth, VSWR, and efficiency with limited ground size.

Table 3.1 Comparison of Proposed Antenna Performance with the Already Published Work

Reference	Type	Substrate	Gain	Radiation Efficiency	Bandwidth
[25]	Compact Printed slot coupled Bow -Tie	FR4	-2dBi to 1dBi	50%	470MHz-860MHz
[188]	Printed Monopole	FR4	$1-2$dBi	-	460-870MHz
[42]	Triangular patch with meander Line and passive ring	FR4	-	-	470-806MHz
[127]	Wire Antenna	Wire Antenna	1.87dBi	99.6%	13.7MHz
[185]	U-Shaped Printed Patch	FR4	1.4dBi 1.9dBi	76.2%	474-1212MHz
[206]	Circular Patch with rings	Rogers5880	2.5dBi	-	470-987MHz
Present Work	Circular Patch with 3 rings etched	FR4	1.3dBi	92%	400-900MHz

3.7 Conclusion

In this chapter, the compact circular patch antenna is designed and analyzed for the white space TV band. The required bandwidth is achieved by adding circular ring slots at 500MHz, 700MHz, and 900MHz frequencies. Further bandwidth is increased by converting the infinite ground plane into a finite ground plane. The lumped parameters of the equivalent circuit are

calculated and the equivalent circuit is simulated in ADS software. The results of equivalent circuits, simulation, and hardware are in the best agreement. The resonance of the fabricated antenna is 553 MHz with a return loss of -31 dB. The impedance bandwidth is from 400MHz to 900MHz for $|S_{11}| < 10dB$. The gain of the antenna is 1.3dBi with a radiation efficiency of 92%. The value of cross-polarization in dB is very large so, less power is radiated in the undesired direction. The electric field intensity of the antenna is checked at three different frequencies and it is found that all three rings are radiated in the principle plane.

CHAPTER 4

Inverted Stacked Parasitic Patch Antenna for Communication in White Space TV Band

4.1 Introduction

The slotting and shorting techniques were discussed in previous chapters for bandwidth enhancement. But, these two techniques did not contribute to high gain. One of the concerns of the microstrip patch antenna is the low gain. In literature [61,154,156,43,36,118,101], many designs have been proposed to alleviate the problems of narrow bandwidth and gain. These methods can be broadly classified and briefly explained below:

- Broadband matching

- Increasing the thickness of the substrate

- Introducing parasitic elements either in coplanar or in a multilayer configuration

- Performing slots in the patch radiator

- High permittivity material

- Combination of the above-said techniques

Broadband matching [125] involves the joining of a lossless matching network to the patch antenna. The matching network can be a part of the feed to the antenna without changing the shape of the antenna. In this method, maximum input can be coupled to the antenna.

By changing the substrate thickness the antenna parameter can be improved but the use of a thicker substrate with low permittivity is not usually desirable [203].

Multilayer or stacking [114, 115, 24, 69, 60, 8, 105, 106, 137, 50] of microstrip patches may also increase the bandwidth, gain, and efficiency of the antenna. Multilayer elements are used more widely than broadband matching [82]. It involves the use of more than one patch element to provide multiple closely spaced resonant frequencies. The dimensions of the antenna may be decreased by embedding it in a high-permittivity material. Microstrip patch radiator using the stacked configuration increases the bandwidth [139]. To obtain larger bandwidth and good surface wave efficiency, it is shown that the thickness of each layer should be more with less dielectric constant. If a combination of different dielectric constant materials is used for the patches better impedance matching is achieved. In the design process of stacked patch antennas, generally, the lower patch is designed as more capacitive rather than for minimum return loss in the desired band of frequency. This is accomplished by exciting the antenna at the edge of the patch. Also, by adding the second patch the capacitive impedance region can be shifted to a near impedance matching so that the bandwidth and gain are improved [136]. Several techniques have been proposed to reduce the dimensions of the antenna [204]. These include introducing slots, shorting pins or plates, and combinations of these techniques [185]. The ultimate purpose of these techniques is to make the antenna smaller and obtain resonance at a desired frequency in a smaller dimension. But this smallness of dimension in the antenna is achieved at the cost of bandwidth and sometimes the radiation or antenna efficiency. At times decrease in bandwidth is acceptable depending on what applications the antennas are to be used for. The main tools for reducing the size of the patch such as making slots in the patch have been dealt with in chapter 3. Using of the shorting pins or plates to reduce the antenna size is explained in the literature [155, 197, 91, 137]. If a standard microstrip antenna is designed for one particular frequency, then the antenna loaded with shorting post or plate can realize the same frequency at half of the size of the microstrip antenna [91]. Placing a shorting pin means

that the ground plane or zero-potential plane is short-circuited to the patch with the dominant mode. Generally, these pins are used to reduce the size, operate at multi-frequency, change polarization, etc [51]. The parameters of the ordinary microstrip antenna can be changed depending on the radius of the post, its length, and the number of posts placed.

In this chapter, larger bandwidth is achieved through two stacked configurations. In the first layer circular patch is used which is shorted to the ground at the center and feed is provided to patch from the edge of the patch. In the second layer, two circular patches on FR4 substrate are placed in the inverted position. 2nd layer is parasitically attached to the first layer. The dielectric used between 1st and 2nd layers is air.

The design methodology used in this chapter is explained in Figure 4.1.
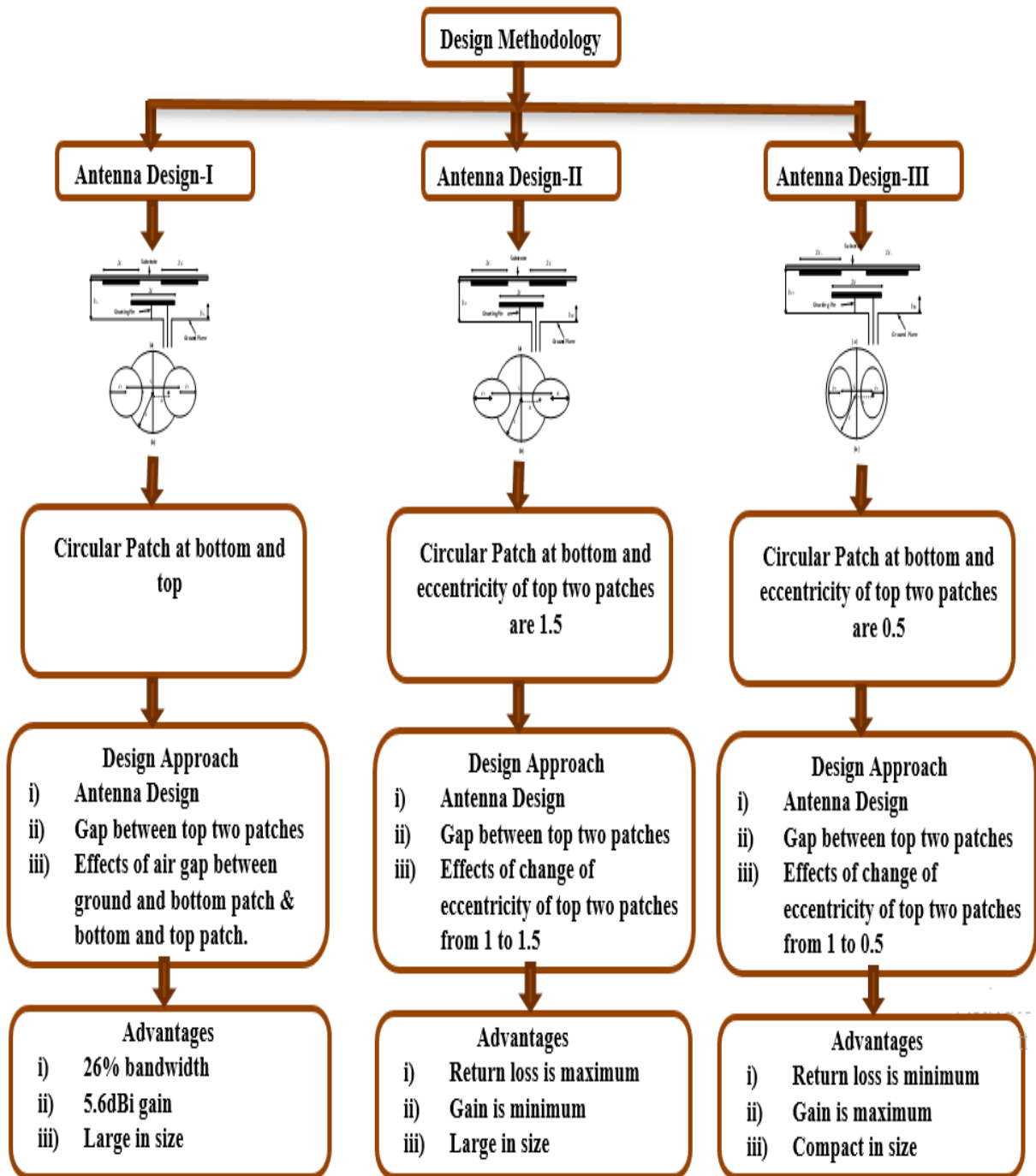
Fig.4.1 Design Methodology of proposed antenna

4.2 Antenna Design

To increase the performance parameters of an antenna, a stacked configuration is explained in detail in this chapter. The effect of the shorting pin along with the stack has also been studied. The stacked microstrip patch antenna consists of two printed patches. Two layers of dielectrics should be placed one over the other. On the dielectric layers, the patches are printed. Generally, the excitation is given to the lower patch, hence this patch is known as the driven patch. The patch placed over the lower patch is known as the parasitic patch and is coupled to the driven patch electromagnetically. The dielectric constant of the lower patch should be high when compared to that of the upper patch to achieve a higher magnitude of the first-order mode on the driven patch than on the parasitic patch. Also, the current distribution on the lower patch will contribute to increasing the bandwidth by coupling the power to the upper patch. In this chapter three different stacked configuration is proposed so that the designer will not depend only on one design. The designer can use any configuration depending on the requirements and parameters of the antenna.

4.2.1 Design and Analysis of Antenna Design-I

In Antenna Design-I lower dielectric used is air. FR4 is used at the upper layer and placed in an inverted position as shown in Figure 4.2. 'r' is the radius of a lower patch, placed 18mm above the ground plane. 'r_1' is the radius of upper patches which are placed at 47mm above the lower patch. FR4 is placed 65mm above the ground plane with a thickness of 1.6mm. The spacing between the center of the top patches is 105mm.
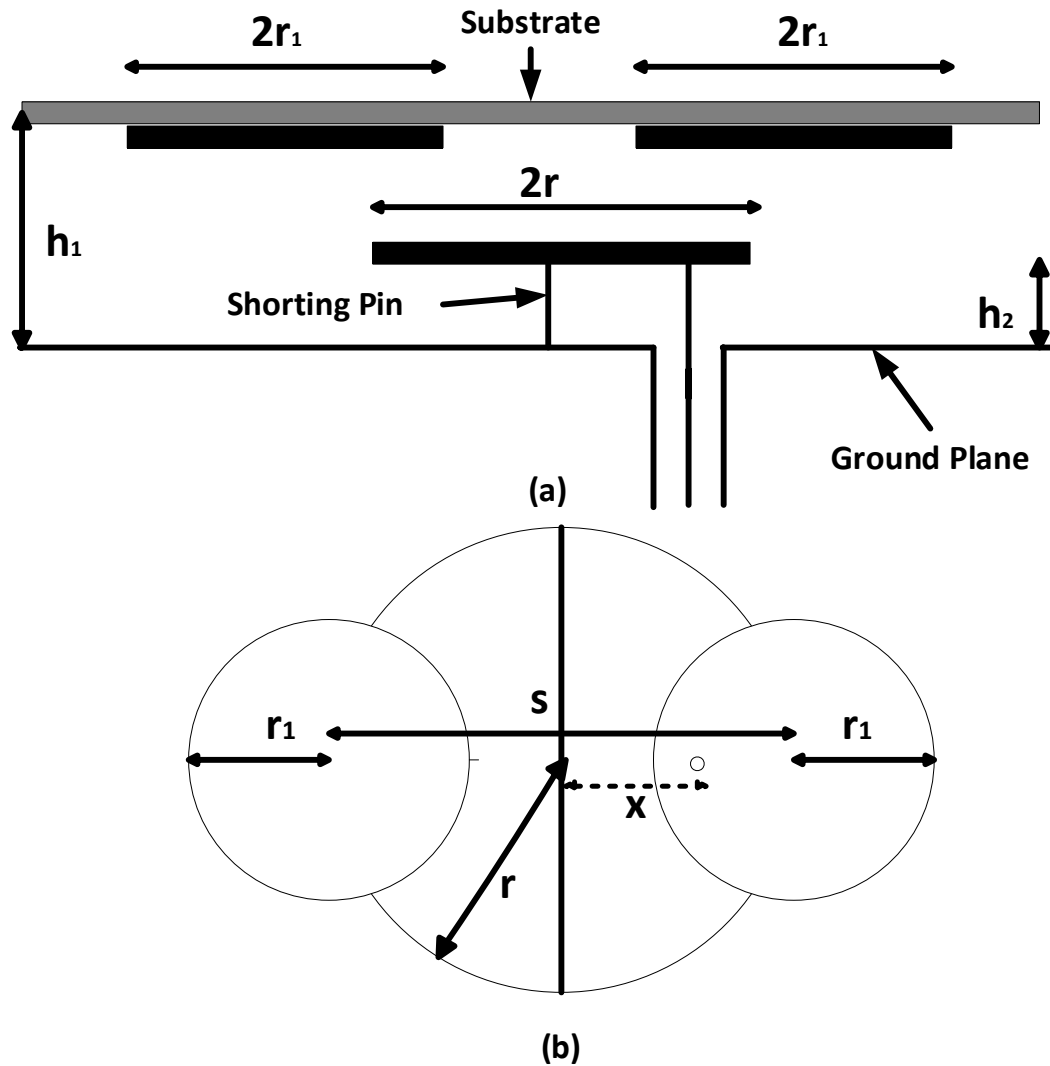
Fig. 4.2 (a) Side view of antenna design-I (b) Top view

All these dimensions are taken after parametric analysis which will be discussed further. In this chapter, the antenna is designed for a frequency band of 470-770MHz. The lower patch is designed for the lower frequency with the help of circular patch design equations given in Chapter 2. Upper patches are corresponding to a higher frequency of the desired band. Co-axial feed is used to provide the excitation to the lower patch. The upper patch is parasitic and excited due to electromagnetic effects from the driven patch. The driven patch is shorted to the ground with the help of shorting pin of 10mm diameter. The final size of the antenna is 0.6λ x 0.7λ x 0.1λ.

4.2.2 Design and Analysis of Antenna Design-II

In this design, the top circles are converted into ellipses in the x-direction. All remaining parameters are kept constant. By changing the circle in to ellipse the conducting part of the top two patches changed. The dimensions of patch are given in mm as: r_1= 80, r=165, s=135, x=120, h_1 =65, h_2 =18, substrate thickness=1.6, eccentricity of top two patches=1.5. The proposed design is shown in Figure 4.3.
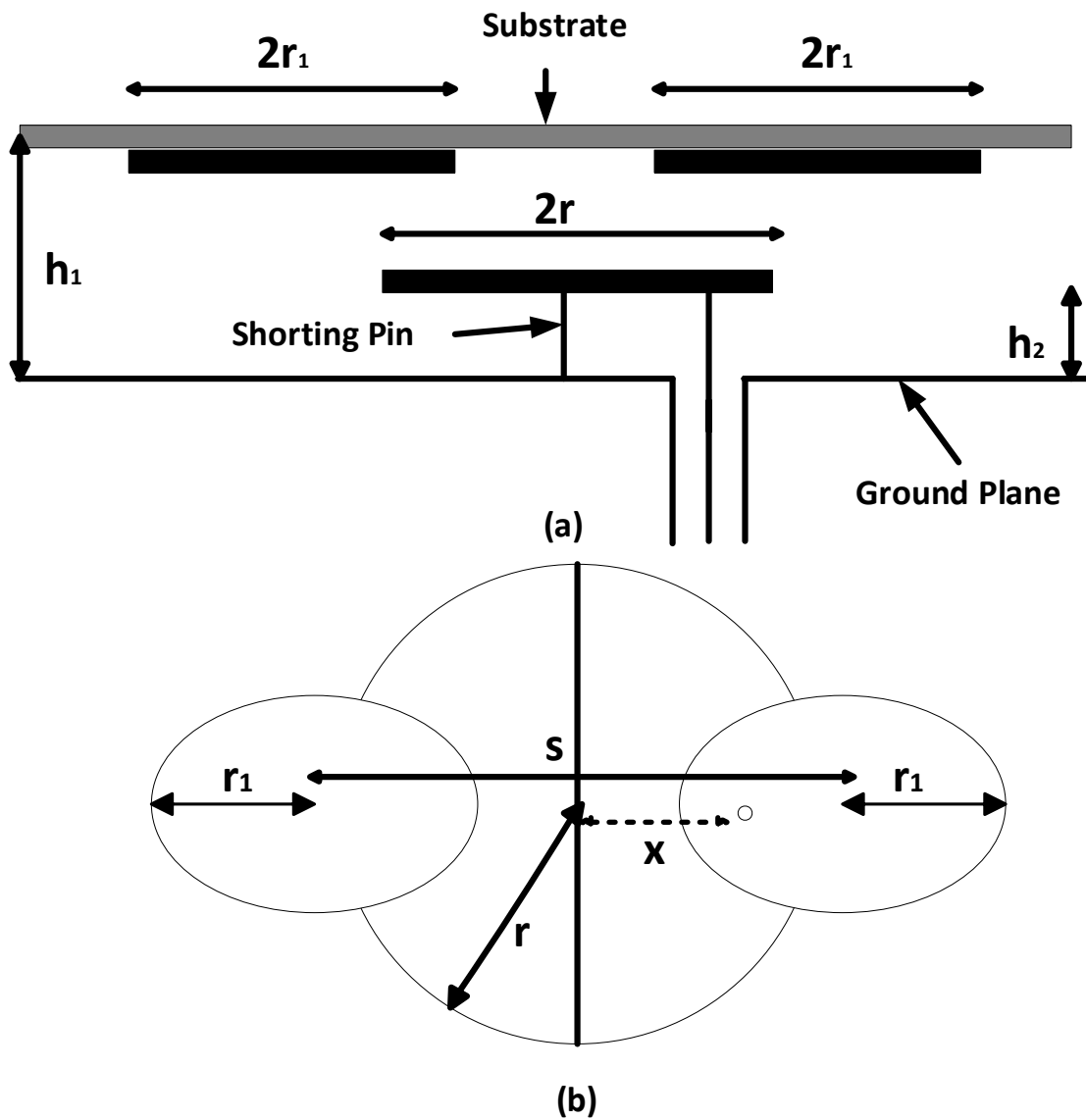
Fig. 4.3. (a) Side and (b) top view of antenna design- II (e=1.5)

4.2.3 Design and Analysis of Antenna Design-III

In antenna, design-III the orientation of the top two parasitic patches of antenna design-II is changed from x to y. Keeping all other parameters constant the dimensions of the proposed design are (all dimensions in mm): r_1= 80, r=165, s=80, x=120, h_1 =65, h_2 =18, substrate thickness=1.6, the eccentricity of top two patches=0.5. The proposed design is shown in Figure 4.4. If the size of all three designs is compared then design-III is having lowest physical dimensions.
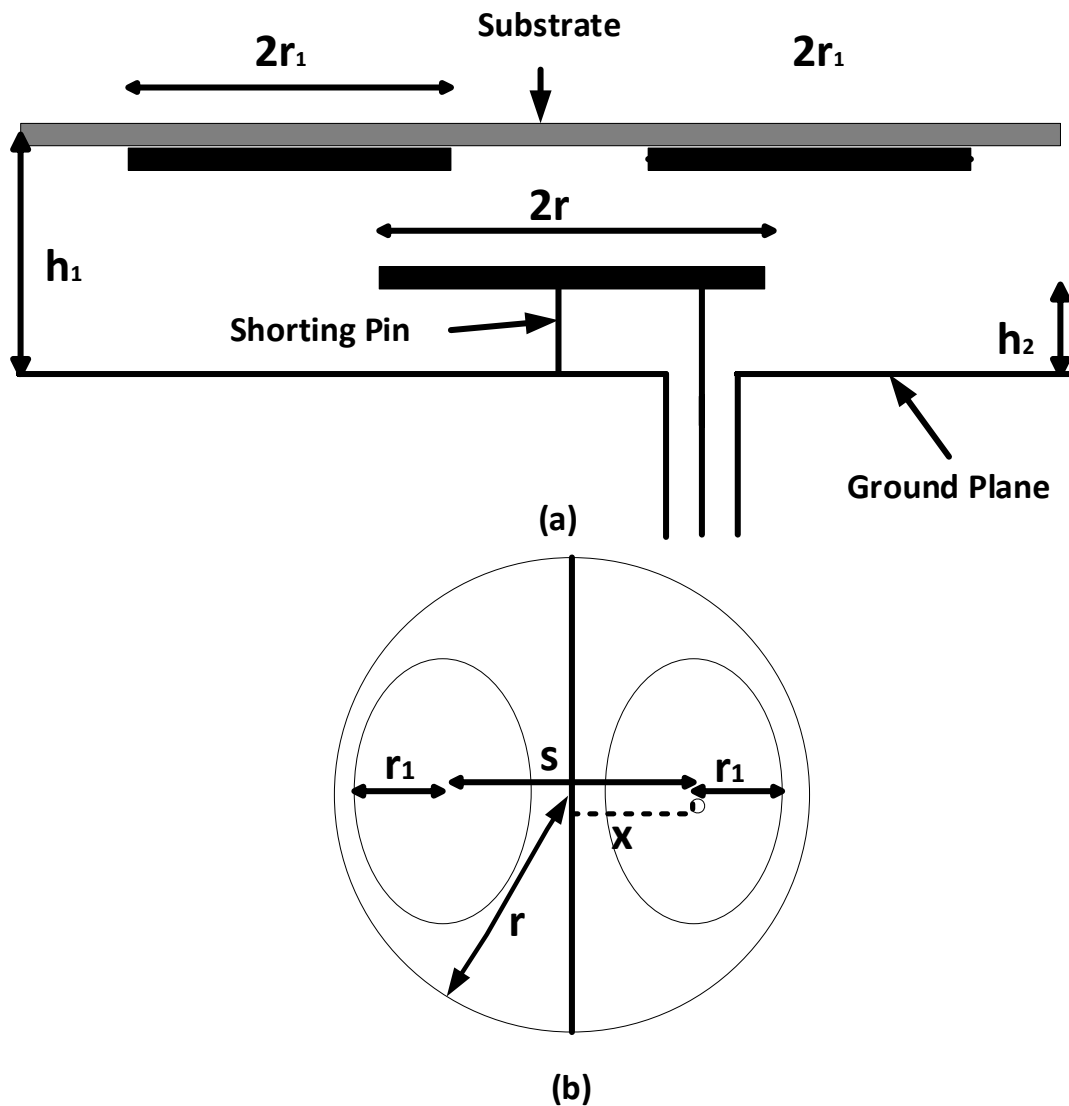
Fig. 4.4. (a) Side and (b) top view of antenna design-III (e=0.5)

4.3 Parametric analysis of the antenna

This section contains the antenna design procedure and parametric studies (the gap between the ground and lower patch "h2", the gap between ground and upper patch "h1", the distance between the top two patches "s", and feed location "x").

4.3.1 Effects of air gap between the ground and lower patch (h_2)

The air gap between the ground and 1st layer is varied from 0mm to 21mm. It is found that as the air gap increased from 0mm the return loss gets improved but after a certain value return loss again starts to deteriorate. The optimized value of h_2 is 18mm at which return loss is best as compared to other values of h_2 as shown in Figure 4.5. The design is less sensitive to the air gap between the patch and ground as by varying the distance only return loss is changing without a change in resonance of the antenna. Hight of the feed is also varying corresponding to the gap between the driven patch and the ground that's why the design is less sensitive to the air gap between the driven patch and the ground.
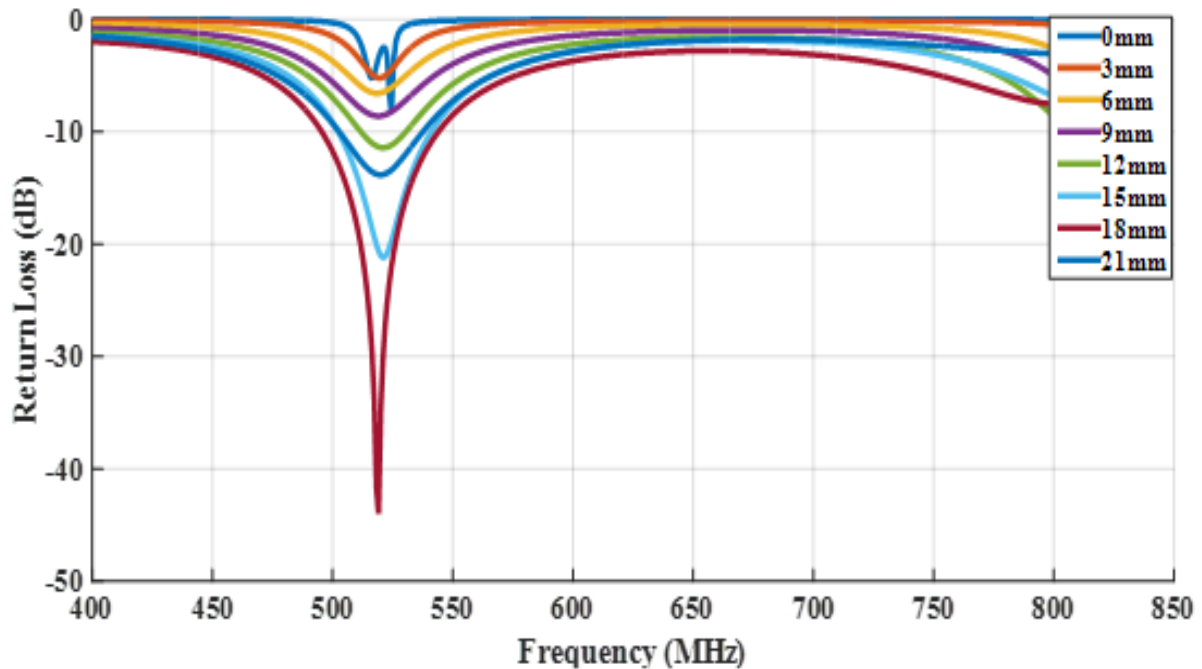
Fig. 4.5 Parametric analysis of the antenna using gap between ground & patch 'h_2'

4.3.2 Effects of air gap between the ground and passive patch (h_1)

The air gap between the ground and parasitic patch is varied in this section. "h_1" is varied from 20mm to 70mm to find out the effects on the performance of the design-I as shown in Figure 4.6. It is observed from the figure that the resonance has been varied from 425MHz to 534MHz. The design is sensitive to the air gap between ground and parasitic patches as the air gap is varied the electromagnetic signal coupled to the parasitic patch is also varied. The return loss is varied between -10.9 dB to -43 dB. The optimized value of "h_1" is 65mm which gives a return loss value of -43 dB at 521 MHz frequency.
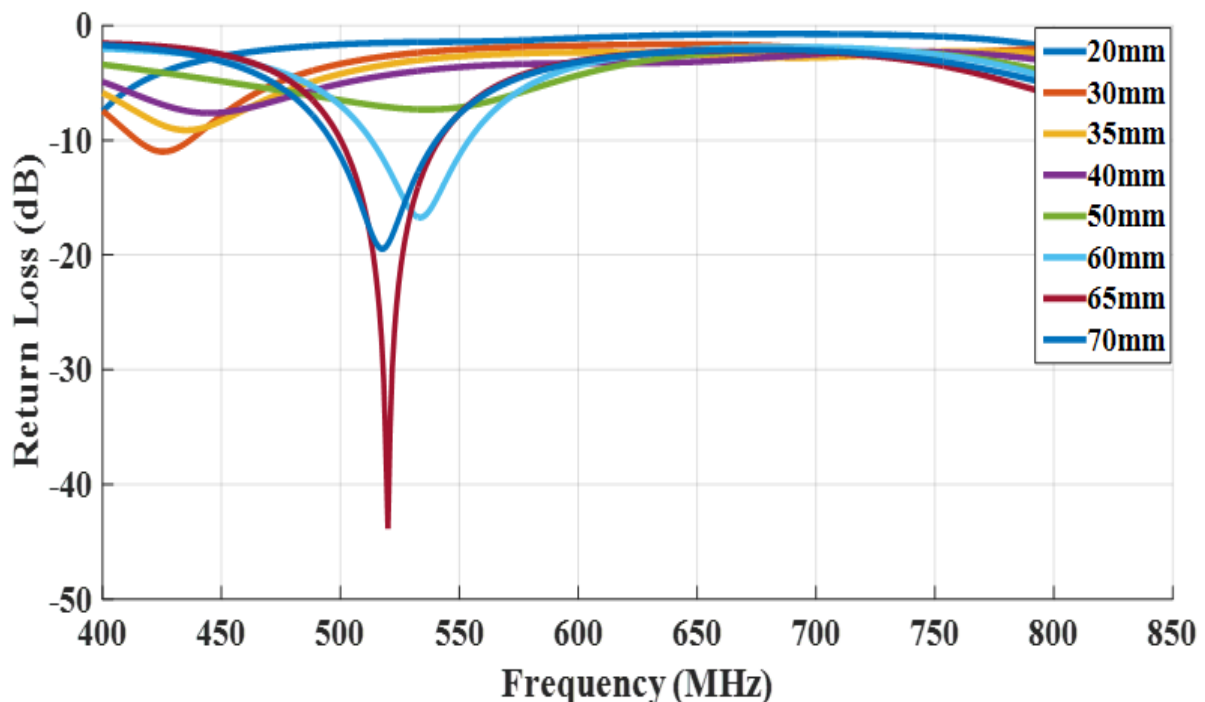
Fig. 4.6 Parametric analysis of the antenna using gap between ground & passive patch 'h_1'

4.3.3 Feed location 'x'

Co-axial feed is given to the driven patch at the 1st layer. The optimized position of the feed is calculated by parametric analysis. The location of the feed is varied from 95mm to 125 mm in the x-direction. As the location of the feed is moving away from the center return loss is

improved. The optimized position of the feed is 120mm as shown in Figure 4.7. At the 120mm location return loss is -43 dB at 521 MHz frequency. If the location is changed further from 120mm to 125mm return loss start reducing from -43dB to -29 dB.
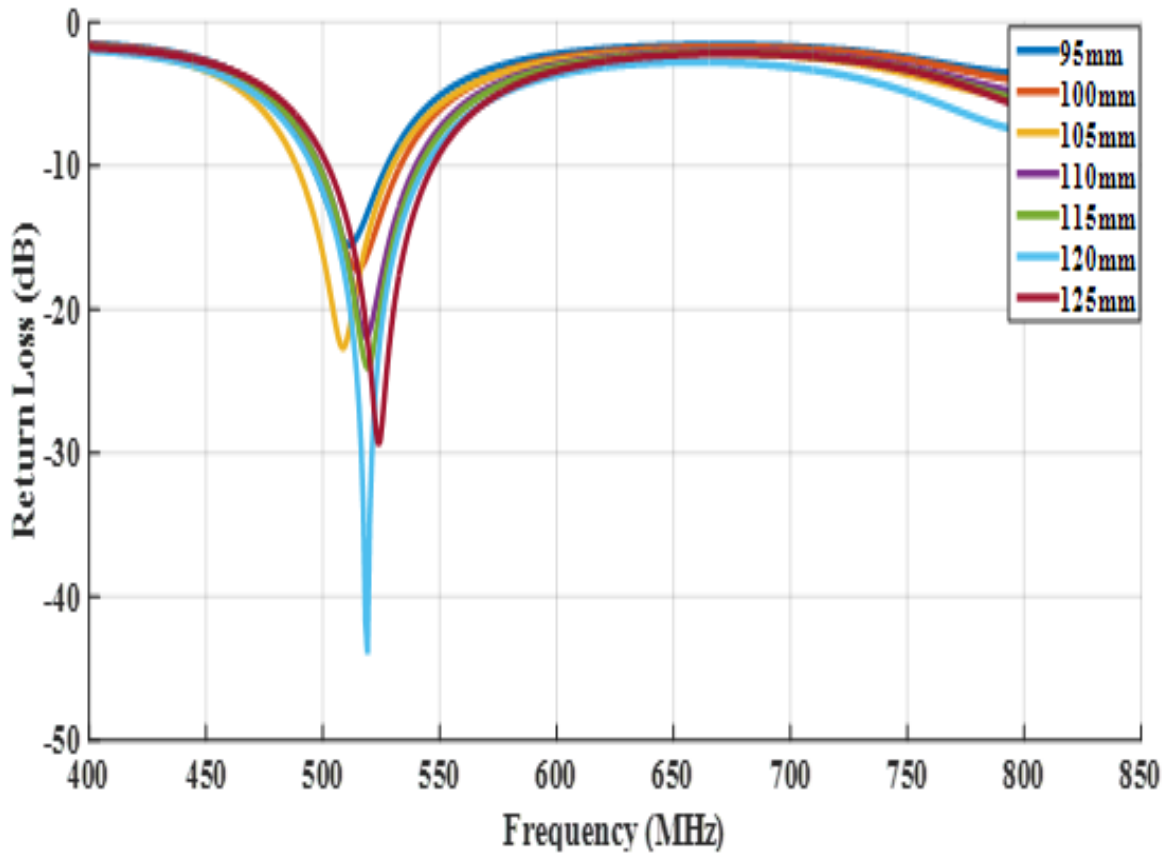
Fig. 4.7 Parametric analysis of the feed location 'x'

4.3.4 Effects of the distance between the top two patches (s)

After optimization of all other parameters, the distance between the top two circular patches is also found by parametric analysis. The distance between the center of the top two patches varied from 90mm to 170mm. From Figure 4.8 the optimized value of 's' is 105mm.
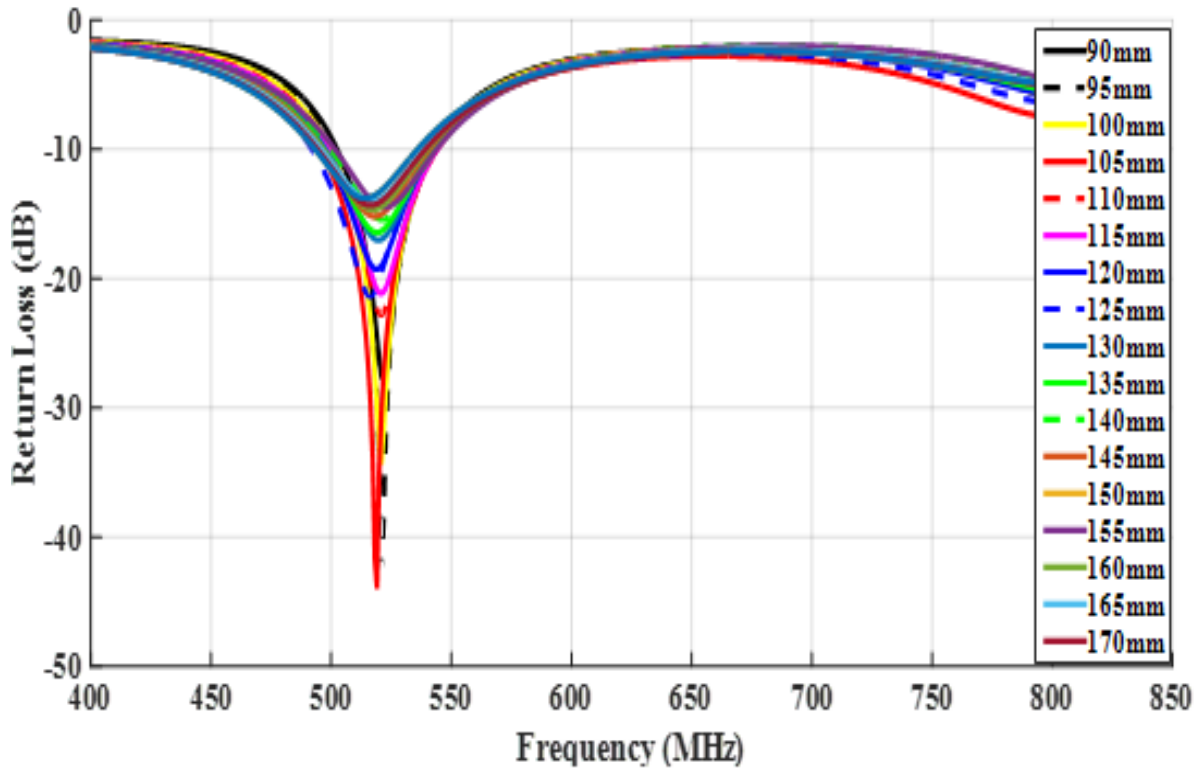
Fig. 4.8. Return loss as a function of 's'

Parametric studies for the height of the driven patch, parasitic patches, air gap between the ground and driven patch, and air gap between driven and parasitic patches are presented here. The proposed antenna design parameters are given in Table 4.1.

Table 4.1 Design parameters of the proposed design

Parameters	Size
Desired Frequency	470-770MHz
h	1.6mm
Dielectric constant	4.4mm
r1	80mm
r	165mm
s	50mm
x	120mm
h2	18mm
h1	65mm

4.3.5 Effects of the eccentricity of top patches

The effects of changing the value of eccentricity of parasitic patches have been discussed here. The return loss of all three antenna designs is compared in Figure 4.9. In antenna design-I, the value of eccentricity is 1. In antenna designs II and III, the value of eccentricity is 1.5 and 0.5 respectively. When the eccentricity is changed from 1.5 to 0.5 the ellipse orientation is changed from the x to y-axis. The return loss for eccentricity values of 0.5,1 and 1.5 is -26dB, -40dB, and -43dB respectively at 1MHz resonant frequency difference. As the value of eccentricity is changed from 0.5 to 1.5 the return loss improved from -26dB to -43dB. The total gain at $\phi = 0^0$ and $\phi = 90^0$ is shown in Figure 4.10. The total gain at e=0.5 and 1.5 is 5.6dBi and 4.5dBi respectively. It is found that for antenna design-III, the S_{11} is lowest (-26dB), but the gain is highest (5.6dBi).
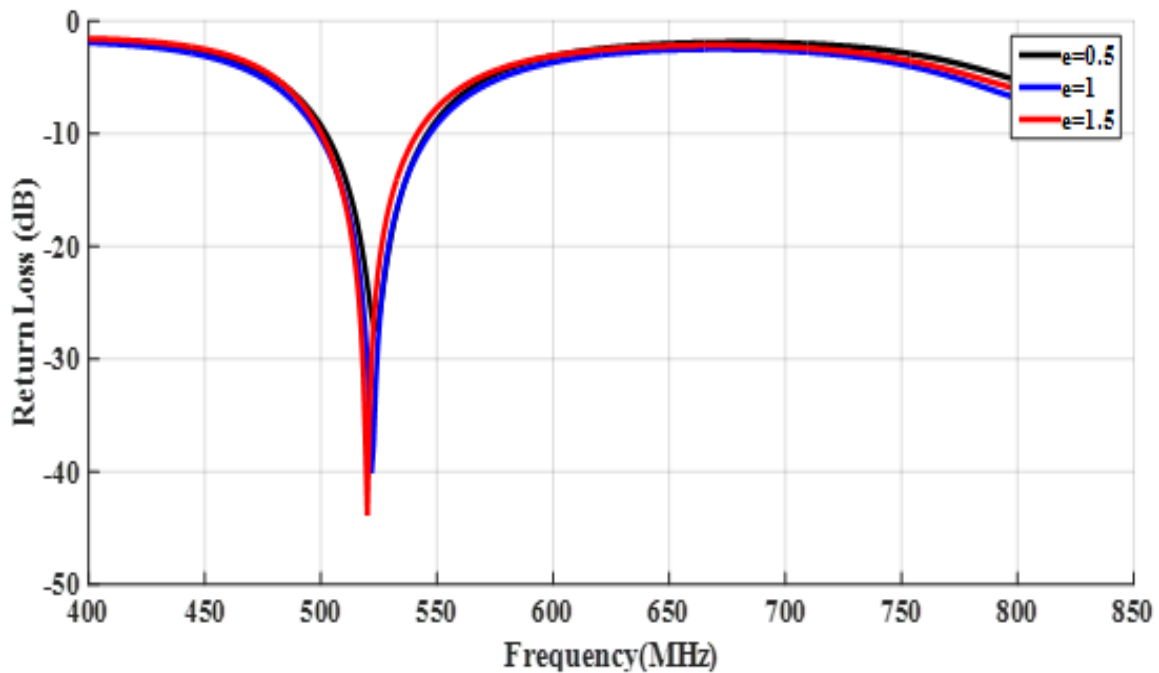
Fig. 4.9. Return loss for different values of eccentricity

Radiation efficiency for antenna designs-I, II, and III are given in Figure 4.11. It varies from 96% to 97%. for antenna design-I (e=1). The radiation efficiency of antenna design-II(e=1.5)

varies from 94% to 99%, and for antenna design-III, it varies from 86% to 99%. For the required band of frequencies, the radiation efficiency of design-I is 98%.

(a)   (b)
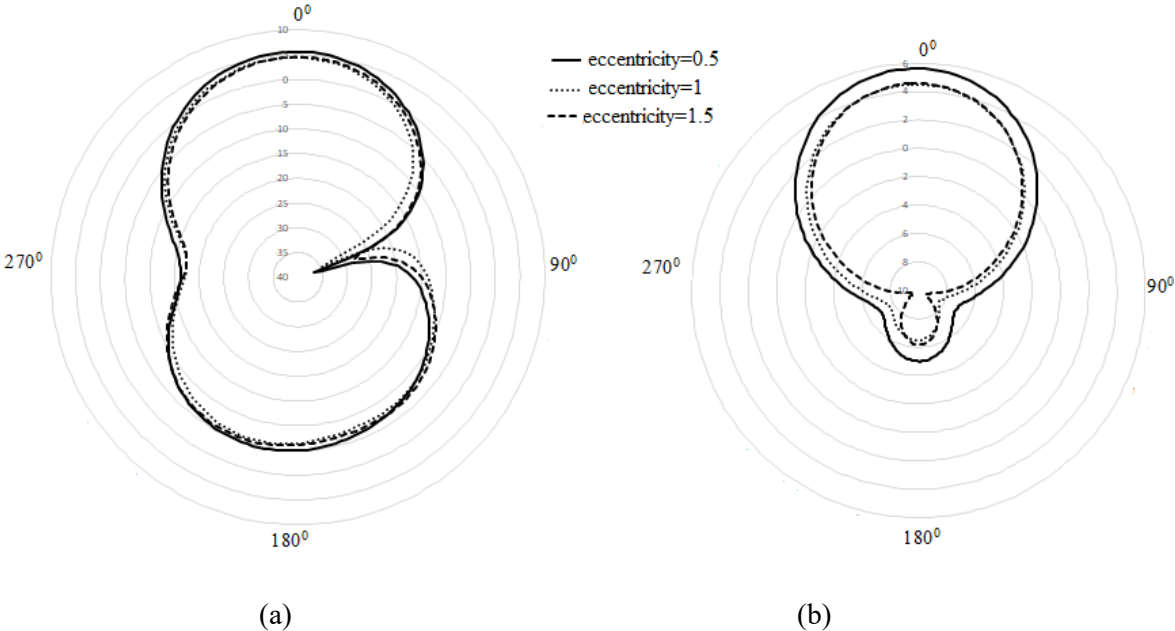
Fig. 4.10. Comparison of Gain for antenna designs- I, II, and III (a) Phi=0^0 and (b) Phi=90^0
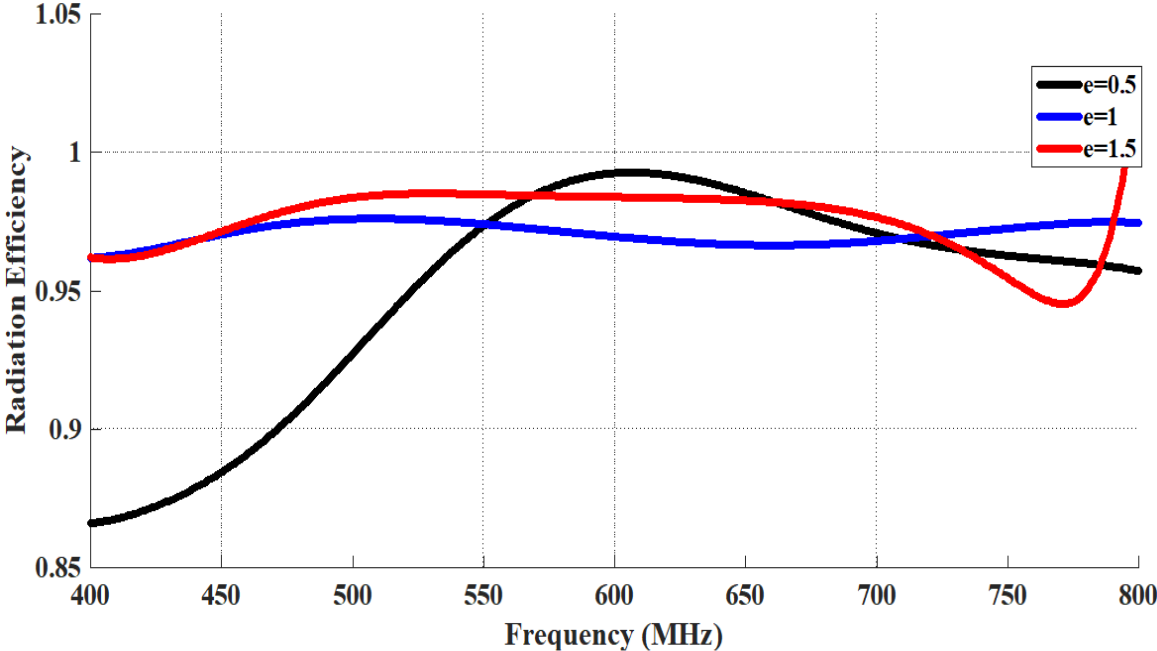
Fig. 4.11. Radiation efficiency of antenna designs- I, II, and III

4.4 Equivalent Circuit

Figure 4.12 displays the equivalent circuit of the proposed design, which was developed using the S_{11} graph. The real impedance corresponding to the resonant frequency of 521MHz is noted down. From equations 3.1 and 3.2 of Chapter 3, the value of capacitance and inductance are calculated to make a resonant circuit.
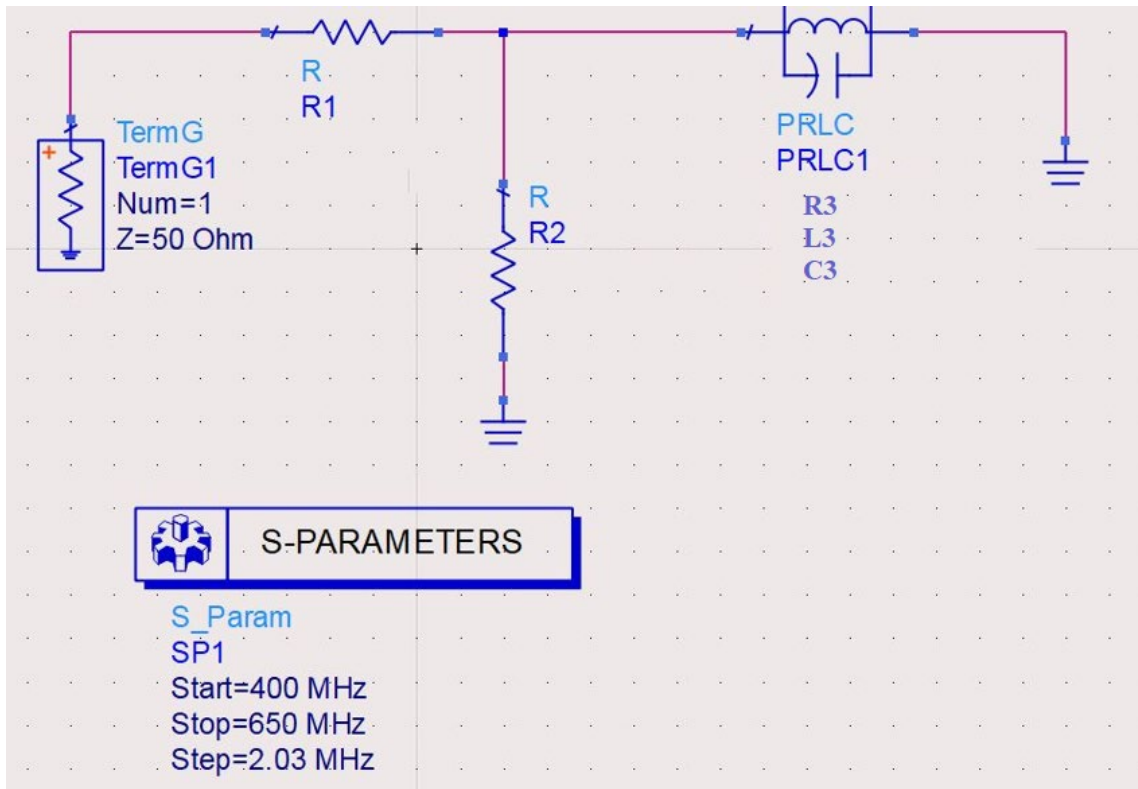
Fig. 4.12 Equivalent Circuit

After optimization, the values of components are R1=10Ω, R2=75Ω, R3=77 Ω, L1=1.517nH, and C1=0.0607nF. The S_{11} graph from ADS software is shown in Figure 4.13. The resonance of the electrical circuit is 523MHz while the simulated antenna resonance is 521MHz. The return loss of the electrical circuit is reduced to -33dB as compared to -40 dB. Figure 4.14 compares the S_{11} of the electrical circuit with the antenna simulation results. The electrical equivalent circuit bandwidth is 10MHz more as compared to the simulated antenna.
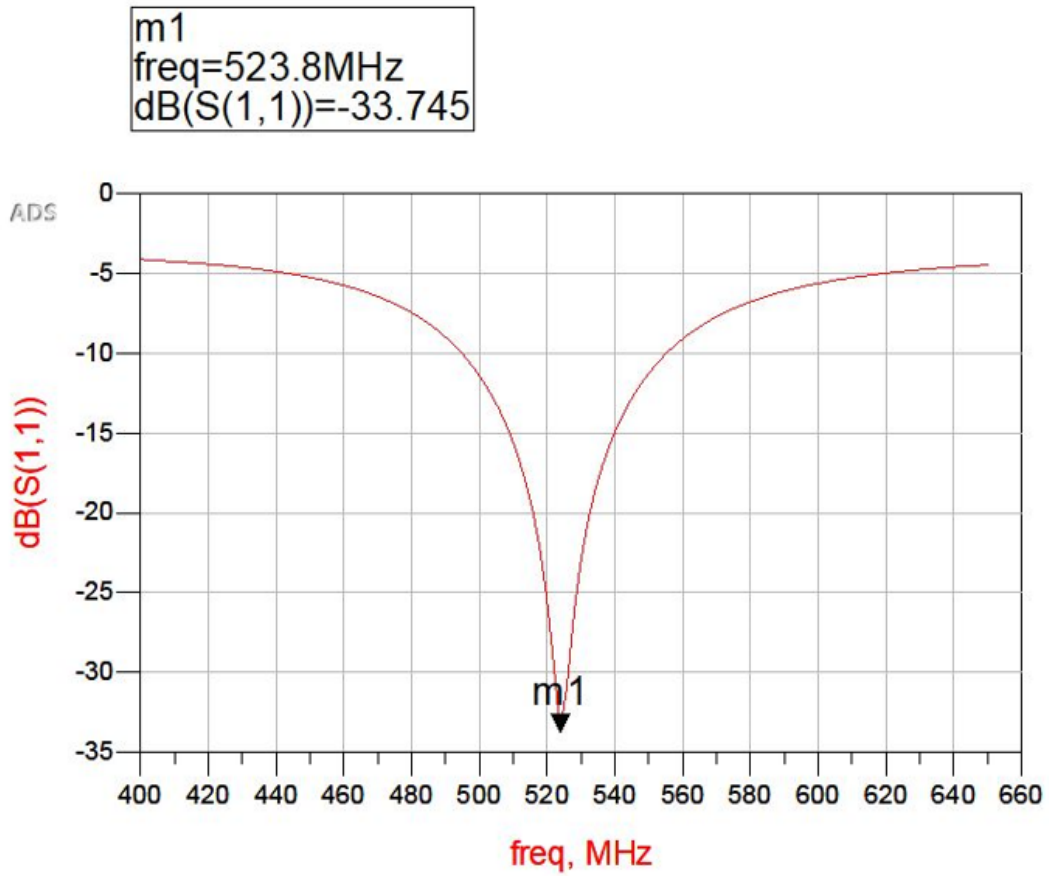
Fig. 4.13 S_{11} plot of equivalent circuit
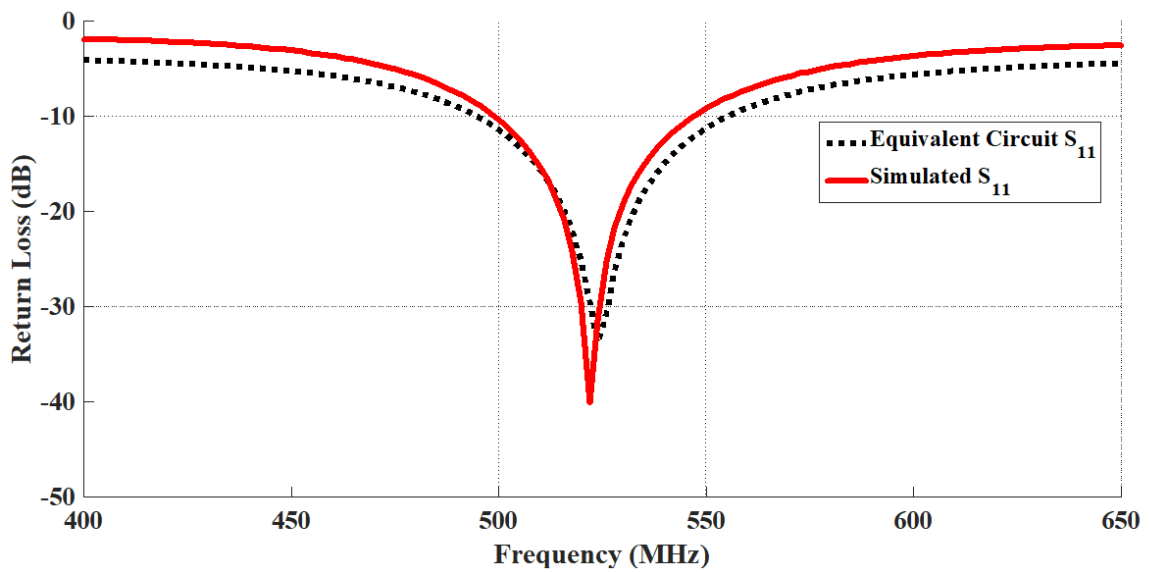
Fig. 4.14 Comparison between equivalent circuit and antenna simulation results

4.5 Measurements and testing

Fabrication of the antenna was done after receiving satisfactory results of the proposed design (S_{11}, VSWR, gain, etc.). To construct the antenna on FR4 substrate, the antenna design layout is initially exported from the HFSS Simulator to auto cad (extension is. dxf). Here, a common etching method used in PCB printing is used. The DXF file from CAD software is printed on a glossy sheet, positioned in front of the copper board, and laminated to etch the design into the copper. This is then submerged in ferric chloride to remove excess copper (FeCl3). The finished design is then attached to a female coaxial connection to obtain the final antenna design.

In the Indian Institute of Technology, Roorkee's Advance Microwave Lab, the suggested antenna is constructed and tested. A side view of the proposed design-I is shown in Figure 4.15.

Fig. 4.15. Side view of the design-I

The top and bottom views of the antenna design-I are shown in Figure 4.16. S_{11} is measured using a vector network analyzer (VNA). Before measuring S_{11} from VNA it should be ensured that there should not be any RF reflector present. The signal is transmitted from an antenna and if there is some reflection it comes back to the antenna port and it will change the true value of

S_{11}. Figure 4.17 shows the antenna with VNA to measure S_{11} of the proposed design. Connect the test antenna to port 1 of VNA and set the range of frequency for operation and measure return loss. If the antenna is fabricated correctly then a resonance dip will appear on the S_{11} graph. The first resonance tells about the working frequency of the designed antenna and most of the power is radiated at this frequency. Multiple band antenna has more than one resonance which can be visible from measurement. These resonances will combine to give wider bandwidth. If during measurement any disturbance is created it will affect the performance of the design.

(a)   (b)
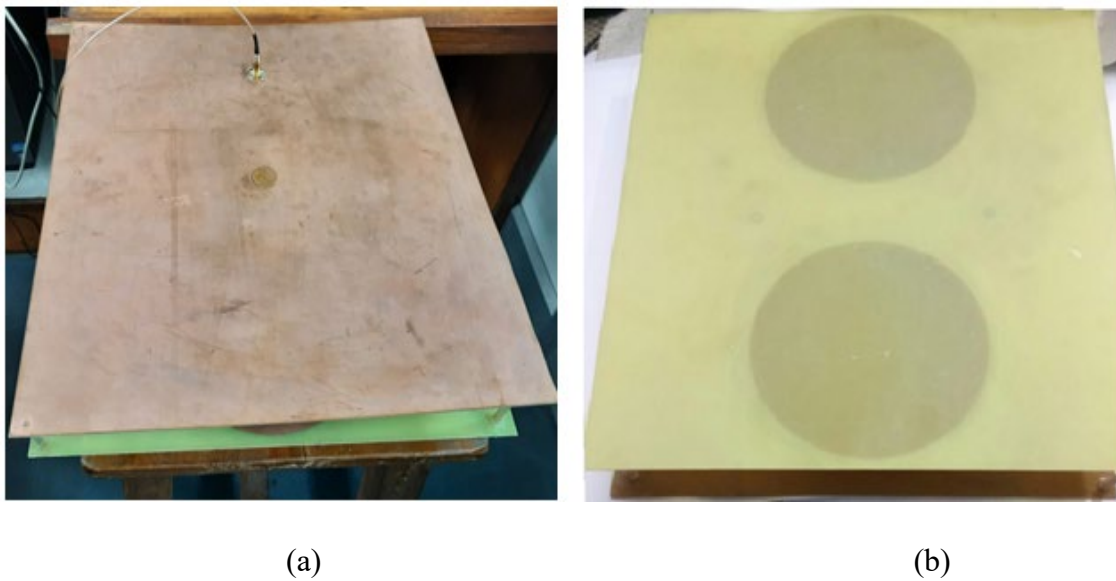
Fig. 4.16 Bottom (a) and top (b) view of design-I

Return loss is measured using VNA as shown in Figure 4.17. The gain of the antenna is measured in an anechoic chamber and the antenna design-I under test is shown in Figure 4.18.
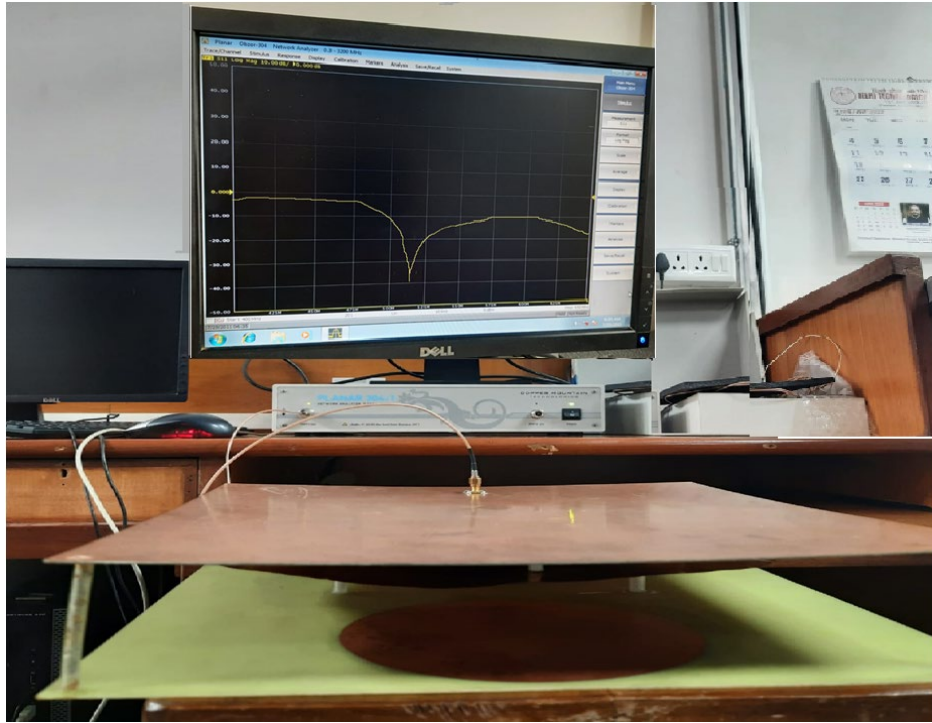
Fig. 4.17. VNA setup for S_{11} measurement

Fig. 4.18 Antenna design-I for gain measurement

4.6 Simulated and Experimental Results

The simulated and experimental results are compared in this section. The simulated and experimental return loss of design-I is shown in Figure 4.19. The simulated return loss is -40dB at 521MHz and the experimental return loss is -37dB at 523MHz. The bandwidth for $|S_{11}| <$ $10dB$ is from 499 - 650 MHz (26%). The recommended antenna's gain is best suited for frequencies between 450 - 650MHz. However, when the frequency grows, the cross-polar level rises as well because of the effective height of the feed line.
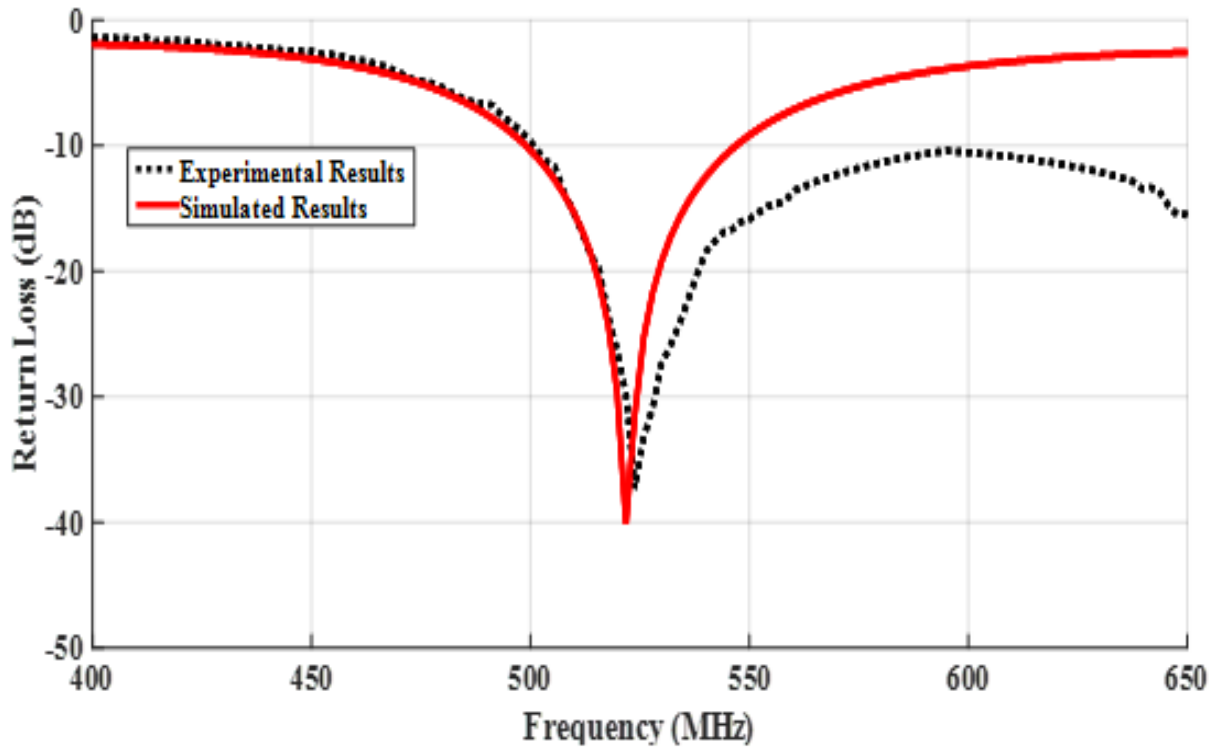
Fig.4.19. Experimental and Simulated S_{11} of design-I

The experimental and simulated gain vs frequency is shown in Figure 4.20. It is observed from the figure that the measured gain is 5.6dBi and the simulated gain is 4.6dBi over the frequency of interest. The simulated and experimental radiation pattern for ϕ=0° and ϕ=90° of the proposed design at 521 MHz is shown in Figure 4.21. The gain ϕ is shown in red color while the gain θ is shown in black color lines. The cross-polarization levels are high which means

less power is radiated in the undesired direction. Most of the power is coupled in the desired direction only.
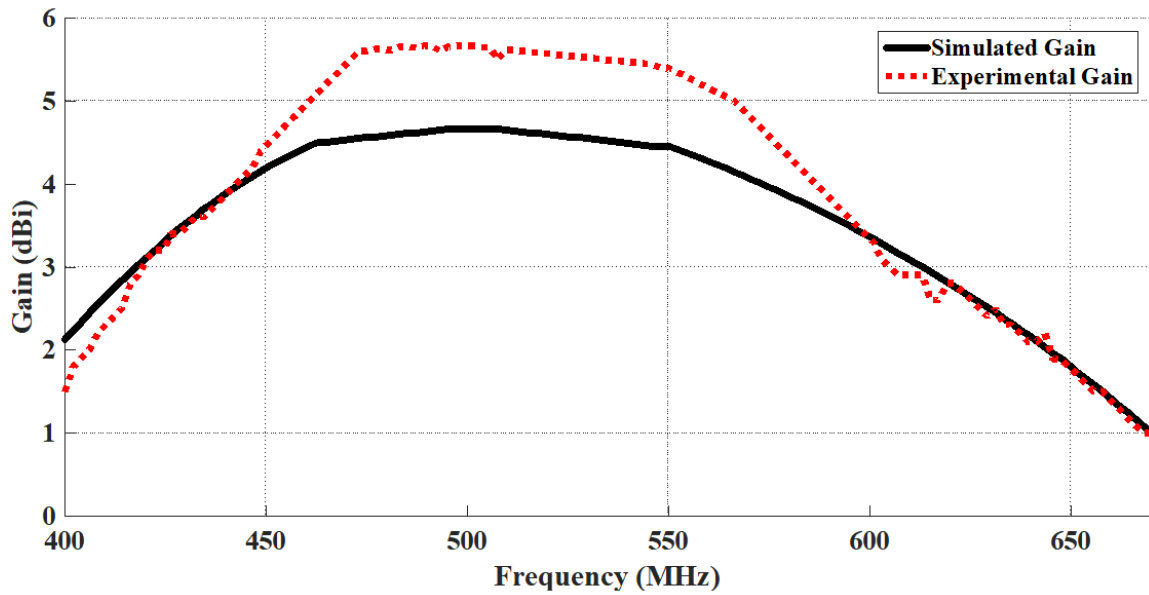
Fig. 4.20. Experimental and Simulated Gain
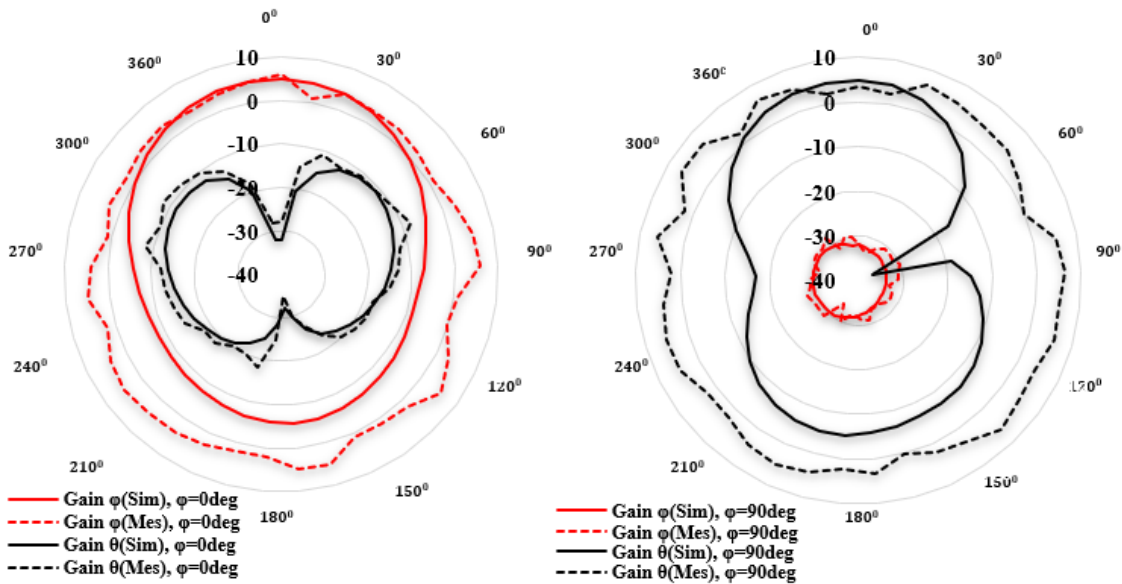
Fig. 4.21 Simulated and experimental radiation patterns of the antenna design-I at 521 MHz

It is possible to compare the proposed design specifications to previously published TVWS band research. As shown in Table 4.2, the performance metrics of the suggested design are compared to previous research.

Table 4.2 Compares performance metrics between the suggested work and previously reported work

Types	Substrate	Gain (dBi)	Radiation Efficiency	BW (MHz)
Bowtie [25]	FR4	-2 to 1	50%	470-860
Wire Antenna [127]	Copper	1.87	99.6%	13.7
U-Shaped [185]	FR4	1.4	76.2%	474-1212
M-shape Monopole [116]	FR4	1.6	63%	470-990
C.P. with rings [159]	FR4	1.3	92%	400-900
Circular Patch [206]	Rogers5880	2.5	-	470-987
Printed Monopole [62]	FR4	1.4-2.1	95%	628-861
Modified ground plane [76]	FR4	2.2-4.6	-	325-815
Two layers stacked parasitic	FR4	5.6	98%	499-650

4.7 Conclusion

In the TV white-space frequency region, which can operate between 470 and 806 MHz, the proposed work attempts to design and construct stacked parasitic microstrip antenna topologies for IEEE 802.11 application. The antenna is made to work with both the user terminal (which has a higher gain) and the base station (compact). With feed at the lower driven patch, two layers are stacked on top of one another in this configuration. The parasitic patches are inverted and electromagnetically connected to a lower patch. FR4 is the substance employed in this design. The suggested antenna has a 5.6dBi gain and can operate in the 499-650MHz frequency range. The proposed antenna has a 98% efficiency and a 26% bandwidth. It was found that antenna design-III has reduced physical size with high gain as compared to designs-I and II. It

is important to note that the design of a stacked structure for gain improvement requires careful optimization and analysis to achieve the desired performance. The number of layers, their dimensions, and the positioning within the antenna structure should be carefully determined to maximize gain while considering other factors such as impedance matching and bandwidth requirements.

CHAPTER 5

Multi-Band Multi-Polarized Fractal Antenna for White Space TV Band

5.1 Introduction

The concept of stacking was addressed in the last chapter. This technique is good to increase the gain of an antenna. But, it compromises the physical size of the design. The designs discussed in the last chapters were single band with wide bandwidth and linearly polarized. The gap between co and cross-polarization levels was more than 20dB. The linear polarized antennas radiate power in the directions of propagation. TVWS technology has high penetration as compared to other technologies. If we use a circular polarized antenna in TVWS technology it will enhance the property of this technology. Researchers are working on finding solutions to these concerns in TVWS technology.

In this chapter, fractals are used to get multi-bands. Fractals are fun-loving shapes that repeat themselves [104]. By increasing the iterations of fractals, the electrical length of an antenna is increased and the size of the design is reduced. The effects of defected ground structure (DGS) are also described in the chapter.

In the literature, various fractals are available for multiband operation. It has been demonstrated that fractal designs if implemented properly, can lead to efficient miniaturized antenna designs. [40,71]. The CP radiation [92] is achieved by an inclined fractal-shaped slot embedded along the diagonal axis of a ground plane [68]. The defected ground is used to increase the bandwidth of the antenna [137,138,111,50,67,164,112]. When defected ground is used with fractal shapes

circular polarization is achieved with a size reduction of 44.7% [87]. Efforts have also been made to improve the bandwidths of these antennas. A stacked antenna configuration with multiple layers of fractal geometries has been found to have some effect in this regard [12]. This configuration has also been made conformal to improve the utilization of the antenna. In this chapter, 4 iteration Koch snowflakes fractal with defected ground structure is used to get multiband and reduced physical size. The design methodology used in this chapter is given in Figure 5.1.
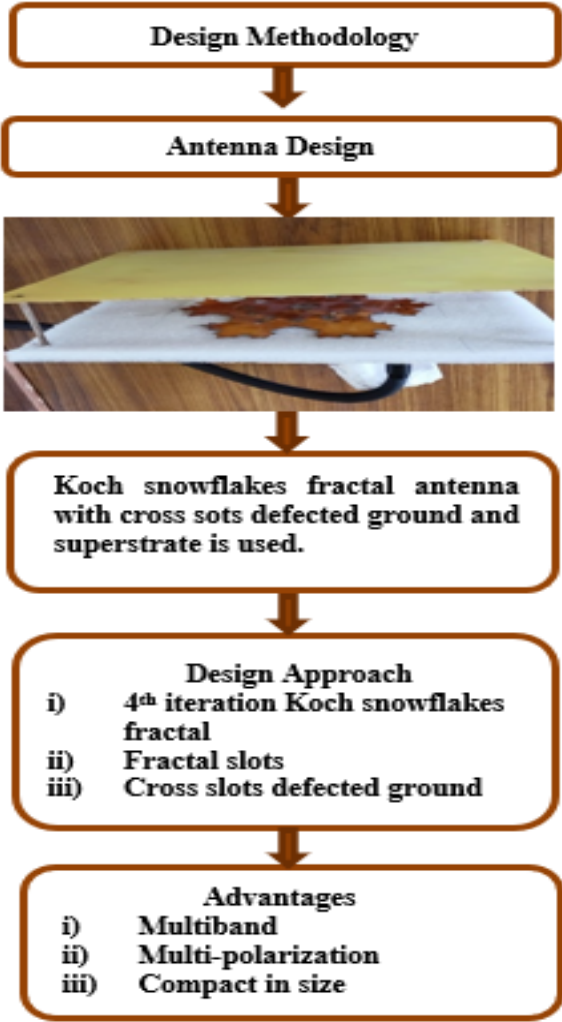
Fig.5.1 Design Methodology used in proposed design

5.2 Antenna Design

The antenna in this chapter is created for the white space TV band frequency. To overcome the requirement of a larger bandwidth triangular antenna is placed on the ground with air as a substrate. To determine where the patch and superstrate should be placed, a parametric study has been conducted. The patch is positioned 18mm above the ground plane, while the superstrate is positioned 65mm away. FR4 superstrate is used at a height of 65mm. The triangular patch is supported with the ground using shorting pin of a diameter of 10mm. A triangular patch is fed by co-axial cable as shown in Figure 5.2.
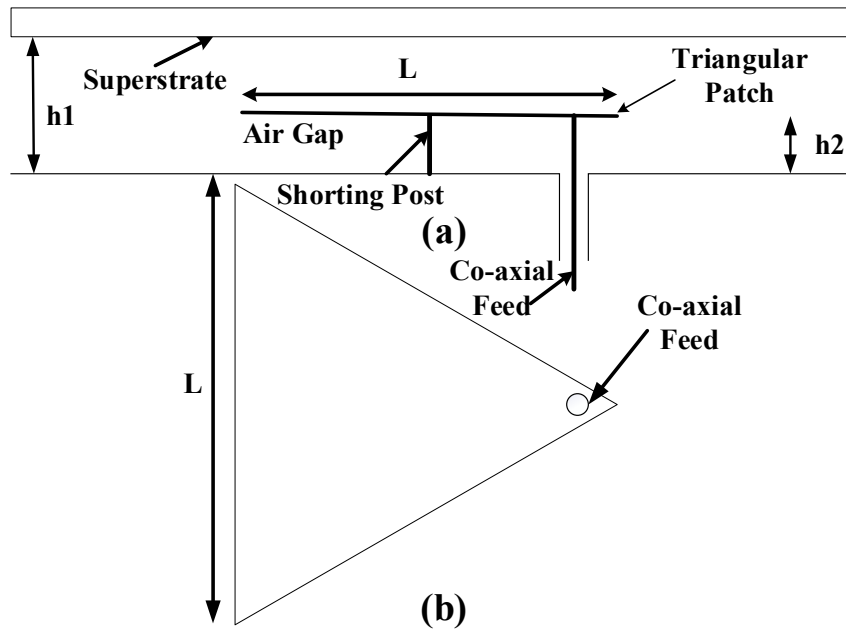
Fig. 5.2 (a) Side and (b) Top view of basic triangular patch antenna

The following formula is used to get the resonance frequency of the equilateral triangular microstrip patch:

$$f_{m,n} = \frac{2v}{3L\sqrt{\varepsilon_r}} (\sqrt{(m^2 + mn + n^2)}) \qquad (5.1)$$

where $'v'$ is the speed of light, substrate effective dielectric constant is denoted by ε_r , "m" and "n" are the number of half-cycle variations in the x and y direction respectively. The resonant

frequency of a triangular patch can be accurately predicted by changing the side length 'L' of the triangular by effective side length L_{eff}. S is the area of the triangle. L_{eff} is given by the following relation

$$L_{eff} = L(\frac{L_e}{L_{equ}}) \tag{5.2}$$

$$L_{equ} = \sqrt{\frac{S}{\pi}} \tag{5.3}$$

$$L_e = L_{equ}[1 + \frac{2h}{\pi\varepsilon_r L_{equ}}\{\ln\left(\frac{L_{equ}}{2h}\right) + 1.77] \tag{5.4}$$

Now equation 5.1 becomes

$$f_{m,n} = \frac{2c}{3L_{eff}\sqrt{\varepsilon_r}}(\sqrt{(m^2 + mn + n^2)} \tag{5.5}$$

After that Koch fractal snowflakes shapes are made with the help of this triangular to get multi-band. Here, the fractal shape is described using iterated function systems (IFSs). They offer a unifying framework for understanding the concept of fractal geometry and serve as an incredibly flexible method for quickly creating a huge range of practical fractal applications. These IFSs are based on a set of contractions attained by applying a number of affine transformations, where p is defined as:

$$p\begin{pmatrix} g \\ h \end{pmatrix} = \begin{pmatrix} i & j \\ k & l \end{pmatrix}\begin{pmatrix} g \\ h \end{pmatrix} + \begin{pmatrix} m \\ n \end{pmatrix} \tag{5.6}$$

$$p\ (g,\ h) = (ig + jh + m,\ kg + lh + n) \tag{5.7}$$

Or equivalently affine matrix is shown in equation (5.7) where $i, j, k, l, m,$ and n are real numbers. Hence affine transformation p is represented by six parameters, which may be expressed using the compact notation $\begin{pmatrix} i & j & m \\ k & l & n \end{pmatrix}$ such that i, j, k and l are control, rotation, and scaling while m and n govern linear translation.

$$p_1(g,h) = (\frac{1}{3}g + (0)h + 0, (0)g + \frac{1}{3}h + 0) \tag{5.8}$$

$$p_2(g,h) = (\frac{1}{6}g - \frac{\sqrt{3}}{6}h + \frac{1}{3}, \frac{\sqrt{3}}{6}g + \frac{1}{6}h + 0) \tag{5.9}$$

$$p_3(g,h) = (\frac{1}{6}g + \frac{\sqrt{3}}{6}h + \frac{1}{2}, -\frac{\sqrt{3}}{6}g + \frac{1}{6}h + \frac{\sqrt{3}}{6}) \tag{5.10}$$

$$p_4(g,h) = (\frac{1}{3}g + (0)h + \frac{2}{3}, (0)g + \frac{1}{3}h + 0) \tag{5.11}$$

With the help of these equations from (5.8) to (5.11) the standard Koch fractal snowflakes curve as an IFS is

$$P(A) = p_1(A) \cup p_2(A) \cup p_3(A) \cup p_4(A) \tag{5.12}$$

Finally, the affine transformation matrix for 4 iterations of the Koch snowflake fractal is:

$$
\begin{array}{ccccccc}
 & i & j & k & l & m & n \\
\end{array}
\tag{5.13}
$$

$$
P(A) =
\begin{array}{cccccc}
\frac{1}{3} & 0 & 0 & \frac{1}{3} & 0 & 0 \\
\frac{1}{6} & -\frac{\sqrt{3}}{6} & \frac{\sqrt{3}}{6}\frac{1}{6} & \frac{1}{3} & 0 \\
\frac{1}{6} & \frac{\sqrt{3}}{6} & -\frac{\sqrt{3}}{6}\frac{1}{6} & \frac{1}{2} & \frac{\sqrt{3}}{6} \\
\frac{1}{3} & 0 & 0 & \frac{1}{3} & \frac{2}{3} & 0 \\
\end{array}
$$

The same 4th iteration Koch fractal slots have been created in the patch as shown in Figure 5.3 and finally, some cross slots are also introduced in the ground. The size of 1st cross slot is taken as $\frac{\lambda}{4}$ further, the 50% scaling is done for 2nd iteration. 3rd and 4th iteration cross slots are created from 50% scaling from 2nd and 3rd cross slots respectively. Cross-slot 4 iterations are shown in Figure 5.4. These cross-slots are repeated on all four quadrants of the suggested antenna design. In Figure 5.5, the final antenna design is displayed. The back view of the design is depicted in Figure 5.6 in which ground fractal slots are coming into the picture.
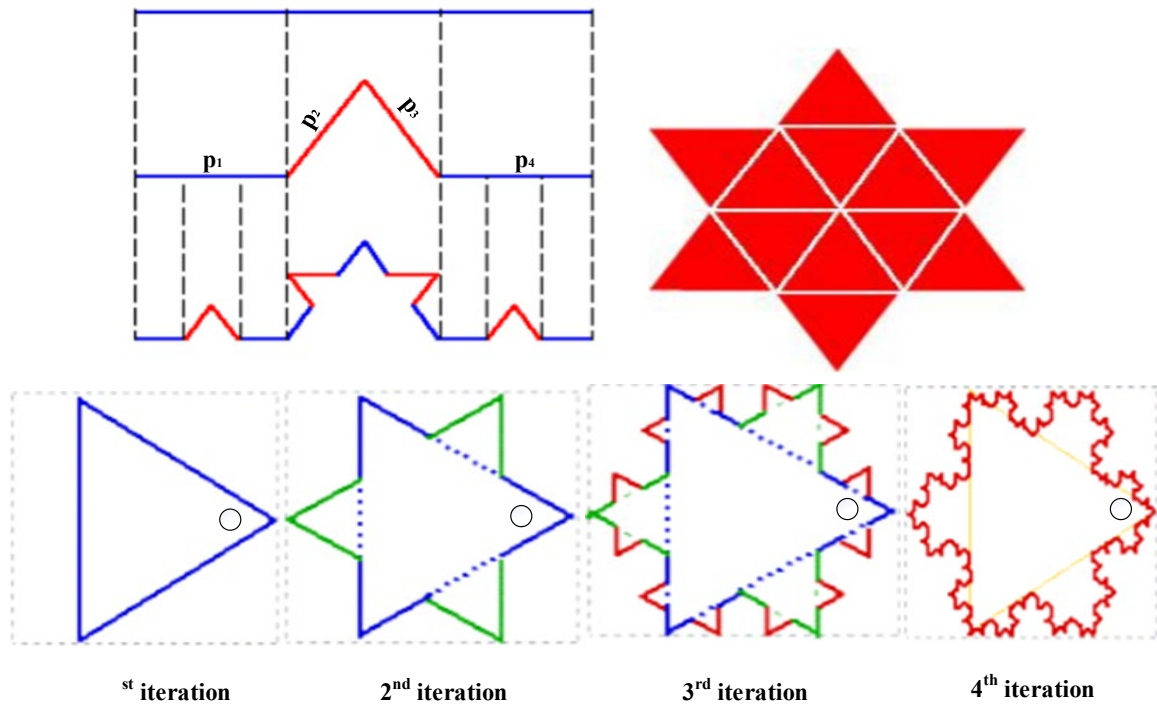
Fig.5.3 The four iterations in the generation of a Koch fractal snowflake

st iteration   2nd iteration   3rd iteration   4th iteration

1st iteration   2nd iteration   3rd iteration   4th iteration
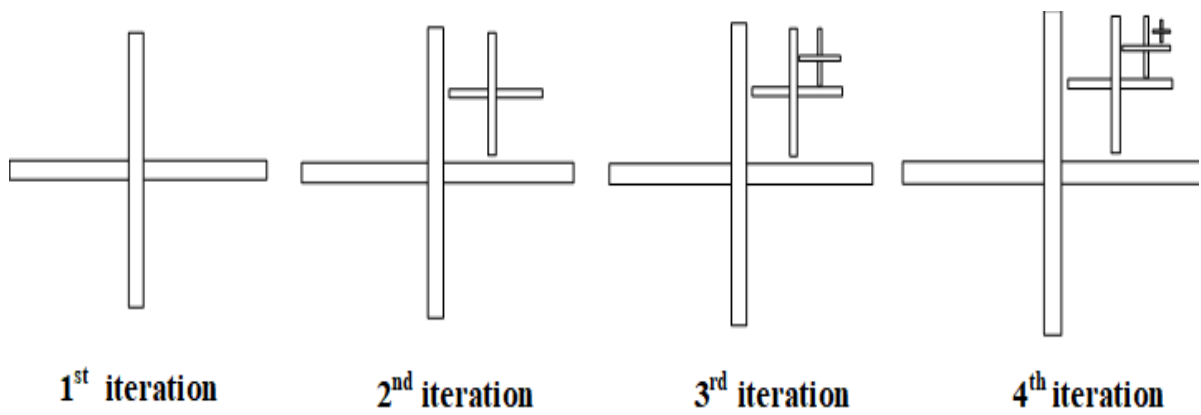
Fig.5.4 The first four stages of cross slot introduced on ground.
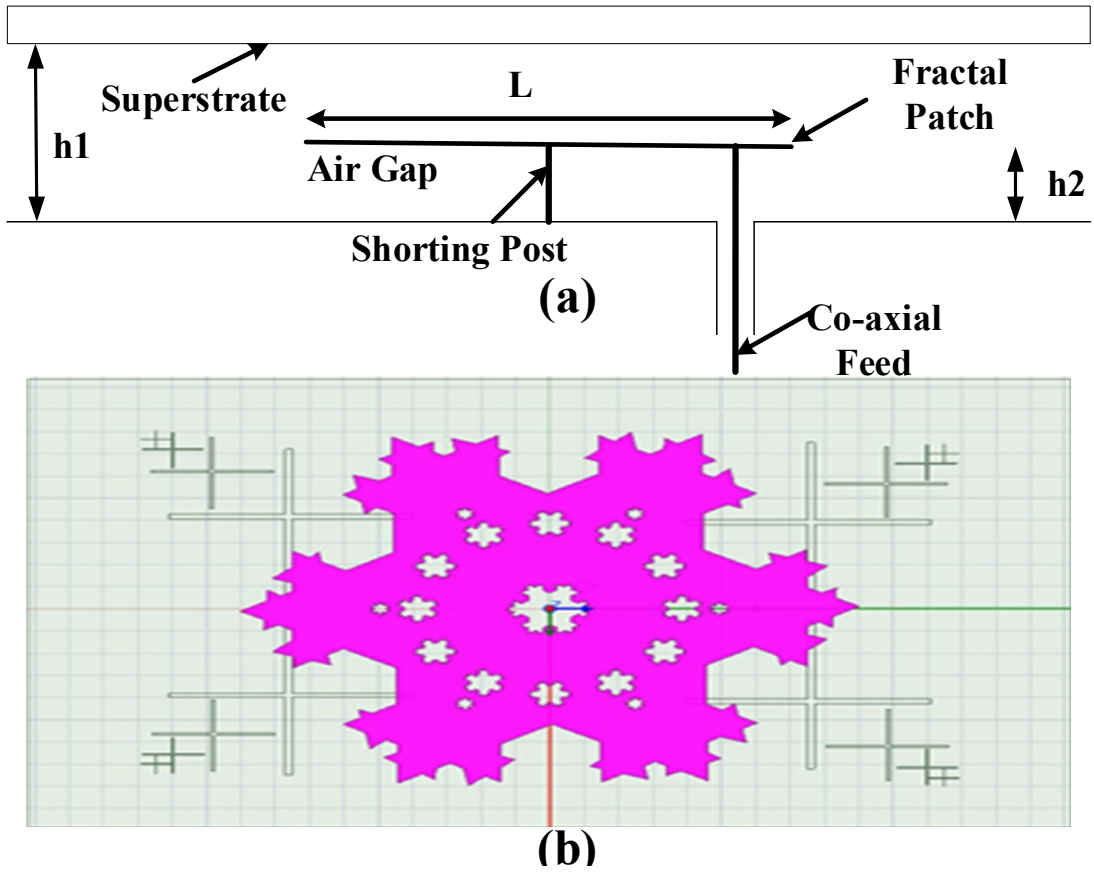
Fig.5.5 (a) Side and (b) Top view of final design
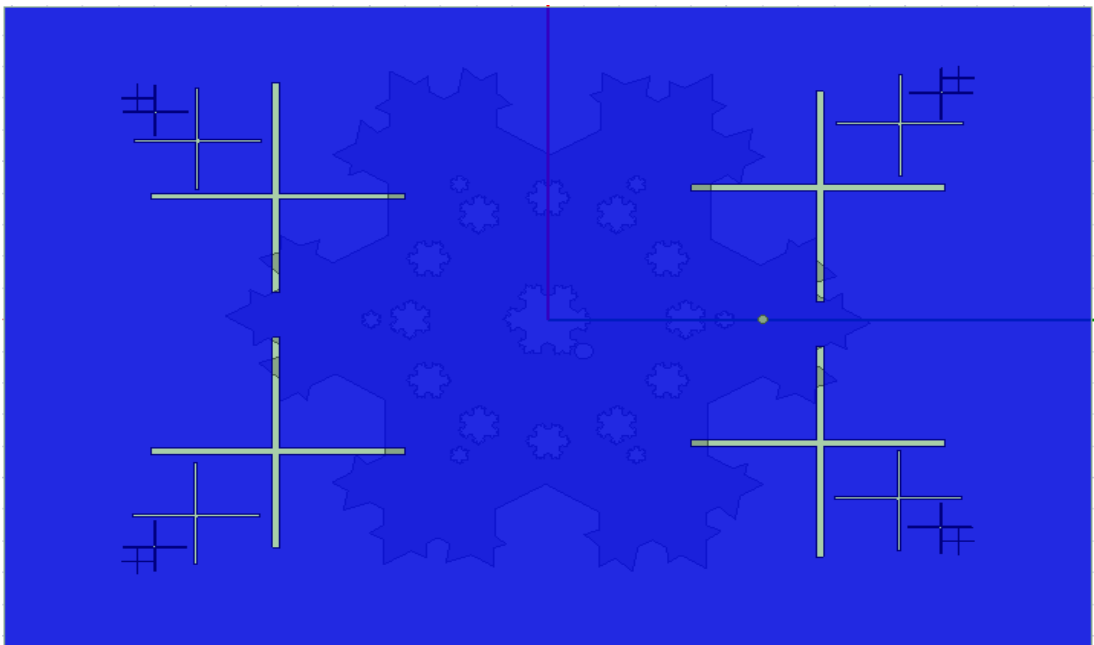
Fig. 5.6 Back view of antenna

5.3 Parametric Analysis

The effects of the number of fractal iteration, fractal slots, and the defected ground plane on the performance of the proposed design is explained in this section.

5.3.1 The effects of the number of iterations

The designed antenna has undergone 4 iterations of the Koch snowflake fractal shape. It is clear from the given Figure 5.7 that as the number of iterations is going to increase resonant frequency is decreased. The resonant frequency has been shifted from 655MHz to 499 MHz with an increase in return loss from -13dB to -20 dB. It means the size of the antenna can be reduced by increasing iteration in fractal design. The physical size of the antenna has been reduced to 38mm. In the same graph, it is also shown that at the 4th iteration, the antenna can work for 2 bands of frequencies from 480 to 517 MHz and 632 to 781 MHz with good gain.
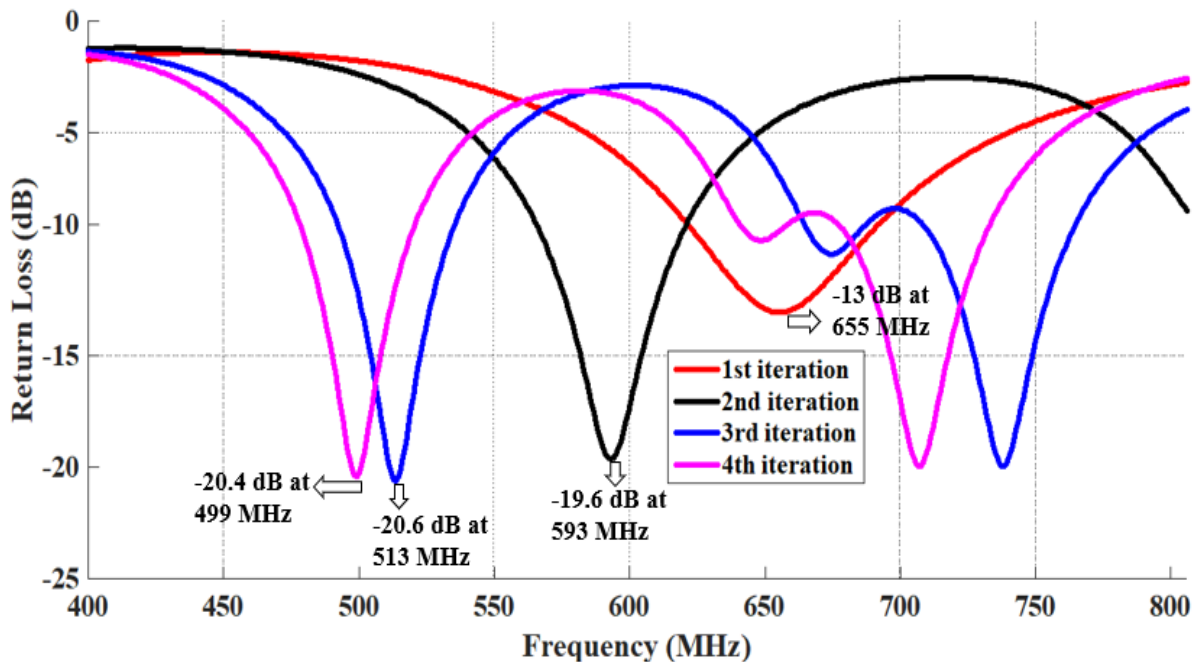
Fig.5.7 Return Loss of 4 iterations of fractal antenna

119

5.3.2 Effects of air gap h_1 between ground and patch

The effect of the air gap between the patch and the ground is depicted in Figure 5.8. The height of h_1 is varied from 3mm to 21mm from the ground plane. It is observed that when height is increased number of bands is increased as well as bandwidth also increased. At h_1 =12mm last two band gets combined. After that last two bands combined to give higher bandwidth. The optimum value of h_1 is 18mm as maximum bandwidth is achieved at this height. If the height is further increased then bandwidth gets reduced with a low value of return loss.
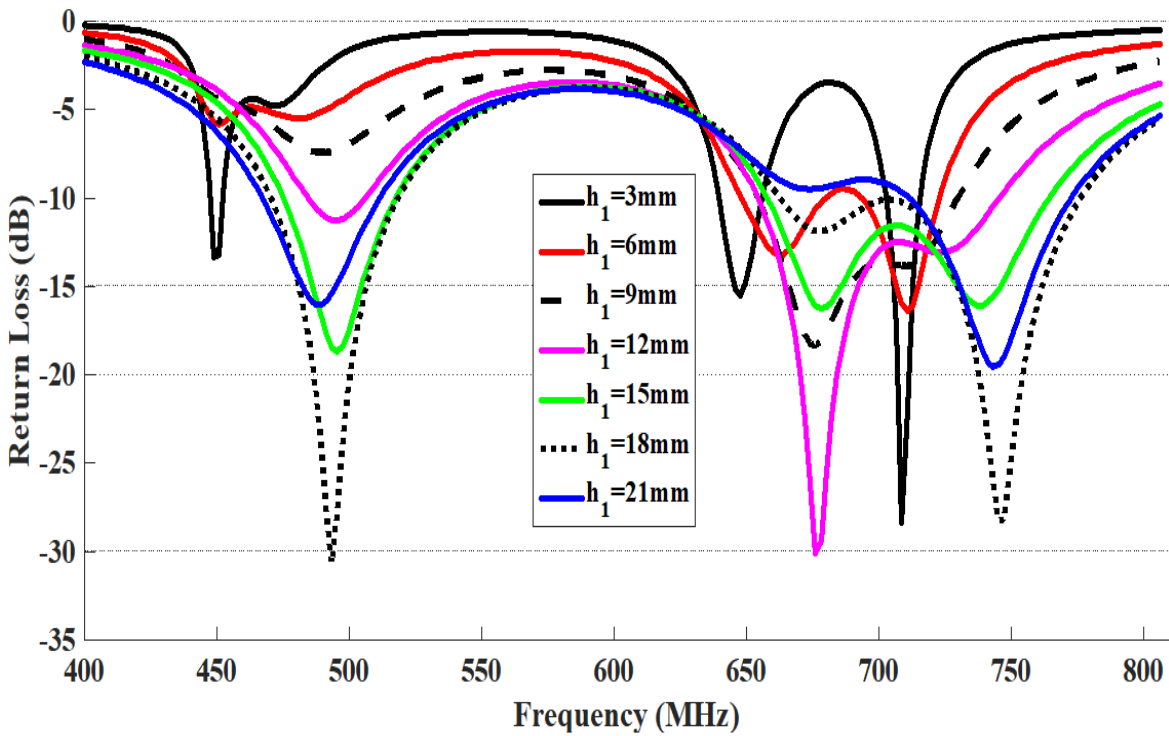
Fig. 5.8 Return Loss as a function of h_1

5.3.3 Effects of air gap h_2 between patch and substrate

The effects of the air gap between the patch and substrate are shown in Figure 5.9. From Figure 5.9, it is clear that when the height of the air gap is increased the value of return loss is improved with increased bandwidth. The value of h_2 is varied between 20mm to 70mm. The optimum value of h_2 is 65mm. When the air gap is further increased, the bandwidth starts reducing.

120
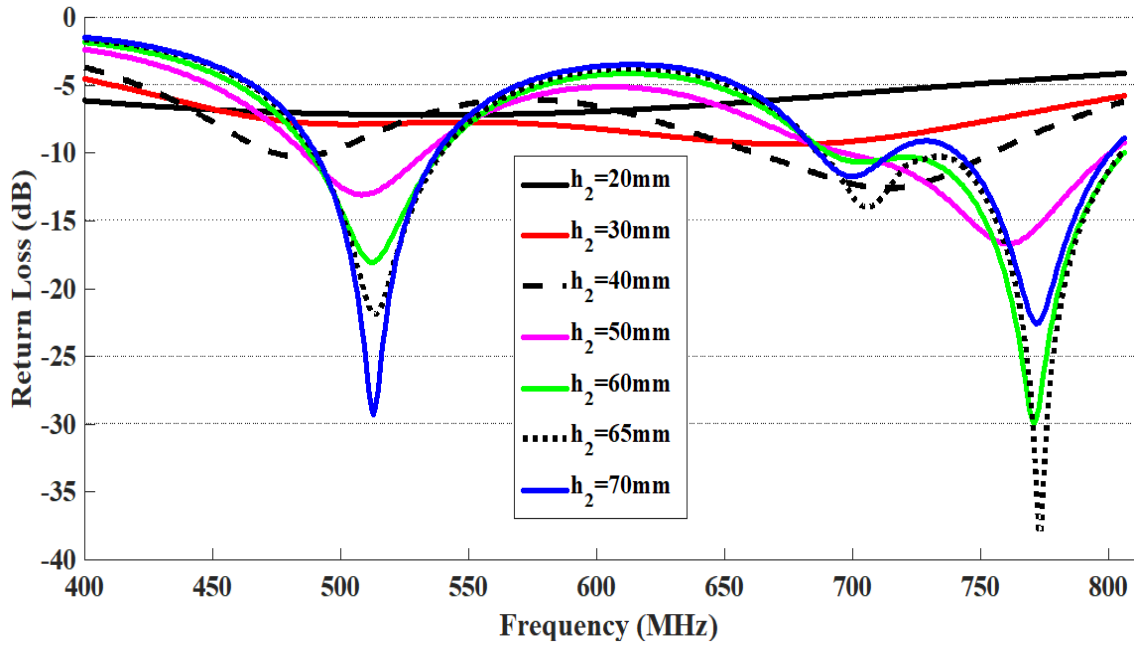
Fig. 5.9 Return Loss as a function of h_2

5.3.4 Effects of fractal slots and cross slots

The effects of fractal slots in the patch and cross slots in the ground are depicted in Figure

5.10. Triple bands are received with the introduction of fractal slots in the patch.
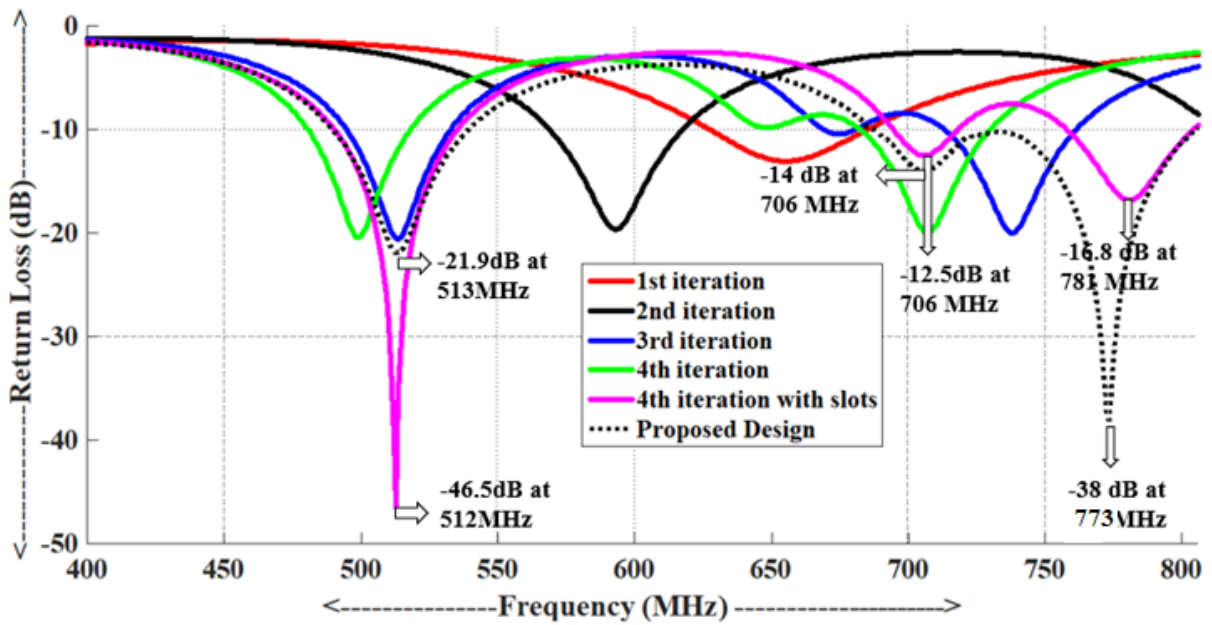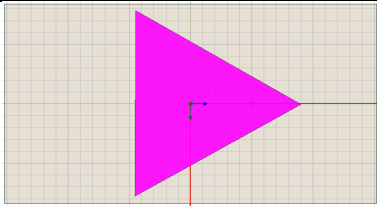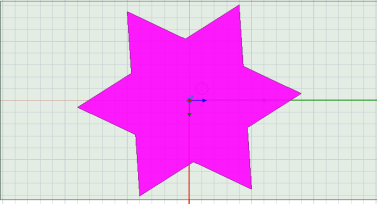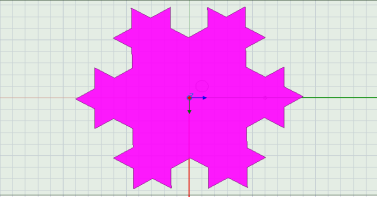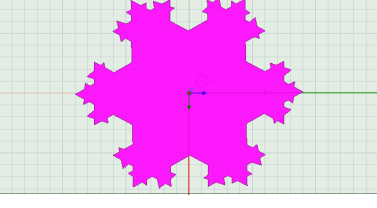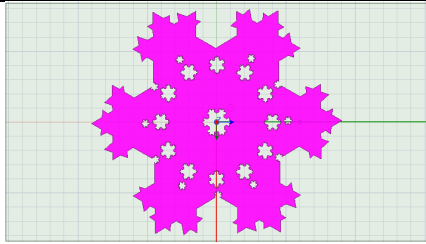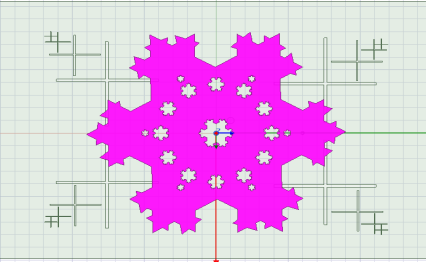
Fig. 5.10 Return Loss of final design

As cross slots are introduced in the design, 2nd and 3rd bands combine to give larger bandwidth. Cross slots work as defected ground planes and increased the bandwidth of the antenna. 1st band works from 489 to 539 MHz and 2nd band works from 689 to 806 MHz respectively. The comparison of antenna paraments step by step is given in Table 5.1. As the number of iterations increased bandwidth and number of bands also increased. Self-symmetry property of fractals is used to get multi-band characteristics as the same structure is available at different parts of the antenna. The increase in the number of iterations shifts resonant frequency due to an increment of electrical length. The shift in resonance does not follow a fixed pattern as the number of iterations changes the size of the fractal at different locations.

Table 5.1 Comparison of antenna parameters

Type	Design	Resonant Frequency	S11	BW	Gain
Fractal patch 1st iteration		655MHz	-13	627-685MHz =58MHz	5.3dBi
Fractal patch 2nd iteration		593MHz	-19.6	568-617MHz =49 MHz	6.4dBi
Fractal patch 3rd iteration		513 MHz 739 MHz	-20.6 -19.8	494-532MHz =38MHz 713-761MHz =48MHz	5.6dBi
Fractal patch 4th iteration		499MHz 707 MHz	-20.4 -19.9	481-518MHz =37 MHz 682-730MHz =48 MHz	5.4dBi

Fractal patch 4th iteration with fractal slots		512MHz	-46.5	489-535MHz =46MHz	5.19dBi
		706 MHz	-12.4	694-718MHz =24MHz	
		780 MHz	-16.8	757-804MHz =47MHz	
Fractal patch 4th iteration with fractal slots and defected ground		513MHz	-21	489-539MHz =50MHZz	4.5dBi
		706 MHz	-14	689-806MHz =117MHz (last two bands merge in the final design and BW increased)	
		773 MHz	-38		

5.4 Electrical Equivalent Circuit

Figure 5.11 displays the equivalent circuit of the proposed design, which was developed using the S_{11} graph. The real impedance corresponding to resonant frequencies of 513MHz, 706MHz, and 773MHz is noted down. From equations 3.1 and 3.2 of Chapter 3, the value of L and C are calculated to make a resonant circuit.
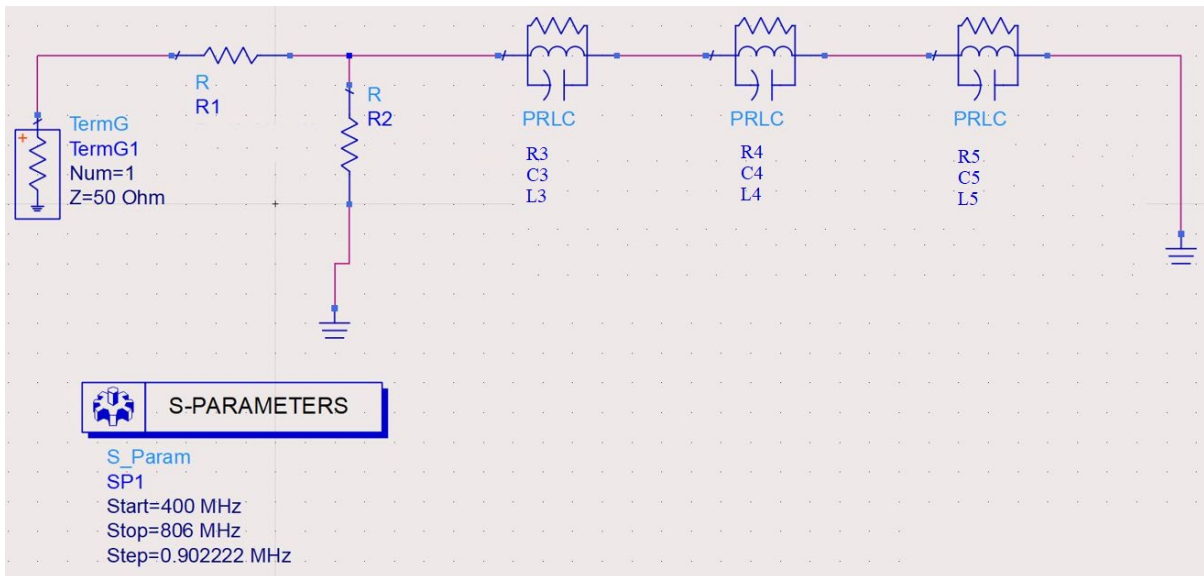
Fig. 5.11 Electrical equivalent circuit of proposed antenna

After optimization the values of components are R1=10Ω, R2=45Ω, R3= 11.7Ω, R4= 31.56Ω,

R5= 274.9Ω, L1=1.663nH, L2=0.619nH, L3=0.943nH, C1=0.059nF, C2=0.082nF and

C3=0.044nF. The S_{11} graph from ADS software is shown in Figure 5.12. The resonance of the

electrical circuit appeared at 506MHZ, 704MHz, and 771MHz. There is a minor shift of

resonance as compared to the simulated antenna. The return loss of the electrical circuit is

matching with the simulated antenna results. Figure 5.13 compares the S_{11} of the electrical

circuit with the antenna simulation results.
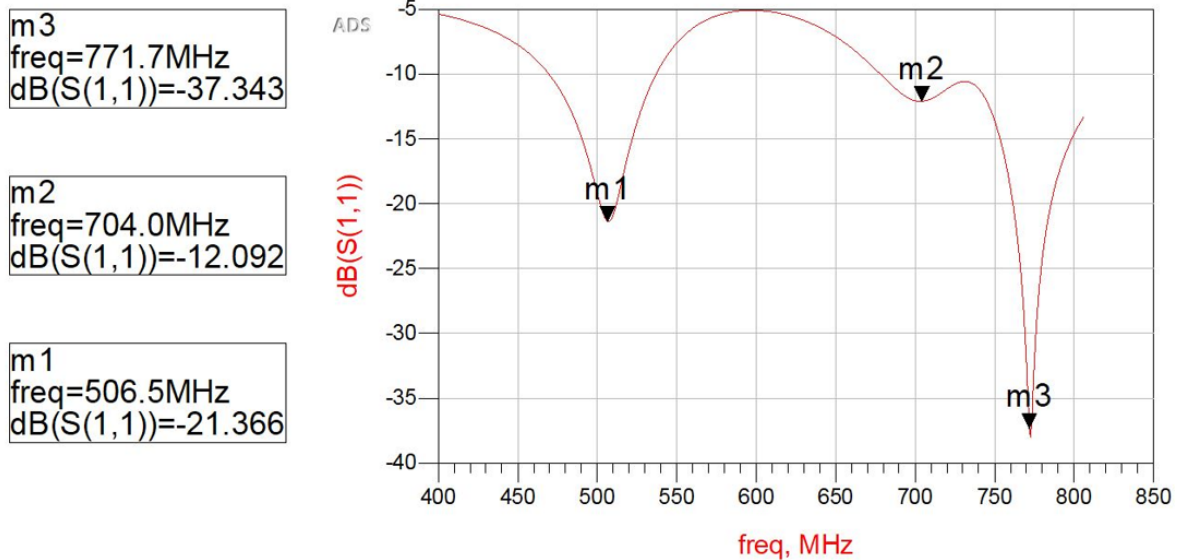
Fig. 5.12 S_{11} of electrical equivalent circuit

The bandwidth of the electrical circuit in 1st band is 66MHz (471-537MHz) and 126MHz in

2nd band (680-806MHz). The bandwidth of the simulated antenna is 50 MHz (489-539MHz)

in the 1st band and 117MHz (689-806MHz) in the 2nd band. It is observed that a 4% bandwidth

is increased in 1st band for the electrical equivalent circuit of the proposed antenna. This is

because of less radiation losses in electrical circuits as compared to antenna.
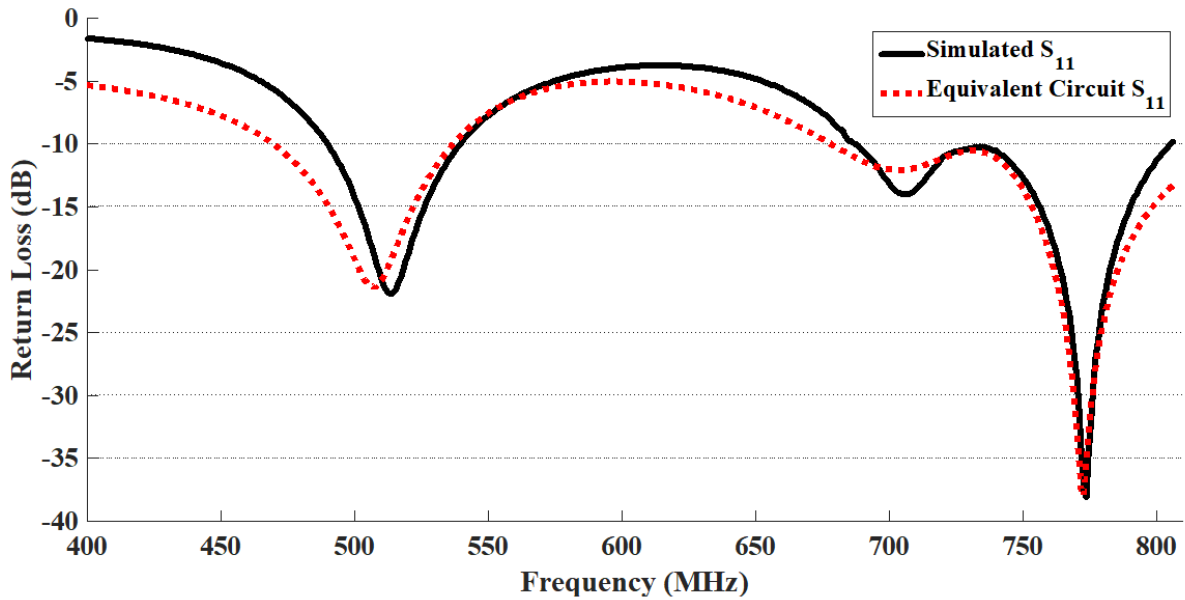
Fig. 5.13 Comparison of S_{11} of equivalent circuit and simulated antenna

5.5 Measurements and Testing

The proposed antenna is fabricated and tested at Advance Microwave Lab at the Indian Institute of Technology, Roorkee. In the first step antenna patch with fractal slots has been fabricated on a copper sheet then the ground plane with cross slots is fabricated. The front patch and background are shown in Figure 5.14.

In the second step, foam is placed between the patch and ground plane for mechanical strength. Finally, the patch is shorted with the ground and FR4 sheet is placed at the optimum height from the ground plane as shown in Figure 5.15.

(a)
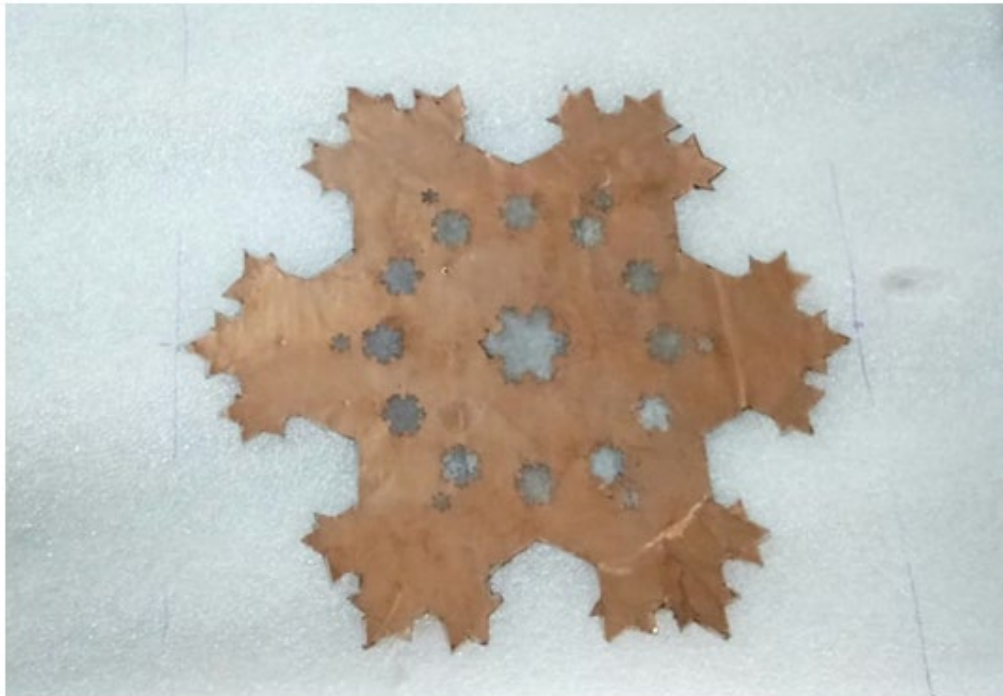
(b)

Fig. 5.14 Fabricated (a) patch and (b) ground plane.

(a)

(b)

Fig. 5.15 (a) Bottom and (b) side view of fabricated antenna

Return loss measurement with the help of VNA is shown in Figure 5.16. The proposed

antenna under test in an anechoic chamber for gain measurement is shown in Figure 5.17.
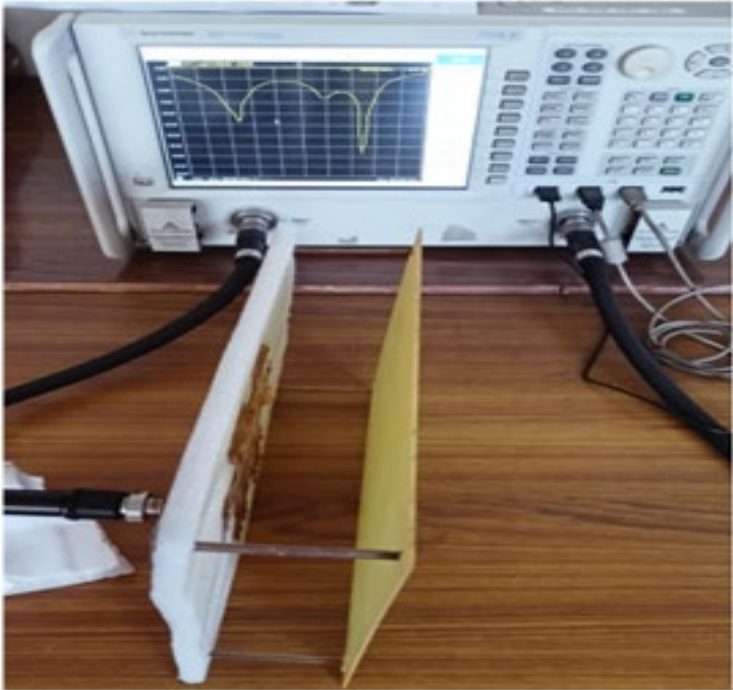
Fig. 5.16 Return loss measurement of fabricated design
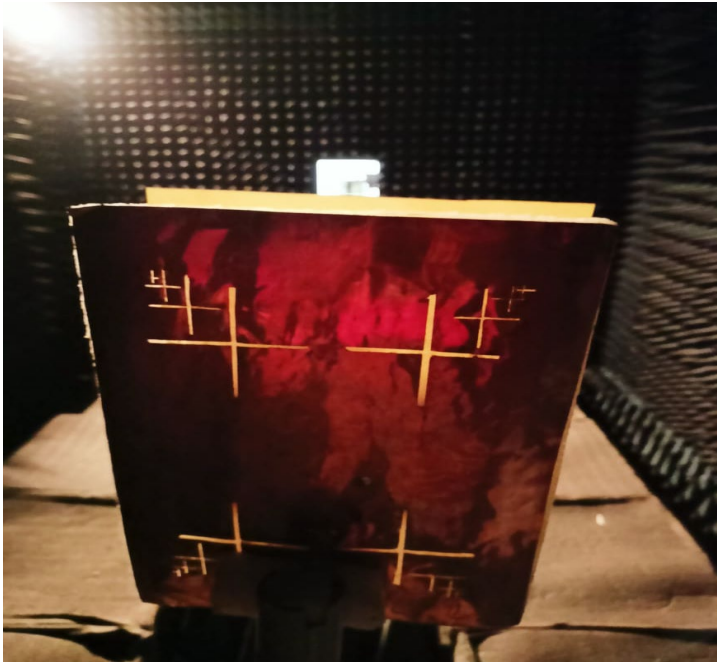
Fig. 5.17 Fabricated antenna

5.6 Simulated and Measured Results

Simulated and measured return loss is compared in Figure 5.18. The measured return loss is in good agreement with the simulated results. The simulated return loss is -21dB at 513MHz frequency and the measured return loss is -20dB at 517MHz frequency. In the 2nd band, the simulated return loss is -38dB at 773MHz and the measured return loss is -36dB at 765 MHz frequency. The measured bandwidth for the 1st band is 50MHz (490 to 540 MHz) and for the 2nd band is 117MHz (689 to 806 MHz).
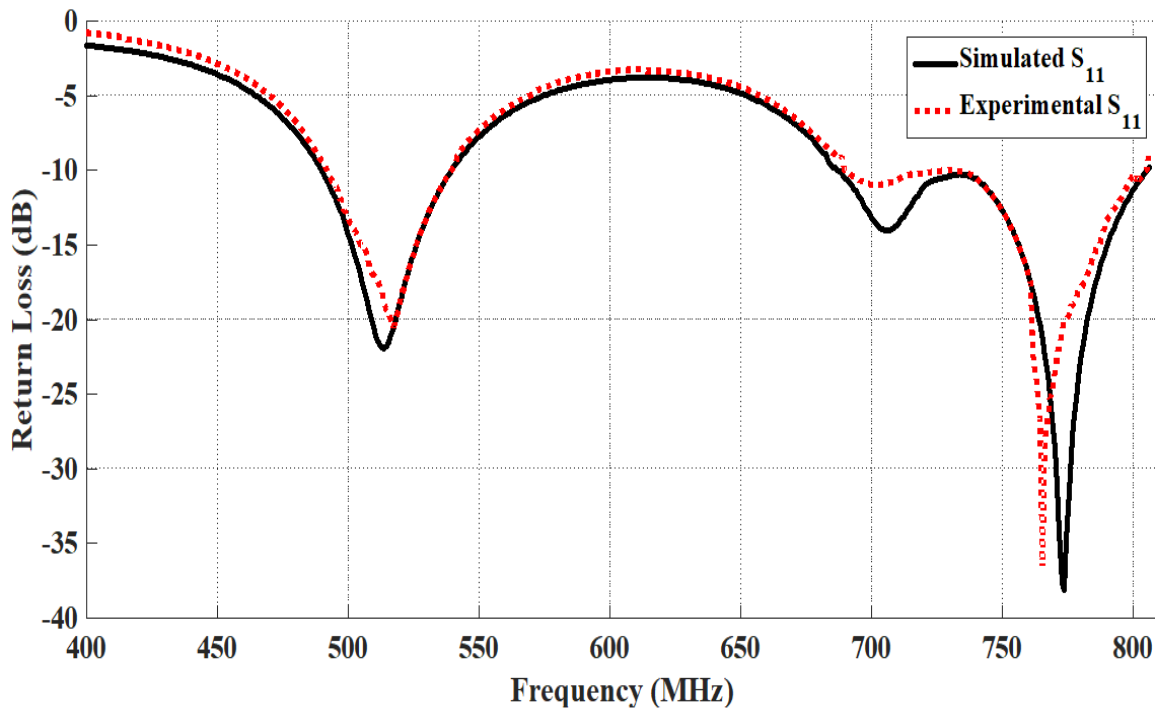
Fig. 5.18 Measured and simulated S_{11} of proposed design

The voltage standing wave ratio (VSWR) is also a key factor to realize the efficiency of any antenna design. Furthermore, VSWR is a reliable indicator of how much power an antenna reflects. For any antenna design, the value of VSWR should always be less than 2. Figure 5.19 it is indicated that the antenna is adequate for practical use as the value of VSWR is less than 2 for dual bands and the low value of VSWR is 1.05.
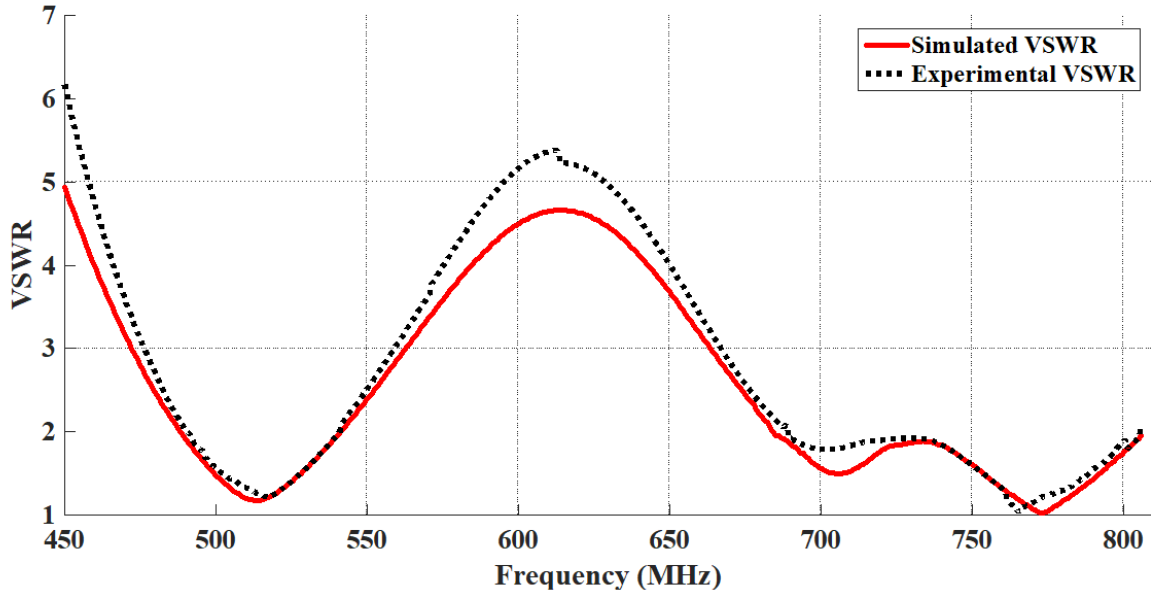
Fig. 5.19 Measured and simulated VSWR Plot of proposed design

The radiation pattern of the proposed antenna at phi=0^0 and 90^0 are shown in Figure 5.20. The graph clearly shows that the maximum gain is 4.5dBi. Some back radiations are also shown in the gain. The presence of back radiation is because of cross slots introduce in the ground plane. This back radiation can be overcome by placing a reflector at a distance of $\lambda/16$ from the ground. The reflector reduces the back lobes and gain is increased to 5.8dBi with some reduction in bandwidth as the gain bandwidth product is one. The gain verse frequency plot is depicted in Figure 5.21. The gain is more in the first band as compared to the second band. The axial ratio plot is shown in Figure.5.22. Axial ratio bandwidth is more as compared to impedance bandwidth (<10dB). The axial ratio bandwidth for 1st band is 78 MHz (480 to 558MHz). The axial ratio is less than 3dB for the first band so, the designed antenna will work in circular polarization in this band. In the 2nd band axial ratio is greater than 3dB so, the designed antenna will work in linear polarization in this band. The same design can be used for multiploidization as circular in the 1st band and linear in the 2nd band. The aim to design multi-polarization is achieved.

(a) Radiation Pattern at Phi=90 degree   (b) Radiation Pattern at Phi=0 degree
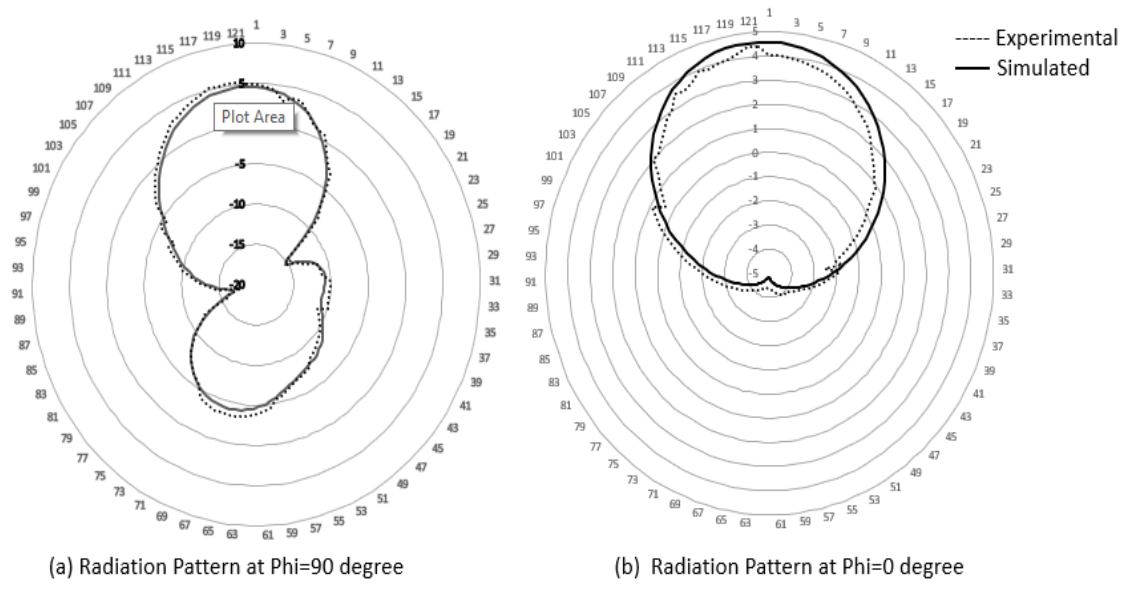
Fig. 5.20 Measured and simulated Radiation Pattern of Proposed Antenna
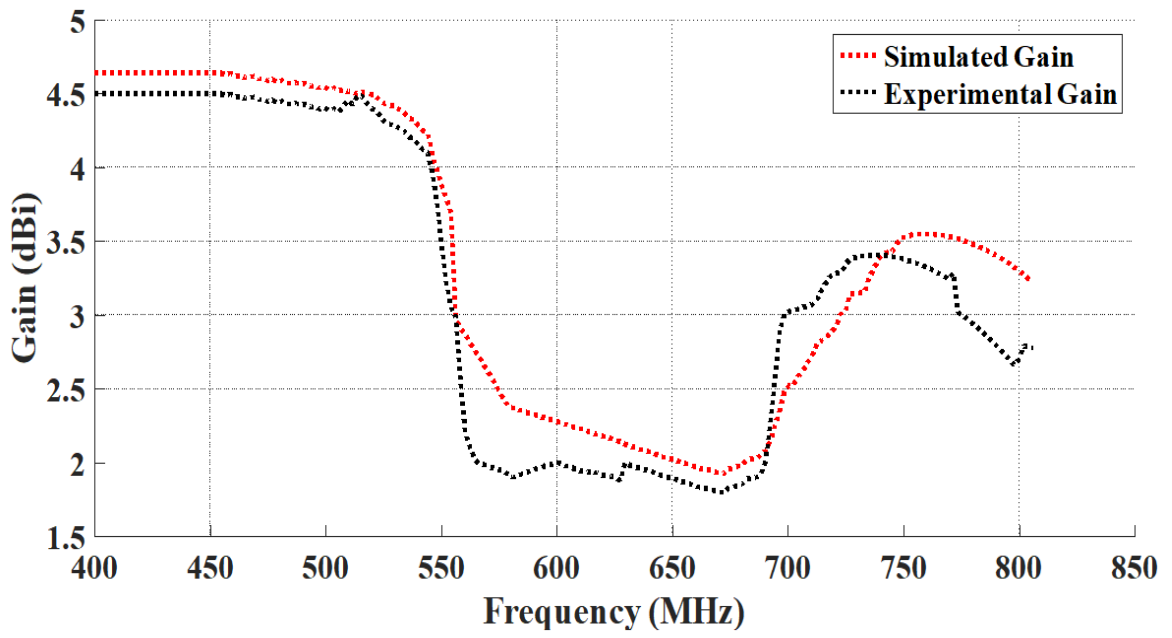
Fig. 5.21 Measured and Simulated Gain of Proposed Antenna
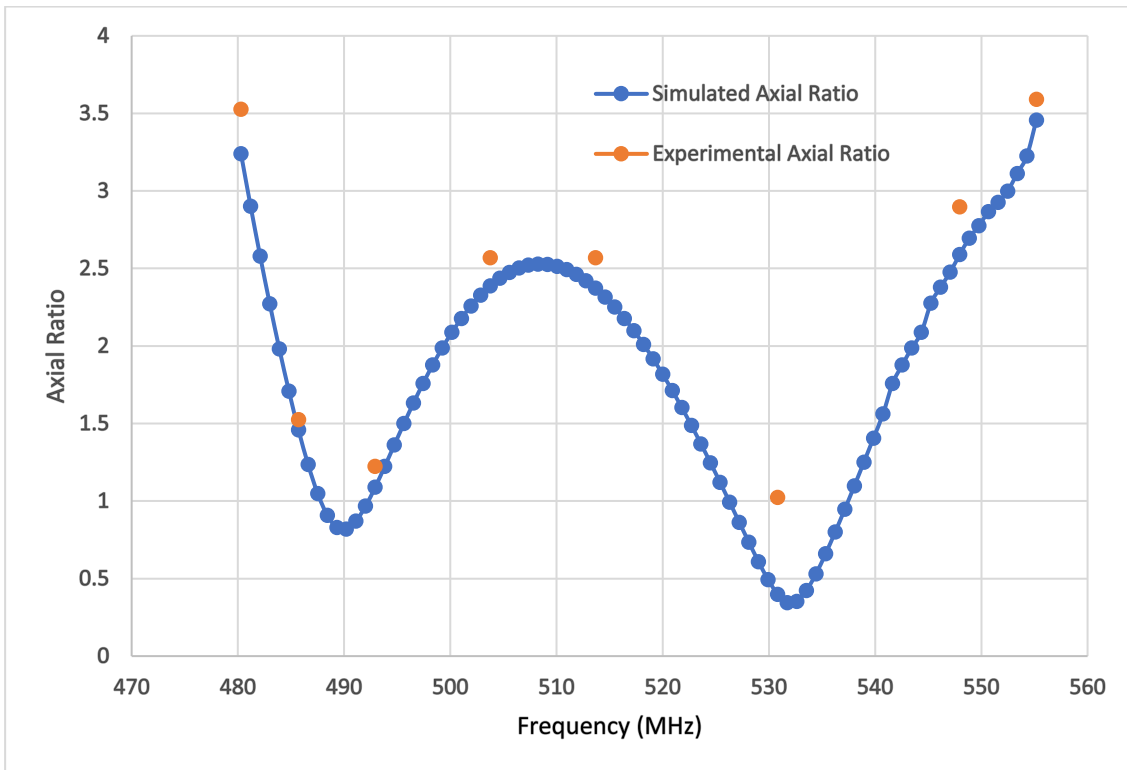
Fig.5.22 Axial Ratio plot

The electrical field vector at different angles is shown in Figure 5.23. From the electrical field vector, it is observed that the electric field is rotated counterclockwise. The electric field is minimum at 0^0 and maximum at 90^0.

(a)

(b)

(c)

(d)

(e)

(f)
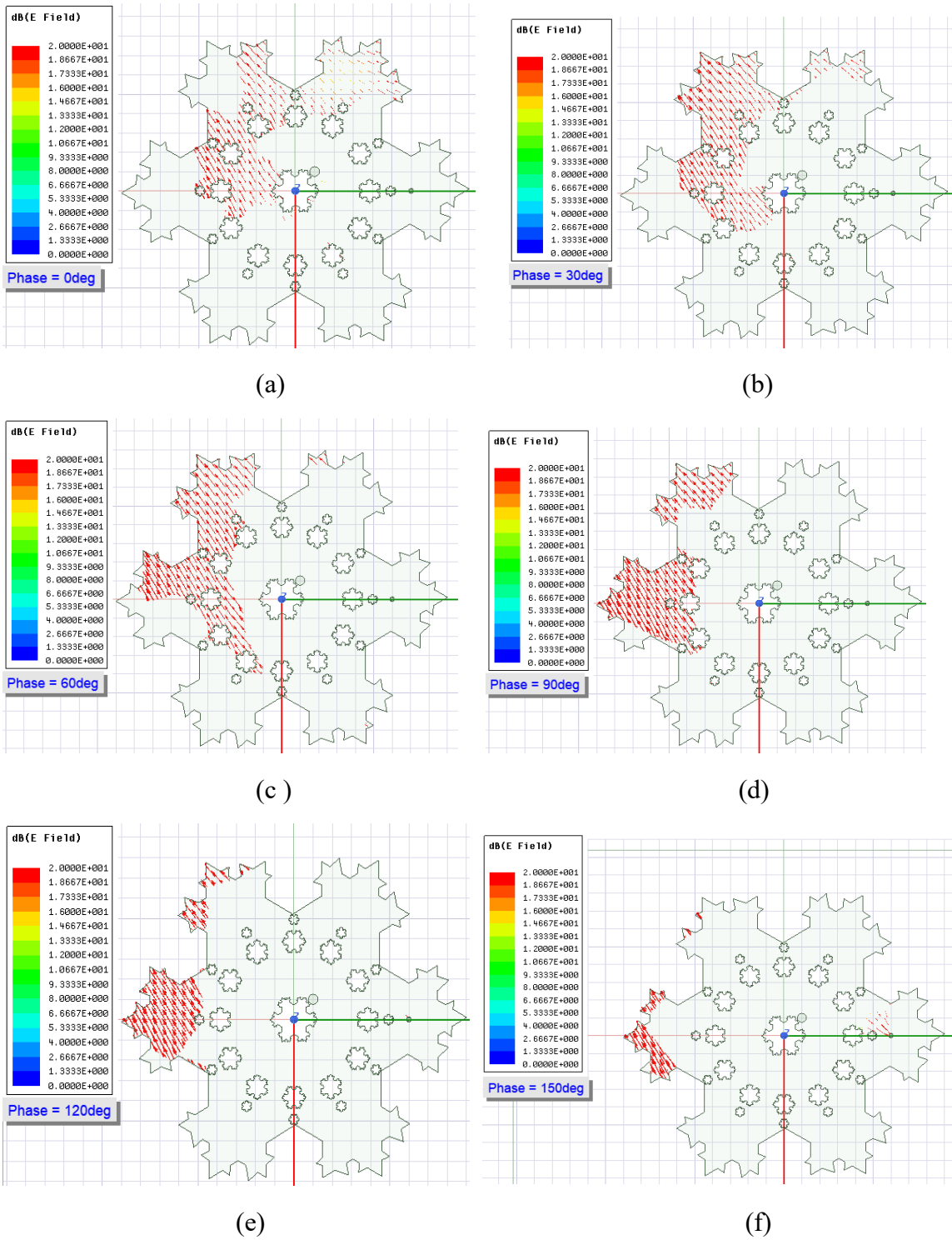
Fig.5.23 Electric field vector (a) 0^0, (b) 30^0, (c) 60^0, (d) 90^0 (e) 120^0, and (f) 150^0

The magnitude plot of the electric field is shown in Figure 5.24. From the figure it is shown that the edges of the fractal patch are more radiated as compared to other parts of the antenna.
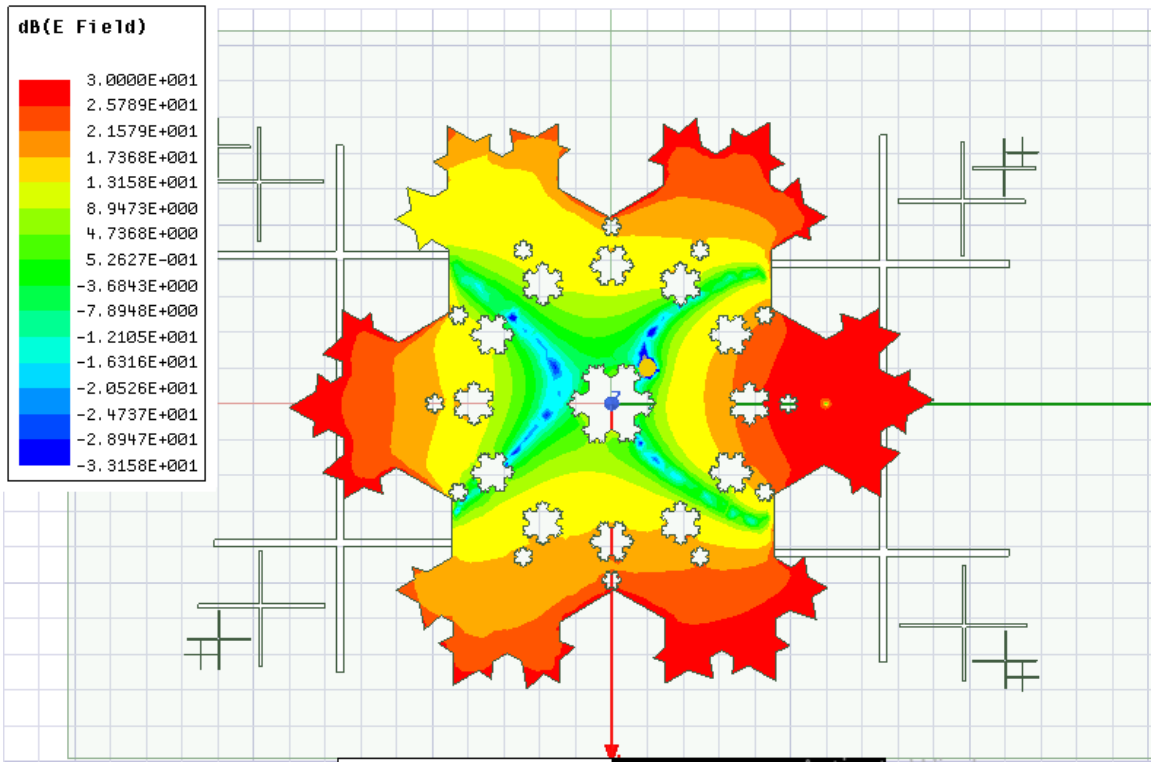
Figure 5.24 Magnitude plot of electric field

5.7 Conclusion

4th iteration of Koch snowflakes is used for the patch and 4th iteration cross slots are cut from the ground plane to get muti-band. As the number of iterations increased size of the antenna is going to reduce. Further 4th iteration Koch snowflakes slots have been created in the patch. By introducing a fourth iteration cross slot into the ground plane, three bands have been created. The antenna operates in the last bands (686-806MHz) of frequencies with linear polarization, but it can also operate in the first band(487-540MHz) of frequencies with left-hand circular polarization (LHCP). The physical size of the antenna is reduced by 38 mm with a gain of 4.5dBi. The axial Ratio bandwidth (480-558MHz) is 78MHz. The axial ratio bandwidth is

18MHz more as compared to the impedance bandwidth of 1st band. The same antenna can work in linear polarization as well as circular polarization. Multi-polarized, multiband antenna with impedance bandwidth of 10.3% (1st band) and 16.08% (last band) is designed for white space TV band frequencies.

CHAPTER 6

Conclusion and Future Scope

In conclusion, the research work in this thesis has provided insights into the design of compact and efficient microstrip patch antennas. The future scope of this research could include exploring new design techniques and testing the performance of the proposed antennas in real-world applications. This chapter is mainly separated into two segments: (i) conclusions of the complete research work, which have been discussed in this thesis, and (ii) the future scope of the given research work.

6.1 Conclusion of the proposed work

The conclusion of the work done is given below chapter-wise:

Chapter 1: In the first chapter of the thesis, the concept of the white space TV band and the TVWS technology is briefly introduced, including the rationale behind the need for TVWS and the specific spectrum requirements for a TVWS antenna. The chapter also provides a short overview of the antenna design approach used in the thesis, along with a review of existing research on enhancing gain, and bandwidth, and reducing the size of antennas. This introductory chapter sets the foundation for understanding the work presented in the rest of the thesis.

Chapter 2: TVWS technology is compared with other communication technologies in Chapter 1. There are lots of advantages of TVWS technology over other communication technologies.

But, the main interest of antenna designers is the compactness of the antenna in this technology. The solution to this problem is to design a microstrip patch antenna in the TVWS band. In this chapter, we are discussing one of the applications of the TVWS band as a radio frequency identification (RFID) antenna. RFID antenna requires better coverage, non-line of sight communication, and better penetration which can achieve with the TVWS technology. However, compactness is also the main desirable factor for RFID antenna.

In Chapter 2, a compact circular patch antenna was designed for RFID applications for India, where the frequency band is 865-867 MHz with 2 MHz bandwidth. The proposed antenna, built on FR4 substrate, had four concentric rings and a shorting pin connecting the patch to the ground. The antenna had a gain of 7.5dBi and a directivity of 9.9 dB. It operated on two bands, 479-492MHz, and 643-653MHz, with bandwidths of 13MHz and 10MHz respectively, and return losses of -29dB and -14 dB. The proposed antenna had the lowest VSWR of 1.07 compared to other commercially available RFID antennas and increased bandwidth of 13MHz compared to 3MHz. The compact size, gain, bandwidth, VSWR, front-to-back ratio, and limited ground size made the proposed design a good candidate for RFID applications.

Chapter 3: In Chapter 2, it is seen that a simple circular patch was studied and additionally, circular ring slots were incorporated into the patch design to reduce its size while maintaining a satisfactory level of gain. The results of the study indicated that this approach was successful to a significant degree. However, it is worth noting that the achieved reduction in size came at the expense of a narrow bandwidth. The main reason for the reduced bandwidth is the introduction of additional resonant modes created by the slots. The narrow bandwidth is a consequence of the interaction and interference between the different resonant modes. The additional modes introduced by the ring slots can cause frequency shifts, impedance mismatch,

and increased losses, leading to a narrower frequency range over which the antenna operates efficiently. To address the issue of narrow bandwidth in circular ring slot patch antennas, further design optimizations and modifications were explored in Chapter 3.

Building on the previous chapter, another circular microstrip patch antenna with three circular rings was designed. By adjusting the ring position and ground plane size, the antenna was improved for use in the entire TV band with low gain. By carefully adjusting the position of the ring relative to the patch, the resonance modes can be modified to cover a broader frequency range. The three rings, with frequencies of 500 MHz, 700 MHz, and 900 MHz, combine to provide wide bandwidth when embedded in a patch with a finite ground plane. Although this increased bandwidth, it reduced the gain value to 1.3dBi. The antenna's performance was compared to previous work in the TV white space spectrum and found to have good bandwidth, efficiency, and low gain. The antenna's lumped parameters were calculated and an equivalent circuit was simulated in ADS, with good agreement between the results. It is worth noting that while slot adjustments can improve the antenna's bandwidth, they may result in a lower gain. The trade-off between bandwidth and gain is a common consideration in antenna design. If maintaining a low gain is a requirement for the application, it may be necessary to sacrifice some gain performance to achieve a wider bandwidth across the TV band. The methods to improve gain will be discussed in the next chapter

Chapter 4: The slotting and shorting techniques were discussed in previous chapters for bandwidth enhancement. But, these two techniques did not contribute to high gain. The presence of ring slots can introduce additional losses in the antenna system. These losses can occur due to the increased surface currents around the slots and the coupling between the different resonant modes. As a result, the overall efficiency of the antenna may be reduced,

leading to decreased performance. Gain improvement can be achieved in a circular patch antenna by using a stacked structure which is discussed in Chapter 4. By adding additional layers or substrates beneath the circular patch, the height of the radiating element can be increased. A taller radiating element allows for a larger aperture, and enables the antenna to radiate more energy in the desired direction, leading to improved gain performance. The additional layers can help in reducing surface wave losses and enhance the coupling between the patch and the feeding mechanism. This increased efficiency allows for a higher percentage of the input power to be radiated, resulting in a gain improvement. The stacked structure can introduce multiple resonant modes, which can be effectively utilized to improve gain.

This chapter covers the study of a two-layer inverted-stacked parasitic patch antenna. The antenna has two layers stacked with coaxial feed at the driven patch and two upper parasitic patches inverted and electromagnetically connected to the lower patch, made of FR4 material. It has a gain of 5.6dBi and operates in the 499-650MHz frequency range with 98% efficiency. A parametric analysis was conducted to optimize size, gain, and radiation pattern, which showed that elliptical top patches gave the smallest size with the highest gain. Optimal top patch eccentricity was found to be 0.5 for an enhanced gain of 5.6dBi and compactness. Can be used as a user terminal or base station depending on the scenario. Low frequencies in the TVWS region between active channels are suitable for various applications like IEEE 802.11 and can penetrate obstacles like walls and trees better than high frequencies. It is important to note that the design of a stacked structure for gain improvement requires careful optimization and analysis to achieve the desired performance. The number of layers, their dimensions, and the positioning within the antenna structure should be carefully determined to maximize gain while considering other factors such as impedance matching and bandwidth requirements.

Chapter 5: The concept of stacking was addressed in the last chapter. This technique is good to increase the gain of an antenna. Stacking additional layers in the antenna structure can result in increased size and weight. This can be a limitation in applications where compactness and lightweight designs are desired. The stacked structure may require more physical space and may not be suitable for applications with strict size and weight constraints. Fractal antennas can achieve compact size while maintaining their multiband or wideband capabilities. The recursive nature of fractal geometries allows for miniaturization without sacrificing performance. This compact size can be advantageous in applications where space limitations or portability are important factors.

In this chapter fractal shapes with stacked structures are used to take benefits of stacking and self-similar properties of fractal shapes. The effects of fractal slots on patch and cross slots in the ground are investigated. The Koch snowflake patch is used to obtain a dual band in the proposed design iteration. 4th iteration Koch snowflake patch is placed 18mm above the air. FR4 is placed 65mm above the ground plane as a superstrate. As the number of iterations increased, the antenna size decreased. In the patch, additional 4th iteration Koch snowflakes slots has been added to get three bands. The last two bands were combined to increase bandwidth by forming a defected ground structure using the fourth iteration cross slot in the ground plane. The axial ratio bandwidth (<3dB) for 1st band is 78MHz. The electric field polarization of the designed antenna is circular in the first band and linear in the last band. The antenna is working in multi-polarization in the received bands. The physical dimensions of an antenna have been decreased by 38 millimeters with a gain of 4.5dBi.

6.2 Subsequent ambit of the thesis

The subsequent ambit of the thesis could involve the following areas of research and development:

1. **Composite Antenna Design**: Building upon the findings of the thesis, the next step could involve the design and optimization of a composite antenna that combines multiple antenna technologies such as microstrip, fractal, and metamaterial. This approach can potentially lead to a synergistic combination of their advantages, such as high gain, high efficiency, wide bandwidth, and reduced physical size. The composite antenna can be developed and tested to assess its performance in the TVWS band and other frequency bands of interest.

2. **Integration with TVWS Systems**: As international standards and specifications for TV band white spaces continue to evolve, it becomes crucial to integrate the proposed antennas into practical TVWS systems. This involves considering the antenna's compatibility with TVWS protocols, regulations, and cognitive radio techniques. Collaborating with relevant standards-development organizations and industry stakeholders can facilitate the integration process and ensure that the antennas meet the requirements of TVWS applications.

3. **Performance Comparison and Evaluation**: Comparative studies can be conducted to evaluate the performance of the proposed antennas against other existing antenna designs for TVWS applications. Performance metrics such as gain, efficiency, bandwidth, radiation patterns, and size can be compared to assess the advantages and limitations of the proposed designs. These studies can help validate the effectiveness and competitiveness of the developed antennas in the TVWS band.

4. **Real-World Deployment and Testing**: Finally, real-world deployment and field testing of the developed antennas can provide valuable insights into their practical performance and feasibility. Deploying the antennas in TVWS networks or pilot projects, and collecting data on their performance in various operating conditions, can further validate their effectiveness and suitability for real-world applications.

By pursuing these research directions, the thesis can contribute to the advancement of TVWS antenna technology, addressing the need for wideband, high-gain, and compact antenna solutions in the evolving landscape of TV band white spaces.

REFERENCES

[1] Abd-Alhameed, Raed A. "Bandwidth Limitations on Linearly Polarized Microstrip Antennas." *IEEE Transactions on Antennas and Propagation*, vol. 58, no. 3, Feb. 2010, pp. 1018-1018.

[2] Abdulghafor, Rawad, et al. "Recent Advances in Passive UHF-RFID Tag Antenna Design for Improved Read Range in Product Packaging Applications: A Comprehensive Review." *IEEE Access*, vol. 9, 2021, pp. 63611-63635.

[3] Abdullah- Al- Mamun, Md., et al. "Performance Analysis of Rectangular, Circular and Elliptical Shape Microstrip Patch Antenna using Coaxial Probe Feed." *2017 2nd International Conference on Electrical & Electronic Engineering (ICEEE)*, 2017, pp. 1-4.

[4] Abdullah, RSA R., et al. "Bandwidth Enhancement for Microstrip Antenna in Wireless Applications." *Modern Applied Science*, vol. 2, no. 6, 2008, pp. 1-8.

[5] Akdagli, Ali, et al. "A Review of Recent Patents on Ultra-Wide Band (UWB) Antennas." *Recent Patents on Electrical Engineering*, vol. 1, no. 1, 2008, pp. 68-75.

[6] Ali, M.T, et al. "Gain enhancement of air substrates at 5.8GHz for microstrip antenna array." *2012 Asia-Pacific Symposium on Electromagnetic Compatibility*, 2012, pp. 477-480.

[7] Al-Zoubi, Asem, et al. "A Broadband Center-Fed Circular Patch-Ring Antenna with a Monopole Like Radiation Pattern." *IEEE Transactions on Antennas and Propagation*, vol. 57, no. 3, 2009, pp. 789-792.

[8] Ang, Irene, and B. L. Ooi. "An ultra-wideband stacked microstrip patch antenna." *Microwave and Optical Technology Letters*, vol. 49, no. 7, 2007, pp. 1659-1665.

[9] Anguera, J., et al. "Miniature monopole antenna based on the fractal Hilbert curve." *IEEE Antennas and Propagation Society International Symposium (IEEE Cat. No.02CH37313)*, vol. 4, June 2002, pp. 546-549.

[10] Anguera, J., et al "Miniature wideband stacked microstrip patch antenna based on the Sierpinski fractal geometry." *IEEE Antennas and Propagation Society International Symposium. Transmitting Waves of Progress to the Next Millennium. 2000 Digest. Held in conjunction with: USNC/URSI National Radio Science Meeting (Cat. No.00CH37118)*, vol. 3, July 2000, pp. 100-1703.

[11] Anguera, J., et al "Bowtie microstrip patch antenna based on the Sierpinski fractal." *IEEE Antennas and Propagation Society International Symposium. 2001 Digest. Held in conjunction with: USNC/URSI National Radio Science Meeting (Cat. No.01CH37229)*, vol. 3, July 2001, pp. 162-165.

[12] Anguera, Jaume, et al. "An undersampled high-directivity microstrip patch array with a reduced number of radiating elements inspired on the Sierpinski fractal." *Microwave and Optical Technology Letters*, vol. 37, no. 2, 2003, pp. 100-103.

[13] Anusudha, K., and M. Karmugil. "Design of circular microstrip patch antenna for ultra-wide band applications." *2016 International Conference on Control, Instrumentation, Communication and Computational Technologies (ICCICCT)*, 2016, pp. 304-308.

[14] Ariff, M. H., et al. "Microstrip antenna based on rectangular patch with arms and partial ground plane for UHF RFID readers." *2015 IEEE 6th Control and System Graduate Research Colloquium (ICSGRC)*, vol. 10, 2015, pp. 61-65.

[15] Ariff, Mohd H., et al. "Circular microstrip patch antenna for UHF RFID reader." *Journal of Telecommunication, Electronic and Computer Engineering*, vol. 10, no. 1-2, Jan. 2018, pp. 61-65.

[16] Arya, Ashwini K., et al. "Defected Ground Structure in the perspective of Microstrip Antennas: A Review." *Frequenz*, vol. 64, no. 5-6, 2010.

[17] Aznabet, Ikram, et al. "A Broadband Modified T-Shaped Planar Dipole Antenna for UHF RFID Tag Applications." *Progress in Electromagnetics Research C*, vol. 73, 2017, pp. 137-144.

[18] Babar, A., et al. "Dual UHF RFID band miniaturized multipurpose planar antenna for compact wireless systems." *2010 International Workshop on Antenna Technology (iWAT)*, 2010, pp. 1-4.

[19] Bahl, I., et al. "Microstrip antennas covered with a dielectric layer." *IEEE Transactions on Antennas and Propagation,* vol. 30, no. 2, Mar. 1982, pp. 314-318.

[20] Bakhtiari, A., et al. "Gain Enhanced Miniaturized Microstrip Patch Antenna Using Metamaterial Superstrates." *IETE Journal of Research*, vol. 65, no. 5, 2018, pp. 635-640.

[21] Balanis, Constantine A. *Antenna Theory: Analysis and Design*. 2nd ed., Wiley, 1996.

[22] Baliarda, C.P., et al. "An iterative model for fractal antennas: application to the Sierpinski gasket antenna." *IEEE Transactions on Antennas and Propagation*, vol. 48, no. 5, 2000, pp. 713-719.

[23] Baliarda, C.P., et al "The Koch monopole: a small fractal antenna." *IEEE Transactions on Antennas and Propagation*, vol. 48, no. 11, 2000, pp. 1773-1781.

[24] Ban-Leong Ooi, et al. "Novel design of broad-band stacked patch antenna." *IEEE Transactions on Antennas and Propagation*, vol. 50, no. 10, 2002, pp. 1391-1395.

[25] Bauer, Jan, and Mario Schuhler "Compact wideband antenna for TV White Spaces." *The 8th European Conference on Antennas and Propagation (EuCAP 2014)*, 2014, pp. 2894-2896.

[26] Bhartia, P., et al. *Millimeter-wave Microstrip and Printed Circuit Antennas*. Artech House Antenna Library, 1991.

[27] Bhattacharya, Manidipa. "An experimental study on compact dual frequency microstrip antenna." *2007 IEEE Applied Electromagnetics Conference (AEMC)*, 2007, pp. 1-4.

[28] Bzeih, Amer, et al. "Empirical Formulation and Design of a Broadband Enhanced E-Patch Antenna." *2007 National Radio Science Conference*, 2007, pp. 1-9.

[29] Chair, R., et al. "Wideband half U-slot patch antennas with shorting pin and shorting wall." *IEEE Antennas and Propagation Society Symposium, 2004*, 2004.

[30] Chakravarty, T., and A. De. "Design of tunable modes and dual-band circular patch antenna using shorting posts." *IEE Proceedings - Microwaves, Antennas and Propagation*, vol. 146, no. 3, 1999, p. 224.

[31] Chakravarty, Tapas, and Asok De. "Investigation of Modes Tunable Circular Patch Radiator with Arbitrarily Located Shorting Posts." *IETE Technical Review*, vol. 16, no. 1, 1999, pp. 109-111.

[32] Chakravarty, Tapas, and Asok De. "Resonant frequency of a shorted circular patch with the use of a modified impedance expression for a metallic post." *Microwave and Optical Technology Letters*, vol. 33, no. 4, 2002, pp. 252-256.

[33] Chakravarty, Tapas, and Asok De. "Using cavity model analysis to design a dual-band dual-slant-polarized microstrip antenna." *Microwave and Optical Technology Letters*, vol. 37, no. 5, 2003, pp. 331-337.

[34] Chakravarty, Tapas, et al. "A novel microstrip patch antenna with large impedance bandwidth in VHF/UHF rang." *Progress in Electromagnetics Research*, vol. 54, 2005, pp. 83-93.

[35] Chen, Sitao, et al. "Circularly Polarized Stacked Circular Microstrip Antenna with an Arc Feeding Network." *Electrical Engineering and Control*, 2011, pp. 927-932.

[36] Chi Yuk Chiu, et al. "Bandwidth enhancement technique for quarter-wave patch antennas." *IEEE Antennas and Wireless Propagation Letters*, vol. 2, 2003, pp. 130-132.

[37] Chiu, C.Y., et al. "Study of slotted microstrip patch antennas with folded patch feed." *IEE Proceedings - Microwaves, Antennas and Propagation*, vol. 152, no. 5, 2005, p. 319.

[38] Cohen, N. "Fractal and Shaped Dipoles." Communications Quarterly, Spring, 1996, pp. 25-36.

[39] Cohen, N. "Fractal Antennas: Part 2." *Communications Quarterly, Summer*, 1996, pp. 53-66.

[40] Cohen, N. "Fractal Antennas: Part I." *Communications s Quarterly, summer, 199*, 1995, pp. 7-22.

[41] Dahele, J., et al. "Dual-frequency stacked annular-ring microstrip antenna." *IEEE Transactions on Antennas and Propagation*, vol. 35, no. 11, 1987, pp. 1281-1285.

[42] Darwhekar, Ishan S., et al. "Wideband Triangular Patch Antenna for Cognitive Radio in TV White Space." *2019 2nd International Conference on Innovations in Electronics, Signal Processing and Communication (IESC)*, 2019, pp. 115-118.

[43] Dastranj, A., and H. Abiri. "Bandwidth Enhancement of Printed E-Shaped Slot Antennas Fed by CPW and Microstrip Line." *IEEE Transactions on Antennas and Propagation*, vol. 58, no. 4, 2010, pp. 1402-1407.

[44] Dawar, Parul, et al. "Directive and Broadband 4-seg SRR Metamaterial Antennas." *International Journal of Advanced Science and Technology*, vol. 97, 2016, pp. 1-12.

[45] Dawar, Parul, et al. "S-Shaped Metamaterial Ultra-Wideband Directive Patch Antenna." *Radio electronics and Communications Systems*, vol. 61, no. 9, 2018, pp. 394-405.

[46] Dawar, Parul, et al. "A novel metamaterial for miniaturization and multi-resonance in antenna." *Cogent Physics*, vol. 2, no. 1, 2015, p. 1123595.

[47] Dawar, Parul, et al. "FEM and Transmission Line based Analysis of 'Closed Ring Pair' Metamaterial." *International Journal of Signal Processing, Image Processing and Pattern Recognition*, vol. 8, no. 12, 2015, pp. 351-356.

[48] Dawar, Parul, et al. "UWB Metamaterial-Loaded Antenna for C-Band Applications." *International Journal of Antennas and Propagation*, vol. 2019, 2019, pp. 1-13.

[49] De, A., and T. Chakravarty. "Theoretical Investigation of Resonant Modes of Shorting Post Loaded Circular Microstrip Antenna on Sphere." *Journal of Electromagnetic Waves and Applications*, vol. 14, no. 8, 2000, pp. 1087-1102.

[50] De, Asok, et al. "Effect of different substrates on Compact stacked square Microstrip Antenna." *Journal of Telecommunications,* vol. 1, no. 1, Feb. 2010, pp. 63-65.

[51] De, Asok. *Study on rectangular and circular microstrip patch radiators*. 1985. Indian Institute of Technology, Kharagpur, India,

[52] Deshmukh, A.A., and G. Kumar. "Half U-slot loaded rectangular microstrip antenna." *IEEE Antennas and Propagation Society International Symposium. Digest. Held in*

conjunction with: *USNC/CNC/URSI North American Radio Sci. Meeting (Cat. No.03CH37450)*, vol. 2, pp. 876-879.

[53] Dey, Supriyo, and Raj Mittra. "Compact microstrip patch antenna." *Microwave and Optical Technology Letters*, vol. 13, no. 1, 1996, pp. 12-14.

[54] Dhande, Tanvi A., et al. "Wideband Patch Antenna for Cognitive Radio Applications in TV White Space." *2019 10th International Conference on Computing, Communication and Networking Technologies (ICCCNT)*, 2019, pp. 1-6.

[55] El-Khamy, S.E., et al. "A simplified Koch multiband fractal array using windowing and quantization techniques." *IEEE Antennas and Propagation Society International Symposium. Transmitting Waves of Progress to the Next Millennium. 2000 Digest. Held in conjunction with: USNC/URSI National Radio Science Meeting (Cat. No.00CH37118)*, vol. 3, 2000, pp. 1716-1719.

[56] Facchine, M. J., and D. H. Werner. "Fractal Spheres as Molecules for Artificial Dielectric Metamaterials." *Electromagnetics*, vol. 26, no. 3-4, 2006, pp. 289-300.

[57] Fan Yang, and Y. Rahmat-Samii. "Wideband dual parallel slot patch antenna (DPSPA) for wireless communications." *IEEE Antennas and Propagation Society International Symposium. Transmitting Waves of Progress to the Next Millennium. 2000 Digest. Held in conjunction with: USNC/URSI National Radio Science Meeting (Cat. No.00CH37118)*, vol. 3, 2000, pp. 1650-1653.

[58] Faudzi, N. M., et al. "Wideband slotted microstrip patch antenna for UHF-RFID reader." *Journal of Physics: Conference Series*, vol. 1755, no. 1, 2021, pp. 1-11.

[59] Gauthier, G.P., et al. "Microstrip antennas on synthesized low dielectric-constant substrates." *IEEE Transactions on Antennas and Propagation*, vol. 45, no. 8, 1997, pp. 1310-1314.

[60] Ghannoum, H., et al. "Probe Fed Stacked Patch Antenna for UWB Sectoral Applications." *2005 IEEE International Conference on Ultra-Wideband*, pp. 97-102.

[61] Ghorbani, A., et al. "Bandwidth Limitations on Linearly Polarized Microstrip Antennas." *IEEE Transactions on Antennas and Propagation*, vol. 58, no. 2, 2010, pp. 250-257.

[62] Gite, Subodh, and Deeplaxmi Niture. "A compact printed monopole antenna for TV white space applications using defected ground structure." *2015 International Conference on Information Processing (ICIP)*, 2015, pp. 198-200.

[63] Guha, D., et al. "Microstrip Patch Antenna with Defected Ground Structure for Cross Polarization Suppression." *IEEE Antennas and Wireless Propagation Letters*, vol. 4, 2005, pp. 455-458.

[64] Guha, D., and Y. M. M. Antar. "Circular Microstrip Patch Loaded with Balanced Shorting Pins for Improved Bandwidth." *IEEE Antennas and Wireless Propagation Letters*, vol. 5, 2006, pp. 217-219.

[65] Guo, Fangzhou, et al. "A Novel Metamaterial Transmission Line with Adjustable Left-Handed Elements and Its Application to H Plane Filter." *IEEE Microwave and Wireless Components Letters*, vol. 28, no. 9, 2018, pp. 774-776.

[66] Guo, Y.-X., et al. "Wide-Band L-Probe Fed Circular Patch Antenna for Conical-Pattern Radiation." *IEEE Transactions on Antennas and Propagation*, vol. 52, no. 4, 2004, pp. 1115-1116.

[67] Gupta, Sakshi, et al. "Dual Band U-Slotted Microstrip Patch Antenna for C Band and X Band Radar Applications." *2013 5th International Conference on Computational Intelligence and Communication Networks*, 2013, pp. 41-43.

[68] Gupta, Sonal, et al. "Design of circularly polarized antenna using inclined fractal defected ground structure for S-band applications." *Electromagnetics*, vol. 40, no. 7, 2020, pp. 526-540.

[69] Hassani, H.R., and D. Mirshekar-syahkal. "Analysis of triangular patch antennas including radome effects." *IEE Proceedings H Microwaves, Antennas and Propagation*, vol. 139, no. 3, 1992, p. 251.

[70] Helmi, Mariam H., and Hassan A. Ragheb. "Monopole Antenna Design for UHF Circularly Polarized RFID Applications." *Progress in Electromagnetics Research Letters*, vol. 106, 2022, pp. 81-88.

[71] Hohlfeld, R.G., and N. Cohen. "Fractal Loops and the Small Loop Approximation." *Communications Quarterly-winter*, 1996, pp. 77-81.

[72] Howell, J. "Microstrip antennas." *IEEE Transactions on Antennas and Propagation*, vol. 23, no. 1, 1975, pp. 90-93.

[73] Hwang, Kuem C. "A Modified Sierpinski Fractal Antenna for Multiband Application." *IEEE Antennas and Wireless Propagation Letters*, vol. 6, 2007, pp. 357-360.

[74] Ilk won Kim, et al. "The Koch island fractal microstrip patch antenna." *IEEE Antennas and Propagation Society International Symposium. 2001 Digest. Held in conjunction with: USNC/URSI National Radio Science Meeting (Cat. No.01CH37229)*, vol. 2, July 2001, pp. 736-739.

[75] Islam, Md Z., et al. "TV White Space Based Wireless Broadband Internet Connectivity: A Case Study with Implementation Details and Performance Analysis." *IEEE Open Journal of the Communications Society*, vol. 2, 2021, pp. 2449-2462.

[76] Jamaluddin, Mohd H., and Mohd Haizal. "A Wideband Dielectric Resonator Antenna with a C shaped Slot Aperture for 5G Applications." *Radio engineering*, vol. 22, no. 3, Sept. 2013, pp. 708-713.

[77] James, R., et al. *Handbook of Microstrip Antennas*. IET, 1989.

[78] Junho Yeo, and R. Mittra. "Modified Sierpinski gasket patch antenna for multiband applications." *IEEE Antennas and Propagation Society International Symposium. 2001 Digest. Held in conjunction with: USNC/URSI National Radio Science Meeting (Cat. No.01CH37229)*, vol. 3, July 2001, pp. 134-137.

[79] Kandwal, Abhishek, and Sunil K. Khah. "A Novel Design of Gap-Coupled Sectoral Patch Antenna." *IEEE Antennas and Wireless Propagation Letters*, vol. 12, 2013, pp. 674-677.

[80] Kang, Kyu-Min, and Byung J. Jeong. "TV band device for TV white space field trial." *2014 IEEE International Conference on Consumer Electronics (ICCE)*, Jan. 2014, pp. 450-451.

[81] Kattimani, Bharamappa, and Rajendra R. Patil. "Bandwidth Enhancement of Microstrip Antenna Using Fractal Geometry for S-Band Applications." *SN Computer Science*, vol. 2, no. 4, 2021, p. 282.

[82] Kaul, Nishant, et al. "Effect of parasitic patch configurations on multi-banding of microstrip antenna." *2015 4th International Conference on Reliability, Infocom Technologies and Optimization (ICRITO) (Trends and Future Directions)*, 2015, pp. 1-4.

[83] Ke-Ren Chen, et al. "A Compact Monopole Antenna for Super Wideband Applications." *IEEE Antennas and Wireless Propagation Letters*, vol. 10, 2011, pp. 488-491.

[84] Khandelwal, Mukesh K., et al. "Defected Ground Structure: Fundamentals, Analysis, and Applications in Modern Wireless Trends." *International Journal of Antennas and Propagation*, vol. 2017, 2017, pp. 1-22.

[85] Khanna, Anshika, et al. "Bandwidth enhancement of modified square fractal microstrip patch antenna using gap-coupling." *Engineering Science and Technology, an International Journal*, vol. 18, no. 2, 2015, pp. 286-293.

[86] Konstantatos, G., et al. "Finite Element Modeling of Minkowski Monopole Antennas Printed on Wireless Devices." *Electromagnetics*, vol. 24, no. 1-2, 2004, pp. 81-93.

[87] Kotla, Sindhu, et al. "Compact Circularly Polarized Fractal Patch Antenna using Defected Ground Structure." *2019 TEQIP III Sponsored International Conference on Microwave Integrated Circuits, Photonics and Wireless Networks (IMICPW)*, 2019, pp. 29-33.

[88] Kumar, Ashwini, and Amar P. Pharwaha. "Development of a Modified Hilbert Curve Fractal Antenna for Multiband Applications." *IETE Journal of Research*, vol. 68, no. 5, 2020, pp. 3597-3606.

[89] Kumar Deb, Partha, et al. "Return loss and bandwidth enhancement of microstrip antenna using Defected Ground Structure (DGS)." *2015 2nd International Conference on Signal Processing and Integrated Networks (SPIN)*, 2015.

[90] Kumar, Hemant, and Girish Kumar. "A broadband planar modified Quasi-Yagi using log-periodic antenna." *Progress in Electromagnetics Research Letters*, vol. 73, 2018, pp. 23-30.

[91] Kumar, Pradeep, and G. Singh. "Microstrip Antennas Loaded with Shorting Post." *Engineering*, vol. 01, no. 01, 2009, pp. 41-45.

[92] Kumar, Sanjeev, et al. "A Frequency Reconfigurable Antenna for Sub-GHz and TV White Space Applications." *Lecture Notes in Electrical Engineering*, 2021, pp. 459-471.

[93] Kumprasert, N., and W. Kiranon. "Simple and accurate formula for the resonant frequency of the circular microstrip disk antenna." *IEEE Transactions on Antennas and Propagation*, vol. 43, no. 11, 1995, pp. 1331-1333.

[94] Lai, Hau W., et al. "Broadband Circularly Polarized Patch Antenna Arrays with Multiple-Layers Structure." *IEEE Antennas and Wireless Propagation Letters*, vol. 16, 2017, pp. 525-528.

[95] Li, Ke, et al. "Design of Electrically Small Metamaterial Antenna with ELC and EBG Loading." *IEEE Antennas and Wireless Propagation Letters*, vol. 12, 2013, pp. 678-681.

[96] Liang, Xu, and Michael Yan Wah Chia. "Multiband characteristics of two fractal antennas." *Microwave and Optical Technology Letters*, vol. 23, no. 4, 1999, pp. 242-245.

[97] Long, S., and M. Walton. "A dual-frequency stacked circular-disc antenna." *IEEE Transactions on Antennas and Propagation*, vol. 27, no. 2, 1979, pp. 270-273.

[98] Maci, S., et al. "Single-layer dual frequency patch antenna." *Electronics Letters*, vol. 29, no. 16, 1993, p. 1441.

[99] Maci, S., and G.B. Gentili. "Dual-frequency patch antennas." *IEEE Antennas and Propagation Magazine*, vol. 39, no. 6, 1997, pp. 13-20.

[100] Mahamuni, Chaitanya V. "Performance enhancement of microstrip patch antenna using metamaterial cover." *2016 International Conference on Global Trends in*

Signal Processing, Information Computing and Communication (ICGTSPICC), 2016.

[101] Mahmoud, M. "Improving the Bandwidth of U-slot Microstrip Antenna Using a New Technique (Trough-Slot Patch)." *2008 IEEE Region 5 Conference*, Apr. 2008, pp. 1-6.

[102] Majrouhi Sardroud, Javad. "Influence of RFID technology on automated management of construction materials and components." *Scientia Iranica*, vol. 19, no. 3, 2012, pp. 381-392.

[103] Mak, C.L., et al. "Half U-slot patch antenna with shorting wall." *Electronics Letters*, vol. 39, no. 25, 2003, p. 1779.

[104] Mandelbrot, Benoit B., and John A. Wheeler. "*The Fractal Geometry of Nature*." *American Journal of Physics*, vol. 51, no. 3, 1983, pp. 286-287.

[105] Matin, M. A., and M. A. Mohd Ali. "Design of broadband stacked E-shaped patch antenna." *2008 International Conference on Microwave and Millimeter Wave Technology*, vol. 4, 2008, pp. 1662-1663.

[106] Matin, M. A., et al. "Probe Fed Stacked Patch Antenna for Wideband Applications." *IEEE Transactions on Antennas and Propagation*, vol. 55, no. 8, 2007, pp. 2385-2388.

[107] "Memorandum Opinion and Order on Reconstruction of the Seventh Report and Order and Eighth report and Order." *fcc,gov*, 20 Aug. 2008, hraunfoss.fcc.gov/edocspublic/attachment/FCC-08-183A1.pdf.

[108] Monebhurrun, Vikass. "Revision of IEEE Standard 145-2013: IEEE Standard for Definitions of Terms for Antennas [Stand on Standards]." *IEEE Antennas and Propagation Magazine*, vol. 62, no. 3, 2020, pp. 117-117.

[109] Moussa, R., et al. "Negative refraction and superlens behavior in a two-dimensional photonic crystal." *Physical Review B*, vol. 71, no. 8, 2005.

[110] Nakano, H., and K. Vichien. "Dual-frequency square patch antenna with rectangular notch." *Electronics Letters*, vol. 25, no. 16, 1989, p. 1067.

[111] Nashaat, Dalia, et al. "Multiband and miniaturized inset feed microstrip patch antenna using multiple spiral-shaped defect ground structure (DGS)." *2009 IEEE Antennas and Propagation Society International Symposium*, 2009, pp. 1-4.

[112] Nayna, Tahsin F., et al. "Bandwidth enhancement of a rectangular patch antenna in X band by introducing diamond shaped slot and ring in patch and defected ground structure." *2017 International Conference on Wireless Communications, Signal Processing and Networking (WiSPNET)*, 2017, pp. 2512-2516.

[113] Oh, Ser W., et al. *TV White Space: The First Step Towards Better Utilization of Frequency Spectrum*. John Wiley & Sons, 2016.

[114] Ooi, B.L., and C.L. Lee. "Broadband air-filled stacked U-slot patch antenna." *Electronics Letters*, vol. 35, no. 7, 1999, p. 515.

[115] Ooi, B.L., and Q. Shen. "A novel stacked E-shaped patch antenna." *IEEE Antennas and Propagation Society International Symposium. 2001 Digest. Held in conjunction with: USNC/URSI National Radio Science Meeting (Cat. No.01CH37229)*, vol. 4, pp. 478-481.

[116] Owusu, Joseph, et al. "Omnidirectional antenna with modified ground plane for wideband DVB in handheld devices." *Scientific African*, vol. 13, 2021, pp. 2468-2276.

[117] Ozpinar, Hurrem, and Sinan Aksimsek. "Fractal interwoven resonator based penta-band metamaterial absorbers for THz sensing and imaging." *Scientific Reports*, vol. 12, no. 1, 2022.

[118] Park, Hoon, et al. "An enhanced bandwidth planar inverted-F antenna with a modified shorting strip." *Microwave and Optical Technology Letters*, vol. 49, no. 3, 2007, pp. 513-515.

[119] Parron, J., et al. "Analysis of a Sierpinski fractal patch antenna using the concept of macro basis functions." *IEEE Antennas and Propagation Society International Symposium. 2001 Digest. Held in conjunction with: USNC/URSI National Radio Science Meeting (Cat. No.01CH37229)*, vol. 3, July 2001, pp. 616-619.

[120] Patel, Jigar M., et al. "Design of S-shaped multiband microstrip patch antenna." *2012 Nirma University International Conference on Engineering (NUiCONE)*, 2012.

[121] Patil, V. P. ""Enhancement of Bandwidth of Rectangular Patch." *International Journal of Engineering Sciences & Emerging Technologies*, vol. 3, no. 2, Oct. 2012, pp. 477-481.

[122] Pedra, A.C.O., et al. "Bandwidth and size optimisation of a wide-band E-shaped patch antenna." *2007 SBMO/IEEE MTT-S International Microwave and Optoelectronics Conference*, 2007.

[123] Pedra, Antonio C., et al. "Optimization of E-shaped patch antenna." *Microwave and Optical Technology Letters*, vol. 52, no. 7, 2010, pp. 1556-1561.

[124] Pendry, J. B., et al. "Low frequency plasmons in thin-wire structures." *Journal of Physics: Condensed Matter*, vol. 10, no. 22, 1998, pp. 4785-4809.

[125] Perini, J., and D. Portofee. "Design of broadband antenna matching networks." *IEEE 1988 International Symposium on Electromagnetic Compatibility*,

[126] Petko, J.S., and D.H. Werner. "Dense 3D fractal tree structures as miniature end-loaded dipole antennas." *IEEE Antennas and Propagation Society International Symposium (IEEE Cat. No.02CH37313)*, June 2002, pp. 94-97.

[127] Pinifolo, Jonathan, et al. "Design of a low-cost television White Space Z antenna." *2015 IST-Africa Conference*, 2015, pp. 1-7.

[128] Pozar, D.M. "Microstrip antennas." *Proceedings of the IEEE*, vol. 80, no. 1, 1992, pp. 79-91.

[129] Prombutr, N., et al. "Bandwidth Enhancement of UWB Microstrip Antenna with a Modified Ground Plane." *International Journal of Microwave Science and Technology*, vol. 2009, 2009, pp. 1-7.

[130] Puente, C., et al. "Multiband properties of a fractal tree antenna generated by electrochemical deposition." *Electronics Letters*, vol. 32, no. 25, 1996, p. 2298.

[131] Puente, C., et al. "Variations on the fractal Sierpinski antenna flare angle." *IEEE Antennas and Propagation Society International Symposium. 1998 Digest. Antennas: Gateways to the Global Network. Held in conjunction with: USNC/URSI National Radio Science Meeting (Cat. No.98CH36194)*, vol. 4, June 1998, pp. 2340-2343.

[132] Puente, C., et al. "Perturbation of the Sierpinski antenna to allocate operating bands." *Electronics Letters*, vol. 32, no. 24, 1996, p. 2186.

[133] Puente, C., et al. "Small but long Koch fractal monopole." *Electronics Letters*, vol. 34, no. 1, 1998, p. 9.

[134] Puente, C., et al. "Fractal multiband antenna based on the Sierpinski gasket." *Electronics Letters*, vol. 32, no. 1, 1996, p. 1.

[135] Puente-Baliarda, C., et al. "On the behavior of the Sierpinski multiband fractal antenna." *IEEE Transactions on Antennas and Propagation*, vol. 46, no. 4, 1998, pp. 517-524.

[136] Raghava, N., et al. "High Gain Patch Antenna for WBAN Applications." *SOP Transactions on Wireless Communications*, vol. 1, no. 2, 2014, pp. 34-41.

[137] Raghava, N. S., and A. De. "Photonic Bandgap Stacked Rectangular Microstrip Antenna for Road Vehicle Communication." *IEEE Antennas and Wireless Propagation Letters*, vol. 5, 2006, pp. 421-423.

[138] Raghava, N. S., and Asok De. "A Novel High-Performance Patch Radiator." *International Journal of Microwave Science and Technology*, vol. 2008, 2008, pp. 1-4.

[139] Raghava, N. S., et al. "A novel patch antenna for ultra-wideband applications." *2011 International Conference on Communications and Signal Processing*, 2011.

[140] Rahman, Mahbubur, and Abusayeed Saifullah. "A comprehensive survey on networking over TV white spaces." *Pervasive and Mobile Computing*, vol. 59, 2019, p. 101072.

[141] Ramalakshmi, Gudla, and P. Mallikarjuna Rao. "A Novel Metamaterial Inspired 2nd Iteration Koch Fractal Antenna for Wi-Fi, WLAN, C band and X band Wireless Communications." *Journal of Physics: Conference Series*, vol. 2062, no. 1, 2021, p. 012004.

[142] Rambabu, K., et al. "Design method for patch antennas short circuited at one end." *Proceedings of 1997 Asia-Pacific Microwave Conference*,

[143] Ray, K. P., and Girish Kumar. "Determination of the resonant frequency of microstrip antennas." *Microwave and Optical Technology Letters*, vol. 23, no. 2, 1999, pp. 114-117.

[144] Reddy, Mekala H., et al. "Bandwidth enhancement of microstrip patch antenna using parasitic patch." *2017 IEEE International Conference on Smart Technologies and Management for Computing, Communication, Controls, Energy and Materials (ICSTM)*, 2017.

[145] "Regulatory status for using RFID in the EPC Gen2 (860 to 960 MHz) band of the UHF spectrum." *The Global language of business*, Mar. 2021, pp. 1-21.

[146] Romeu, J., et al. "High directivity modes in the Koch island fractal patch antenna." *IEEE Antennas and Propagation Society International Symposium. Transmitting Waves of Progress to the Next Millennium. 2000 Digest. Held in conjunction with: USNC/URSI National Radio Science Meeting (Cat. No.00CH37118)*, vol. 3, July 2000, pp. 1696-1699.

[147] Romeu, J., and J. Soler. "Generalized Sierpinski fractal multiband antenna." *IEEE Transactions on Antennas and Propagation*, vol. 49, no. 8, 2001, pp. 1237-1239.

[148] Rusdiyanto, Dian, et al. "Bandwidth and Gain Enhancement of Microstrip Antenna Using Defected Ground Structure and Horizontal Patch Gap." *SINERGI*, vol. 25, no. 2, 2021, p. 153.

[149] Rushingabigwi, Gerard, et al. "The Impact of Substrate Materials to the Design of UWB Modern Antennas." *Journal of Computer and Communications*, vol. 04, no. 03, 2016, pp. 20-27.

[150] Sabapathy, T., et al. "Gain enhancement of circular patch antenna using parasitic ring." *2013 IEEE Antennas and Propagation Society International Symposium (APSURSI)*, 2013.

[151] Salman, Karrar N., et al. "Coplanar UHF RFID tag antenna with U-shaped inductively coupled feed for metallic applications." *PLOS ONE*, vol. 12, no. 6, 2017, p. e0178388.

[152] Salmasi, Mostafa P., et al. "A Novel Broadband Fractal Sierpinski Shaped, Microstrip Antenna." *Progress In Electromagnetics Research C*, vol. 4, 2008, pp. 179-190.

[153] Schurig, D., et al. "Metamaterial Electromagnetic Cloak at Microwave Frequencies." *Science*, vol. 314, no. 5801, 2006, pp. 977-980.

[154] Shackelford, A.K., et al. "Correction to "Design of small-size wide-bandwidth microstrip-patch antennas"." *IEEE Antennas and Propagation Magazine*, vol. 45, no. 2, 2003, pp. 58-58.

[155] Shackelford, A.K., et al. "U-slot patch antenna with shorting pin." *Electronics Letters*, vol. 37, no. 12, 2001, p. 729.

[156] Shackelford, A., et al. "Small-size wide-bandwidth microstrip patch antennas." *IEEE Antennas and Propagation Society International Symposium. 2001 Digest. Held in conjunction with: USNC/URSI National Radio Science Meeting (Cat. No.01CH37229)*, 2001, pp. 86-89.

[157] Shah, Rajvi, and Pravin R. Prajapati. "Slot loaded dielectric resonator antenna for bandwidth enhancement." *2017 International Conference on Wireless Communications, Signal Processing and Networking (WiSPNET)*, 2017, pp. 647-649.

[158] Sharma, Narinder, et al. "Miniaturization of fractal antenna using novel Giuseppe peano geometry for wireless applications." *2016 IEEE 1st International Conference on Power Electronics, Intelligent Control and Energy Systems (ICPEICES)*, 2016, pp. 1-4.

[159] Sharma, Richa, et al. " Design and Analysis of Circular Microstrip Patch Antenna for White Space TV Band Application." *Wireless Pers Commun, vol. 126*, 2022, pp. 3333–3344.

[160] Sharma, Tej R., et al. "Triple Band MSA for WiMAX and WLAN Application." *2015 Second International Conference on Advances in Computing and Communication Engineering*, 2015, pp. 214-218.

[161] Shelby, R. A., et al. "Experimental Verification of a Negative Index of Refraction." *Science*, vol. 292, no. 5514, 2001, pp. 77-79.

[162] Shen, Jun, et al. "A Slot-based RFID Reader Antenna Design with Broad Left to Right Space Detections." *2021 IEEE 4th International Conference on Electronic Information and Communication Technology (ICEICT)*, 2021, pp. 620-622.

[163] Shen, Laiwei, et al. "A Yagi–Uda Antenna With Load and Additional Reflector for Near-Field UHF RFID." *IEEE Antennas and Wireless Propagation Letters*, vol. 16, 2017, pp. 728-731.

[164] Shilpi, Pragya, et al. "Design of dual band antenna with improved gain and bandwidth using defected ground structure." *2016 3rd International Conference on Signal Processing and Integrated Networks (SPIN)*, 2016, pp. 544-548.

[165] Siddiqui, Mohd G., et al. "Koch–Sierpinski Fractal Microstrip antenna for C/X/Ku-band applications." *Australian Journal of Electrical and Electronics Engineering*, vol. 16, no. 4, 2019, pp. 369-377.

[166] Sindou, M., et al. "Multiband and wideband properties of printed fractal branched antennas." *Electronics Letters*, vol. 35, no. 3, 1999, pp. 181-182.

[167] Singh, Arun K., et al. "Seven element wideband planar log-periodic antenna for TVWS base station." *2017 Progress in Electromagnetics Research Symposium - Fall (PIERS - FALL)*, 2017, pp. 2051-2055.

[168] Singh, Ranjit, et al. "Resonant frequency of elliptical microstrip patch radiator." *International Journal of Electronics*, vol. 69, no. 3, 1990, pp. 385-388.

[169] Smierzchalski, M., and K. Mahdjoubi. "A novel approach for the characterization of bi-anisotropic metamaterials using oblique incidence." *2013 7th International Congress on Advanced Electromagnetic Materials in Microwaves and Optics*, 2013, pp. 511-513.

[170] Soler, J., and J. Romeu. "Dual-band Sierpinski fractal monopole antenna." *IEEE Antennas and Propagation Society International Symposium. Transmitting Waves of Progress to the Next Millennium. 2000 Digest. Held in conjunction with: USNC/URSI National Radio Science Meeting (Cat. No.00CH37118)*, vol. 3, July 2000, pp. 1712-1715.

[171] Song, C.T.P., et al. "Fractal stacked monopole with very wide bandwidth." *Electronics Letters*, vol. 35, no. 12, 1999, p. 945.

[172] Song, C.T.P., et al. "Sierpinski monopole antenna with controlled band spacing and input impedance." *Electronics Letters*, vol. 35, no. 13, 1999, p. 1036.

[173] Song, C.T.P., et al. "Shorted fractal Sierpinski monopole antenna." *IEEE Antennas and Propagation Society International Symposium. 2001 Digest. Held in conjunction with: USNC/URSI National Radio Science Meeting (Cat. No.01CH37229)*, vol. 3, 2001, pp. 138-141.

[174] "Spectrum Policy Task Force." *Federal Communications Commission*, 14 Nov. 2018, www.fcc.gov/document/spectrum-policy-task-force.

[175] Staple, G., and K. Werbach. "The End of Spectrum Scarcity." *IEEE Spectrum*, vol. 41, no. 3, 2004, pp. 48-52.

[176] Sung, Y. J. "Bandwidth Enhancement of a Wide Slot Using Fractal-Shaped Sierpinski." *IEEE Transactions on Antennas and Propagation*, vol. 59, no. 8, 2011, pp. 3076-3079.

[177] Tang, P. "Scaling property of the Koch fractal dipole." *IEEE Antennas and Propagation Society International Symposium. 2001 Digest. Held in conjunction with: USNC/URSI National Radio Science Meeting (Cat. No.01CH37229)*, vol. 3, pp. 150-153.

[178] Tashi, et al. "Design, simulation, prototyping and experimentation of planar micro-strip patch antenna for passive UHF RFID to tag for metallic objects." *2016 10th International Conference on Software, Knowledge, Information Management & Applications (SKIMA)*, 2016, pp. 243-249.

[179] Tesneli, Nigar B., et al. "Performance Improvement of a Microstrip Patch Antenna by Using Electromagnetic Band Gap and Defected Ground Structures." *2020 International Conference on Electrical, Communication, and Computer Engineering (ICECCE)*, June 2020, pp. 25-30.

[180] Thakur, S., et al. "L-shaped Microstrip Antenna for Wideband." *2013 International Conference on Communication Systems and Network Technologies*, 2013, pp. 41-43.

[181] "TV White Spaces Unlicensed Access Spectrum in Sub-700 MHz Band." *Frank Rayal | Strategic Insights & Advisory in Telecom and Technology*, Telesystem

Innovations, 2010, frankrayal.files.wordpress.com/2012/04/tv-white-space-whitepaper.pdf. Accessed 7 Apr. 2021.

[182] Verma, M. K., et al. "A novel circularly polarized gap-coupled wideband antenna with DGS for X/Ku-band applications." *Electromagnetics*, vol. 39, no. 3, 2018, pp. 186-197.

[183] Vinoy, K.J., et al. "Resonant frequency of Hilbert curve fractal antennas." *IEEE Antennas and Propagation Society International Symposium. 2001 Digest. Held in conjunction with: USNC/URSI National Radio Science Meeting (Cat. No.01CH37229)*, vol. 3, July 2001, pp. 648-651.

[184] Viswanadha, Karteek, and Nallanthighal S. Raghava. "Design and Analysis of a Multi-band Flower Shaped Patch Antenna for WLAN/WiMAX/ISM Band Applications." *Wireless Personal Communications*, vol. 112, no. 2, 2020, pp. 863-887.

[185] Vithanawasam, Chamath K., et al. "A review of microstrip antenna designs for TV white space applications." *Indonesian Journal of Electrical Engineering and Computer Science*, vol. 19, no. 2, 2020, pp. 855-863.

[186] Wandale, Steven, et al. "Need for TVWS Availability Quantification After the Analogue TV Switch-Off." *2021 International Conference on COMmunication Systems & NETworkS (COMSNETS)*, 2021, pp. 74-77.

[187] Wang, Bo, et al. "A novel wideband circular patch antenna for wireless communication." *2014 International Symposium on Antennas and Propagation Conference Proceedings*, 2014, pp. 545-546.

[188] Wang, Naizhi, et al. "Compact wideband omnidirectional UHF antenna for TV white space cognitive radio application." *AEU - International Journal of Electronics and Communications*, vol. 74, 2017, pp. 158-162.

[189] Wang, Ping, et al. "Wideband Circularly Polarized UHF RFID Reader Antenna with High Gain and Wide Axial Ratio Beam widths." *Progress In Electromagnetics Research*, vol. 129, 2012, pp. 365-385.

[190] Wang, Xiufang, et al. "Analysis of Wireless Power Transfer Using Superconducting Metamaterials." *IEEE Transactions on Applied Superconductivity*, vol. 29, no. 2, 2019, pp. 1-5.

[191] Waterhouse, R. "Small microstrip patch antenna." *Electronics Letters*, vol. 31, no. 8, 1995, p. 604.

[192] Werner, D.H., et al. "A self-similar fractal radiation pattern synthesis technique for reconfigurable multiband arrays." *IEEE Transactions on Antennas and Propagation*, vol. 51, no. 7, 2003, pp. 1486-1498.

[193] Werner, D.H., and Junho Yen. "A novel design approach for small dual-band Sierpinski gasket monopole antennas." *IEEE Antennas and Propagation Society International Symposium. 2001 Digest. Held in conjunction with: USNC/URSI National Radio Science Meeting (Cat. No.01CH37229)*, vol. 3, 2001, pp. 632-635.

[194] Werner, D.H., et al. "Radiation characteristics of thin-wire ternary fractal trees." *Electronics Letters*, vol. 35, no. 8, 1999, p. 609.

[195] Wolff, I., and N. Knoppik. "Rectangular and Circular Microstrip Disk Capacitors and Resonators." *IEEE Transactions on Microwave Theory and Techniques*, vol. 22, no. 10, 1974, pp. 857-864.

[196] Wong, Hang, and Kwai-Man Luk. "Unidirectional antenna composed of a planar dipole and a shorted patch." *2006 Asia-Pacific Microwave Conference*, 2006, pp. 1-4.

[197] Wong, Kin-Lu, et al. "A compact meandered circular microstrip antenna with a shorting pin." *Microwave and Optical Technology Letters*, vol. 15, no. 3, 1997, pp. 147-149.

[198] Xu, Kai D., et al. "Microstrip Patch Antennas with Multiple Parasitic Patches and Shorting vias for Bandwidth Enhancement." *IEEE Access*, vol. 6, 2018, pp. 11624-11633.

[199] Yang, Deqiang, et al. "Bandwidth enhancement of wide-slot antenna array for UWB applications." *2017 IEEE 3rd Information Technology and Mechatronics Engineering Conference (ITOEC)*, 2017.

[200] Yeo, U. B., et al. "An Ultra-Wideband Antenna Design Using Sierpinski Sieve Fractal." *Journal of Electromagnetic Waves and Applications*, vol. 22, no. 11-12, 2008, pp. 1713-1723.

[201] Yong-Xin Guo, and D.C.H. Tan. "Wideband Single-Feed Circularly Polarized Patch Antenna with Conical Radiation Pattern." *IEEE Antennas and Wireless Propagation Letters*, vol. 8, 2009, pp. 924-926.

[202] Yoo, Sungjun, et al. "Design of microstrip patch antennas with parasitic elements for minimized polarization mismatch." *2016 URSI Asia-Pacific Radio Science Conference (URSI AP-RASC)*, 2016, pp. 1845-1846.

[203] Yu, Yin-Hua, et al. "Dielectric Slab Superstrate Electrically Small Antennas with High Gain and Wide Band." *IEEE Antennas and Wireless Propagation Letters*, vol. 19, no. 9, 2020, pp. 1476-1480.

[204] Zhang, Qianyun, and Yue Gao. "Compact low-profile UWB antenna with characteristic mode analysis for UHF TV white space devices." *IET Microwaves, Antennas & Propagation*, vol. 11, no. 11, 2017, pp. 1629-1635.

[205] Zhang, Qianyun, et al. "Compact U-shape ultra-wideband antenna with characteristic mode analysis for TV white space communications." *2016 IEEE International Symposium on Antennas and Propagation (APSURSI)*, 2016, pp. 17-18.

[206] Zhang, Qianyun, et al. "Design of a Multimode UWB Antenna Using Characteristic Mode Analysis." *IEEE Transactions on Antennas and Propagation*, vol. 66, no. 7, 2018, pp. 3712-3717.

[207] Zhang, Wenjie, et al. "TV white space and its applications in future wireless networks and communications: a survey." *IET Communications*, vol. 12, no. 20, 2018, pp. 2521-2532.

[208] Zhu, Feng, et al. "Exploring Tag Distribution in Multi-Reader RFID Systems." *IEEE Transactions on Mobile Computing*, vol. 16, no. 5, 2017, pp. 1300-1314.

[209] Ziolkowski, R.W. "Design, fabrication, and testing of double negative metamaterials." *IEEE Transactions on Antennas and Propagation*, vol. 51, no. 7, 2003, pp. 1516-1529.